

**INVESTIGATING WATER SOLUBLE ORGANIC AEROSOLS:  
SOURCES AND EVOLUTION**

A Dissertation  
Presented to  
The Academic Faculty

by

Arsineh N. Hecobian

In Partial Fulfillment  
of the Requirements for the Degree  
Doctor of Philosophy in the  
School of Earth and Atmospheric Sciences

Georgia Institute of Technology  
May 2010

**INVESTIGATING WATER SOLUBLE ORGANIC AEROSOLS:  
SOURCES AND EVOLUTION**

Approved by:

Dr. Rodney J. Weber, Advisor  
School of Earth and Atmospheric Sciences  
*Georgia Institute of Technology*

Dr. Paul H. Wine  
School of Earth and Atmospheric  
Sciences  
*Georgia Institute of Technology*

Dr. L. Gregory Huey  
School of Earth and Atmospheric Sciences  
*Georgia Institute of Technology*

Dr. Michael Bergin  
School of Civil and Environmental  
Engineering  
*Georgia Institute of Technology*

Dr. Athanasios Nenes  
School of Earth and Atmospheric Sciences  
*Georgia Institute of Technology*

Date Approved: March 31, 2010



To the guiding light of my life,  
my mom

## ACKNOWLEDGEMENTS

My special thanks to my adviser Dr. Rodney Weber for his guidance and support throughout the years that I have worked with him. I also would like to thank my committee members Dr-s Paul Wine, Mike Bergin and Thanos Nenes for the comments on my thesis. My sincere thanks to Dr. Greg Huey and his group members Mr. David Tanner and Dr. Robert Stickel for their support during the years of my study.

I would like to thank my current and former group members, Dr-s Amy Sullivan, Rick Peltier and Chris Hennigan for their help in the different aspects of my research. Also, Ms. Michelle Oakes-Jones and Jiumeng Liu for making the lab a fun place to be. My special thanks to Ms. Xiaolu Zhang for her help with my thesis research and defense presentation, and her friendship.

Many thanks to my friends Dr.-s Violeta Toma, Kremena Darmenova and Anton Darmenov and Ms. Kelly Smolinski for keeping me sane.

And finally, thanks to my family without whose unconditional and continuous help and support I would not be here today. Mere words cannot express how much their support means to me. I am grateful to Armen and Rima, especially. And finally, thanks to my mom, for listening to my talks on data analysis over the phone.

# TABLE OF CONTENTS

	Page
ACKNOWLEDGEMENTS	iv
LIST OF TABLES	viii
LIST OF FIGURES	ix
LIST OF SYMBOLS AND ABBREVIATIONS	xii
SUMMARY	xiv
CHAPTER 1: INTRODUCTION	1
1.1. Why Are Aerosols Important?	1
1.2. Organic Aerosols	3
1.2.1. Primary Organic Aerosols (POA)	4
1.2.2. Secondary Organic Aerosols (SOA)	5
1.2.3. HOA and OOA	6
1.3. Emerging Issues on POA and SOA	7
CHAPTER 2: MEASUREMENT OF AEROSOLS BY CIMS	9
2.1. Background	9
2.2. Experimental Techniques	9
2.2.1. CIMS Modifications	10
2.2.2. PILS-IC Setup	14
2.2.3. Calibration Setup	15
2.3. Results	17
2.3.1. Calibration	17
2.3.2. Ambient measurements	19

2.4. Conclusions	22
CHAPTER 3: ARCTAS-2008	24
3.1. Introduction	24
3.2. Methods	30
3.2.1. Aircraft Instrumentation	30
3.2.2. Plume Analysis	31
3.2.3. Identification of Fire Sources	32
3.2.4. Data Processing and Analysis	35
3.3. Analysis Complications and Simplifications	39
3.3.1. Detailed Segregation vs. Counting Statistics	39
3.3.2. Transport Age vs. Photochemical Age	39
3.3.3. Mixing of Various Emissions into Single Smoke Plumes	39
3.3.4. Different Loss Process of Species Relative to CO	40
3.4. Results	42
3.4.1. Canadian Boreal Forest Fires	42
3.4.2. Comparison of NEMRs for All Biomass Burning Categories	46
3.4.2.1. $\Delta\text{AN}/\Delta\text{CO}$ and $\Delta\text{HCN}/\Delta\text{CO}$	50
3.4.2.2. $\Delta\text{CO}_2/\Delta\text{CO}$ and $\text{CH}_4/\Delta\text{CO}$	51
3.4.2.3. $\Delta\text{BZ}/\Delta\text{CO}$ and $\Delta\text{TU}/\Delta\text{CO}$	51
3.4.2.4. $\Delta\text{NO}_x/\Delta\text{CO}$ , $\Delta\text{NO}_y/\Delta\text{CO}$ and $\Delta\text{O}_3/\Delta\text{CO}$	52
3.4.2.5. $\Delta\text{NO}_3^-/\Delta\text{CO}$ , $\Delta\text{SO}_4^{2-}/\Delta\text{CO}$ and $\Delta\text{NH}_4^+/\Delta\text{CO}$	53
3.4.2.6. $\Delta\text{OA}/\Delta\text{CO}$ and $\Delta\text{WSOC}/\Delta\text{CO}$	55
3.4.2.7. $\Delta\text{BC}_{\text{Mass}}/\Delta\text{CO}$	56
3.5. Conclusions	56
CHAPTER 4: WATER SOLUBLE ORGANIC CARBON LIGHT ABSORPTION	59

4.1. Introduction	59
4.2. Methods	64
4.2.1. Light Absorption Measurements	64
4.2.2. Filter Measurements	65
4.2.3. Online Measurements	71
4.2.4. Interpretation of Absorption Data	76
4.3. Results	78
4.3.1. Absorption Data	78
4.3.2. FRM Filter Results	82
4.3.3. Online Measurement Results	90
4.4. Conclusions	95
CHAPTER 5: FUTURE WORK	98
CHAPTER 6: CONCLUSIONS	101
REFERENCES	104



## LIST OF TABLES

	Page
Table 3.1: Measurements from ARCTAS-2008 aboard the NASA DC-8 aircraft used for the analysis presented in this chapter	31
Table 3.2: Abbreviations and descriptions of plume categories selected during the ARCTAS-2008 study	35
Table 3.3: Results of ANOVA analysis for the differences in the means of different species in categorized plumes	50
Table 4.1: Summary of linear regression results for 24-hr FRM filter $Ab_{8365}$ versus WSOC concentration for each site, separated by high and low levels of levoglucosan ( $>50\text{ng/m}^3$ and $<50\text{ng/m}$ , respectively). The mean result exclude the LCRK site and the non-biomass burning also excluded the ATH site, which all had very low correlations	88

## LIST OF FIGURES

	Page
Figure 1.1: Global average radiative forcing (RF) estimates and ranges in 2005 for anthropogenic emissions and other agents and mechanisms (IPCC, 2007)	2
Figure 2.1: Schematic of negative ion chemical ionization mass spectrometer (CIMS) for the measurement of sulfuric acid. The equation above the figure presents the ionization scheme of this instrument (modified from Thompson, 2006)	12
Figure 2.2: Schematic of the heated inlet used for modifying the CIMS instrument for aerosol measurements. The thermally denuded system had four heater cartridges, inside a 1"x1"x1" stainless steel block. The stainless steel block encompasses a 0.5" ID stainless steel tube	13
Figure 2.3: Calibration setup for generation of sulfate aerosol for the aerosol CIMS system	16
Figure 2.4: Thermal profile of ammonium sulfate at different temperatures (of the heater) for the CIMS system. The aerosol generation system was used to produce sulfate aerosols and the optimum temperature was around 360° C	18
Figure 2.5: Mass spectrum of ambient air from Atlanta, GA, measured by the aerosol CIMS system. The temperature of the inlet of the heater was set at 360° C. The red trace on the graph is a spectrum of ambient air and the blue trace is a spectrum of ambient air with a HEPA filter inline	19
Figure 2.6: Signal count for 97 amu, using the aerosol CIMS. Background measurements highlighted in this figure were performed by directing the sample flow through an inline HEPA filter	20
Figure 2.7: Results of comparison of PILS-IC and aerosol CIMS sulfate measurements for ambient air collected on March 28, 2005 in Atlanta, GA. The error bars are 1σ of the uncertainty of the PILS_IC system	21
Figure 2.8: Mass Spectrum of oxalate aerosol (in red) compared with the spectrum of filtered air (in black) is presented in this figure	22
Figure 3.1: Location of selected biomass burning plumes recorded during the ARCTAS-2008 experiment aboard the DC-8 aircraft. The plumes are identified by source categories	29

Figure 3.2: Evolution of emission ratios for trace-gas and aerosol chemical components in four large boreal forest fires detected during ARCTAS-B. Specific fires are identified by the date on which they were intercepted (month/day/year). For cases where transport times were within $\pm 10\%$ for a fire measured on a given day, the mean normalized excess mixing ratio is given and the data range is shown as an error bar of $\pm 1$ standard deviation	38
Figure 3.3: Comparison of median (25 <sup>th</sup> and 75 <sup>th</sup> %-ile and mean) for various trace-gas and aerosol components in all biomass burning plumes intercepted by the NASA DC-8 during ARCTAS-A, ARCTAS-B and ARCTAS-CARB. Numbers inside the graphs represent the number of points present in each category	41
Figure 3.4: A cumulative representation of observed Boreal forest fires during the period of June 29 to July 10, 2008 (ARCTAS-B), from FIRMS website	42
Figure 3.5: A cumulative representation of the fires in California from June 18 to June 24, 2008 from FIRMS website	48
Figure 4.1: The locations and designation (urban/rural) of FRM filter collection sites in the Southeastern United States	67
Figure 4.2: Schematic of Online Light Absorption and WSOC measurement. The area highlighted and enlarged is the LWCC schematic, which presents the setup that was used for the filter measurements	72
Figure 4.3: Raw light absorption data from online measurements of light absorption in Atlanta, GA; July 2009	75
Figure 4.4: Examples of absorption spectra from FRM filters collected at two sites during 2007	79
Figure 4.5: Monthly average concentration for all sites for 2007. Variability is shown as the standard error. The number of filters averaged for each month is roughly 75	83
Figure 4.6: Correlation between Abs <sub>365</sub> and levoglucosan at a representative rural (6a. Yorkville) and urban (6b. South Dekalb) site. The data for the cooler months (J, F, M, A, O, N, D) are presented in blue and the data for the warmer months are (M, J, J, A, S) are shown in red. The regression fit is only for the cooler month's data.	85
Figure 4.7: Comparison of Absorption vs. WSOC for all filter data. The data points have been color coded based on levoglucosan values. Light colors indicate high concentrations of levoglucosan (i.e. filters influenced by biomass burning plumes) and dark colors show low levels of levoglucosan (i.e. filters that were less affected by biomass burning plumes)	86

Figure 4.8: Comparison of daily averages of online measurements of light absorption and WSOC in Atlanta, GA (July – September 2009) 91

Figure 4.9: Hourly means of ozone, CO, WSOC and light absorption from online measurements in Atlanta, GA. Ozone and CO data are from SEARCH monitoring site at Jefferson street, Atlanta, GA (2008) and included for only general comparison purposes. WSOC and Abs are from July-Sep 2009. Variability in the hourly averages is the standard error, where n=120 for each hourly average 92

## LIST OF ABBREVIATIONS

AMS: Aerosol Mass Spectrometer

AN: Acetonitrile

ARCTAS: Arctic Research of the Composition of the Troposphere from Aircraft and Satellites

BB: Biomass Burning

BC: Black Carbon

BZ: Benzene

CARB: California Air Resource Board

CH<sub>4</sub>: methane

CIMS: Chemical Ionization Mass Spectrometer

CO: carbon monoxide

CO<sub>2</sub>: carbon dioxide

DI Water: de-ionized water

HCN: hydrogen cyanide

HOA: Hydrocarbon-like organic aerosol

HULIS: Humic-like substances found in aerosols

HYSPLIT: hybrid single particle lagrangian integrated trajectory model

IC: Ion Chromatograph

NEMR: Normalized Excess Mixing Ratio

NO<sub>3</sub><sup>-</sup>: Nitrate ion

OA: Organic Aerosol

OOA: Oxygenated organic aerosol

OVOC: Oxygenated Volatile Organic Carbon

PILS: Particle-into-Liquid Sampler

PILS-IC: Particle-into-Liquid Sampler Ion Chromatogram

PM<sub>1</sub>: particles with aerodynamic diameters less than 1 μm

PM<sub>2.5</sub>: particles with aerodynamic diameters less than 2.5 μm

PTR-MS: proton transfer reaction – mass spectrometer

SOA: secondary organic aerosol

SO<sub>2</sub>: sulfur dioxide

SO<sub>4</sub><sup>-2</sup>: sulfate

TOC: Total Organic Carbon (analyzer)

UTC: coordinated universal time

UV: ultraviolet (light)

VOC(s): Volatile Organic Compound(s)

WIOC: water-insoluble organic carbon (calculated from OC – WSOC)

WSOC: water-soluble organic carbon

## SUMMARY

Many studies are being conducted on the different properties of organic aerosols (OA-s) as it is first emitted into the atmosphere and the consequent changes in these characteristics as OA-s age and secondary organic aerosol (SOA) is produced and in turn aged. This thesis attempts to address some of the significant and emerging issues that deal with the formation and transformation of water-soluble organic aerosols in the atmosphere.

First, a proven method for the measurement of gaseous sulfuric acid, negative ion chemical ionization mass spectrometry (CIMS), has been modified for fast and sensitive measurements of particulate phase sulfuric acid (i.e. sulfate). The modifications implemented on this system have also been the subject of preliminary verifications for measurements of aerosol phase oxalic acid (an organic acid).

Second, chemical and physical characteristics of a wide range of biomass-burning plumes intercepted by the NASA DC-8 research aircraft during the three phases of the ARCTAS experiment are presented here. A statistical summary of the emission (or enhancement) ratios relative to carbon monoxide is presented for various gaseous and aerosol species. Extensive investigations of fire plume evolutions were undertaken during the second part of this field campaign. For four distinct Boreal fires, where plumes were intercepted by the aircraft over a wide range of down-wind distances, emissions of various compounds and the effect of aging on them were investigated in detail. No clear evidence of production of secondary compounds (e.g., WSOC and OA) was observed. High variability in emissions between the different plumes may have obscured any clear

evidence of changes in the mass of various species with increasing plume age. Also, the lack of tropospheric oxidizing species (e.g.,  $O_3$  and OH) may have contributed to the lack of SOA formation. Individual intercepts of smoke plumes in this study were segregated by source regions. The normalized excess mixing ratios (NEMR-s) of some gaseous and aerosol compounds were compared. The NEMRs of most species had a high degree of variability that tended to obscure any significant differences between various smoke sources; however, some trends were observed.

Smoke plumes associated with long-range transport from Asia and Siberia showed enhanced sulfate and HCN levels. The fire plumes that were influenced by urban emissions (e.g., intercepted over California) had higher levels of  $CO_2$ ,  $CH_4$ ,  $NO_y$  and toluene. Overall, pronounced differences were observed when comparing the plumes subject to long-range transport to the ones that were intercepted closer to the fire sources (e.g., the plumes intercepted over California and the ones from Canadian Boreal forest fires). Additionally, when comparing the plumes near the fires, the ones that were influenced by urban emissions (some of the plumes encountered over California) displayed more distinct characteristics than the ones that were less or not influenced by urban emissions.

Data from Teflon filters from the Southeastern United States were analyzed. The filter data show that the fraction of water-soluble light absorbing carbonaceous material is larger in biomass burning plumes regardless of the urban or rural location of the collection of the filter. Indeed, the slope of light absorption at 365 nm ( $Ab_{s365}$ ) vs. WSOC was about 3.5 times higher in filters that were influenced by biomass burning plumes. Also, when the filters were separated into biomass burning and non-biomass



burning categories, the slopes of  $\text{Abs}_{365}$  vs. WSOC for each category were uniform for all the sites where the filters were collected.

Finally, a new method of simultaneous online measurement of water-soluble aerosol light absorption and WSOC has been presented. The results from an online study are in reasonable agreement with filter studies, although the measurements were collected during two different years and using two different techniques. The hourly averages of the online data showed that the morning rush hour production of WSOC coincides with an increase in  $\text{Abs}_{365}$ . However, there was no corresponding increase in  $\text{Abs}_{365}$  for the daytime photochemical production of WSOC.

As new challenges arise in the area of organic aerosols and their production and fate, the results of this thesis can be used to augment our knowledge of the field and provide information that can be useful in future research.

# CHAPTER 1

## INTRODUCTION

### 1.1. Why Are Aerosols Important?

Atmospheric aerosols can have important local, regional and global impacts. Ambient aerosols have been extensively studied because of their significant influence on air pollution, human health [*Kroll and Seinfeld, 2008*] and climate [e.g., *Saxena et al. 1995; Malm et al. 1996; Ramanathan et al., 2001, Charlson et al., 1992*]. On a local scale, urban air pollution from anthropogenic emissions (e.g., vehicular exhaust, biofuel or anthropogenic biomass burning and industrial emissions) can cause significant adverse health [e.g., *Brimblecombe and Bowle, 1992; Studnicka et al., 1993; Harrison and Yin, 2000; Pope et al., 2002*] or socioeconomic (e.g., reduction in visibility in national parks [*Malm, 1989*]) effects. On a regional and global scale, aerosols can be transported over long distances and affect the ambient conditions of places far away from the location of their original emission [*Ravishankara, 1997*]. Particulate matter in the atmosphere can influence cloud condensation nuclei (CCN) and cloud albedo; thus, they can significantly affect global climate [*Charlson et al., 1992; Penner et al., 2001; Ramanathan et al., 2001, Gunthe et al., 2009; Shinozuka et al., 2009*]. Additionally, aerosols can scatter and absorb solar radiation and consequently affect the earth's radiation budget and climate [*Haywood and Boucher, 2000; Claeys et al., 2004a; Claeys et al., 2004b*]. The radiative effect of aerosols contributes the largest degree of uncertainty in the prediction of global climate change due to anthropogenic activities (Figure 1.1).

# Radiative Forcing Components

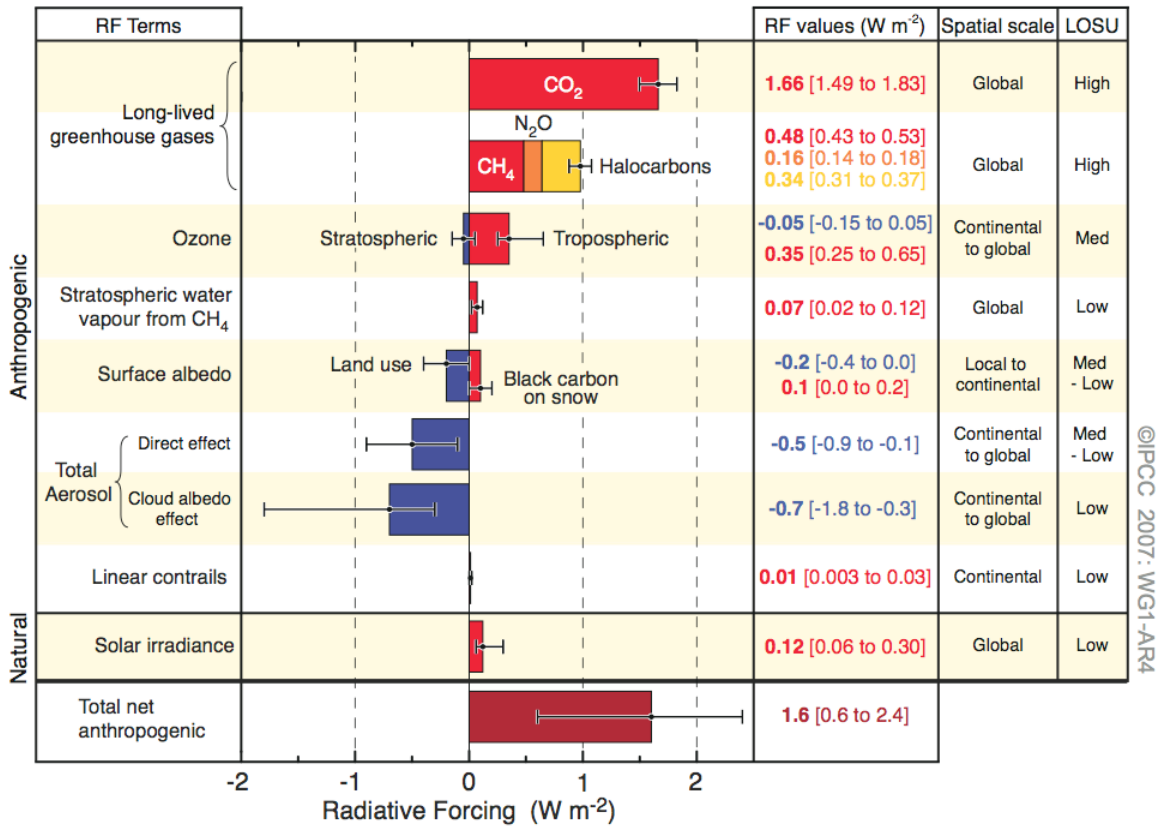


**Figure 1.1 Global-average radiative forcing (RF) estimates and ranges in 2005 for anthropogenic emissions and other agents and mechanisms (IPCC, 2007)**

Thus, the study of aerosols and the processes involved in their production and loss are vital to our understanding of atmospheric mechanism and their effect on ecology and human health.

In general, atmospheric aerosols (or particulate matter) are composed of some water-soluble inorganic compounds (such as sulfate and nitrate), water insoluble mineral dust and soluble and insoluble carbonaceous materials. The carbonaceous compounds in turn, can be made up of soluble and insoluble organic compounds and elemental carbon.

Organic aerosols (OA-s) can comprise about 20-90% of fine aerosols (particulate matter with diameter of  $\leq 2.5 \mu\text{m}$ ) [e.g., *Talbot et al., 1988; Artaxo et al., 1990; Talbot et al., 1990; Saxena and Hildemann, 1996; Andreae and Crutzen, 1997; Kanakidou et al., 2005; Zhang et al., 2007; Kroll and Seinfeld, 2008*]. OA-s and the mechanisms leading to their production and evolution are the least understood part of atmospheric aerosols [e.g., *Novakov et al., 1997; Zappoli et al., 1999; Decesari et al., 2000; Fuzzi et al., 2001; Jimenez et al., 2009*].

The presence of organic compounds in the particulate matter affects some important properties of aerosols such as hygroscopicity [*Rubel and Gentry, 1985; Hansson et al., 1990; Andrews and Larson, 1993; Novakov and Corrigan, 1996; Hansson et al., 1998*] and thus, cloud condensation nuclei activity [*Asa-Awuku et al., 2008*]. Organic compounds and their effect on cloud condensation nuclei (CCN) have been the subject of many studies [e.g., *Novakov and Penner, 1993; Noone et al., 1996*]. A clear understanding of the processes producing and affecting OA-s will greatly reduce the uncertainty associated with the climate change predictions as they pertain to direct and indirect effects of aerosols on the global radiation budget [*Kanakidou et al., 2005 and references therein; Menon, 2004*], especially since the estimation of the direct and indirect forcing of OA-s on climate is not well understood [*Jimenez et al., 2009*].

## **1.2. Organic Aerosols**

Organic aerosols are released to the atmosphere as primary emissions (i.e. direct emissions) from anthropogenic and natural sources, or they are produced as secondary compounds from physio-chemical processes involving other aerosols and trace gases, which can have precursors from natural or anthropogenic emissions [e.g., *Khwaja et al.,*

1995; Forstner et al., 1997a; Forstner et al., 1997b; Pandis et al., 1991; Edney et al., 2005; Sullivan et al., 2006].

### **1.2.1. Primary Organic Aerosols (POA)**

There are many emission sources than can contribute to the production of primary organic aerosols (POA-s). Some examples are: biomass and biofuel burning [*Kanadidou et al, 2005 and references therein*], charbroilers and meat cooking operations [*Rogge et al., 1991*], non-catalyst and catalyst-equipped vehicles and heavy-duty diesel trucks [*Rogge et al., 1993a*], road dust, tire debris and organometallic brake lining dust [*Rogge et al., 1993b*], residential fuel burning [*Rogge et al., 1993c and d*], etc. Additionally, direct emissions from plants and agricultural waste can also produce POA [*Rogge et al., 1998*]. Indeed, disintegration, stress and degradation of bulk plant material have been recognized as a small natural source of POA [*Simoneit, 1977; Sicre et al., 1990; Hildemann et al., 1996; Jacob, 2000*]. In the following sections only the major sources of POA have been discussed.

One of the major sources of POA is biomass burning [*Rogge et al. 1998; Fine et al., 2001; Streets et al., 2003; Iinuma et al., 2007; De Gouw and Jimenez, 2009*], which can be both natural or anthropogenic in origin. The differences in OA emissions from diverse biomass-burning sources have been discussed in Chapter 3.

Traditionally, it has been assumed that POA is a smaller fraction of OA when compared to SOA, especially in urban areas. However, recently it has been suggested that the POA may constitute a larger fraction of OA than previously thought [*Donahue et al., 2009*]. In their paper, *Donahue et al. (2009)* suggest that more studies need to be conducted to clarify the oxygenated nature of POA, which will lead to a better

segregation of POA and SOA and thus a better understanding of the nature and contribution of POA to aerosols.

### **1.2.2. Secondary Organic Aerosol (SOA)**

The sources and pathways leading to the production of secondary organic aerosols (SOA-s) in the atmosphere are very complex. SOA-s can be produced from the oxidation products of many anthropogenic [Volkamer *et al.*, 2006] or biogenic [Went 1960; Goetz and Pueschel, 1967; Trainer *et al.*, 1987; Jacob and Wofsy, 1988; Andreae and Crutzen, 1997; Kavouras *et al.*, 1999; Pandis *et al.*, 1992; Hoffmann and Klockow, 1998; Yu *et al.*, 1999a and 1999b; Tsigaridis and Kanakidou, 2003; Claeys *et al.*, 2004a and 2004b; Kanakidou *et al.*, 2005; Hamilton *et al.*, 2009] volatile organic compounds (VOC-s) [De Gouw *et al.*, 2005; Volkamer *et al.*, 2006; Zhang *et al.*, 2007; Hallquist *et al.*, 2009].

Major families of VOC-s in the atmosphere are alkanes, alkenes/monoterpenes and aromatics. Alkenes/monoterpenes have been studied as a major source of global SOA [Engelhart *et al.*, 2008]. Aromatics are considered a major source of urban SOA. For example, isoprene (a biogenic VOC) has been extensively studied as a precursor for the formation of SOA [Henze and Seinfeld, 2006]. Anthropogenic VOC-s such as toluene (an aromatic VOC) have been known to act as SOA precursor by undergoing oxidation in the atmosphere [Atkinson, 2000; Kleindienst *et al.*, 2004].

One of the pathways of production of SOA is through oxidation of biogenic or anthropogenic VOC-s by oxidizing compounds such as ozone (O<sub>3</sub>), the hydroxyl radical (OH) and the nitrate radical (NO<sub>3</sub><sup>°</sup>) [Kroll and Seinfeld, 2008]. Additionally, gaseous VOC-s can be absorbed into cloud droplets and undergo chemical oxidation by aqueous phase OH [Kanakidou *et al.*, 2005; and references therein]. SOA formation through this

mechanism is accomplished by the integration of first and second generation oxidized VOC-s into the particle phase. As noted before, particle phase oxidation (via OH) is also a possible pathway of production of SOA.

Another proposed mechanism for the formation of SOA is through oligomerization of carbonyl + alcohol, carbonyl + gem-diol (or alcohol-ROH) or carboxylic acid + alcohol compounds [e.g., *Hastings et al., 2005; Ervens and Kreidenweis, 2007; Mang et al., 2008*]. Additionally, some evidence of acid catalyzed production of SOA has been shown in laboratory studies [e.g., *Jang et al., 2002 and references therein; Iinuma et al., 2007; De Haan et al., 2009a, 2009b and 2009c*]. A more in depth discussion of these studies has been presented in Chapter 4.

### **1.2.3. HOA and OOA**

A different categorization of OA is hydrocarbon-like organic aerosol (HOA) and oxygenated organic aerosol (OOA). This designation is generally similar to that of POA and SOA [e.g., *Zhang et al., 2005; Zhang et al., 2007; Jimenez et al., 2009*].

*Zhang et al. (2007)* have averaged the results from many studies (see references in *Zhang et al., (2007)*), to show that of total OA, 63% is OOA in urban areas, 83% downwind of urban areas and 95% in rural locations. Since it is possible that OOA can be both SOA and POA [*Donahue et al., 2009*], clearly this pattern of OOA requires further investigation.

More information on the chemical composition and pathways of SOA formation is an important tool that can reduce the ambiguity associated with the effect of aerosols on climate [*Kiehl, 2007*]. In fact, estimating the amount of production of SOA using its

known precursors and pathways leading to its production are vital parts of understanding the direct and indirect effects of aerosols on the climate [*Maria et al., 2004*].

### **1.3. Emerging Issues on POA and SOA**

In recent years, many studies have tried to address the relationship and fraction of POA and SOA in different air masses. The consensus seems to be that in urban areas SOA is the dominant fraction of OA, whereas when studying sources such as biomass burning, such agreement does not exist [*Capes et al., 2009; Yokelson et al., 2009; and the results from Chapter 3 of this thesis*]. Additionally, the oxygenated nature of POA and SOA and the relationship of their aging with the ratio of atomic oxygen to carbon have been studied [*Jimenez et al., 2009*].

Another area where the OA-s have been studied closely is the light absorbing nature of OA, especially at the ultra-violet region of the electromagnetic spectrum. In recent years, many studies have evaluated the nature of such material and the possible pathways of formation of these molecules. Chapter 4 of this thesis provides an overview of such studies and the results from two experiments in the Southeastern United States.

In summary, the papers presented in this thesis address some of the different aspects of production of POA and SOA (specifically from biomass burning sources, in Chapter 3) and the different chemical and physical properties (such as light absorption), that can be used to distinguish the processes affecting the production of POA and the changes in SOA with time (Chapter 4). Chapter 2 presents a proven method of measurement of atmospheric gaseous sulfuric acid, which has been modified to measure aerosol phase sulfuric acid (i.e. sulfate) and has the potential for the measurement of particulate phase organic compounds. Some of the questions answered here are:



- Can CIMS combined with a thermally denuded inlet be used for fast and accurate measurements of some organic aerosol components?
- Do the normalized emission ratios from different fires (in different locations) differ from each other?
- Is there any evidence of SOA formation in the diverse biomass burning plumes encountered on board the NASA DC-8 aircraft during ARCTAS-2008?
- Is there a difference between the light absorbing properties of water soluble OC for biomass burning and non-biomass burning plumes?
- Do fresh and aged SOA contain different quantities of water soluble light absorbing carbon?
- Is PILS-LWCC a viable method of near real time measurement of light absorbing properties of WSOC?

## CHAPTER 2

### MEASUREMENT OF AEROSOLS BY CIMS

#### 2.1. Background Information

Chemical Ionization Mass Spectroscopy (CIMS) technique has been used to measure various gaseous compounds such as  $\text{HNO}_3$ ,  $\text{SO}_2$ ,  $\text{H}_2\text{SO}_4$ ,  $\text{NH}_3$ , PAN,  $\text{HO}_2\text{NO}_2$  and many others, from direct ambient measurements or in laboratory studies [e.g., *Mohler and Arnold, 1991; Viggiano, 1993 and references therein; Huey et al., 1995; Huey et al., 1996; Tanner et al., 1997; Fehsenfeld et al., 1998; Slusher et al., 2001; Huey et al., 2004; Huey, 2007 and references therein; Nowak et al., 2007*]. Also, in recent years, CIMS has been modified to measure various inorganic and organic aerosol compounds [e.g., *Curtius and Arnold, 2001; Hearn and Smith 2004a and 2004b; Hearn and Smith, 2006*].

In this study, the modification of a CIMS system to measure aerosol sulfate by the addition of a thermally denuded inlet is reported. This system was used for the measurement of atmospheric aerosol phase sulfuric acid. *Arnold et al. (1998)* and *Curtius et al. (1998)* used a similar system for airborne measurements of aerosol sulfuric acid.  $\text{NO}_3^-$  was used as the reagent ion in this system and a particle into liquid sampler coupled with an ion chromatography system (PILS-IC) was used for verifying the aerosol CIMS measurements.

#### 2.2. Experimental Techniques

Two instruments were used for the measurement of atmospheric sulfate in the aerosol phase in this experiment. A CIMS was modified to provide measurements of

aerosol sulfuric acid (sulfate) and a PILS-IC was used to verify the CIMS measurements. The setup and specifications of these two systems have been discussed in the following sections. Additionally, a setup that was used for the calibration of CIMS has been discussed.

### 2.2.1. CIMS Modifications

A negative-ion detection CIMS instrument was used to measure concentrations of sulfate in aerosol phase in the atmosphere. This system utilizes negative chemical ionization technique to convert sulfuric acid ( $\text{H}_2\text{SO}_4$ ) molecules into  $\text{HSO}_4^-$  ions, using  $\text{NO}_3^-$  as the ionizing agent. This technique or ones similar to it have been previously used in many other studies for gaseous or aerosol measurements [e.g., *Viggiano et al., 1982; Eisle and Tanner, 1993; Mohler et al., 1993; Clemitshaw, 2004 and references therein; McNiell et al., 2007*] and [*Curtius et al., 1998*]. *Berrensheim et al. (2000)* used a modified version of CIMS and ambient atmospheric  $\text{H}_2\text{SO}_4$  measurements to make indirect measurements of ambient OH. Additionally, *Curtius and Arnold (2001)* have reported the details of setup and operation of a similar method for the direct, in situ measurement of aerosol sulfuric acid.

In this system, the sheath gas is inundated with  $\text{HNO}_3$  (see Figure 2.1); the  $\text{NO}_3^-$  ions are produced by  $^{120}\text{Po}$  (a radioactive  $\alpha$  emitter) from the ion source [*Huey et al., 2004*]. The  $\text{NO}_3^-$  ions are carried by the sheath gas flow to mix and react with the  $\text{H}_2\text{SO}_4$  molecules present in the sample flow air. The reaction between  $\text{H}_2\text{SO}_4$  and  $\text{NO}_3^-$  is shown below:



The signal count from the  $\text{HSO}_4^-$  ions that result from this Reaction 2.1 are measured using a quadrupole mass spectrometer. The concentration of  $\text{H}_2\text{SO}_4$  is calculated using the measured  $\text{NO}_3^-$  and  $\text{HSO}_4^-$  ion signal counts via Equation 2.2 [Berresheim *et al.*, 2000].

$$[\text{H}_2\text{SO}_4] = 1/kt \ln \{[(\text{NO}_3^-) + (\text{HSO}_4^-)]/(\text{NO}_3^-)\} \quad (2.2)$$

Where,  $[\text{H}_2\text{SO}_4]$  is the concentration of  $\text{H}_2\text{SO}_4$ ,  $(\text{NO}_3^-)$  is the signal count for  $\text{NO}_3^-$  (at 62 amu) and  $(\text{HSO}_4^-)$  is the signal count for  $\text{HSO}_4^-$  (at 97 amu),  $k$  is the rate constant of Reaction 1, and  $t$  is the interface time between  $\text{NO}_3^-$  and sample flow.

The configuration of the CIMS used for this experiment is a modified version of the one utilized by *Slusher et al.*, (2004). Figure 2.1 shows the setup of the basic components for this instrument.

## CIMS for H<sub>2</sub>SO<sub>4</sub> Detection

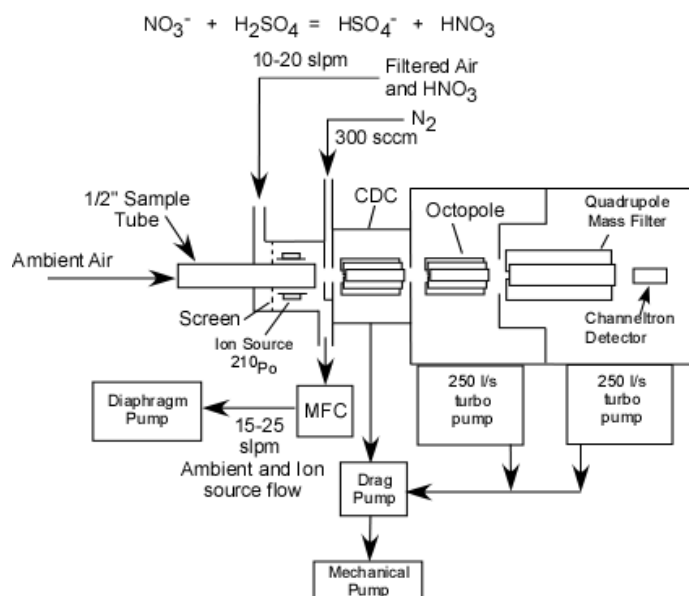


**Figure 2.1: Schematic of negative ion chemical ionization mass spectrometer (CIMS) for the measurement of sulfuric acid. The equation above the figure presents the ionization scheme of this instrument. (modified from *Thompson, (2006)*)**

The information on the setup of this system has been discussed in great detail by *Thompson, (2006)*. Very briefly, the CIMS instrument consists of a quadrupole mass spectrometer housed in a high vacuum chamber combined with an ion source that operates at a pressure that ranges from a few millibars to atmospheric pressure. In the current setup the ion source region is separated from the high vacuum area of the mass spectrometer by a collisional dissociation chamber (CDC) at an intermediate pressure [*Tanner et al, 1997*]. The ion current is transmitted from the CDC to the mass spectrometer with the octopole ion guide [*Slusher et al, 2001*]. Further details on the operation and specifications of the CIMS system are provided by *Eisele and Tanner (1991)*; *Eisele and Tanner (1993)*; *Tanner and Eisele (1995)* and *Eisele et al. (1996)*.

In the modified version of the CIMS for aerosol measurements, ambient air is drawn into the CIMS system through a thermally denuded stainless steel tube. A special heated inlet is used for the ambient flow in this instrument. This inlet is made up of a 12" long stainless steel tube (1/2" ID), encompassed in a stainless steel block with 1"x1"x1" dimensions (see Figure 2.2). Four non-stick high-temperature cartridge heaters (McMaster Carr, Atlanta, GA) were used to heat the stainless steel block and thus the tube and consequently the air-flow. The range of the temperatures for the heated block is from 25 °C to 550°C. The temperature of the sample flow was not measured. The temperature of the block was observed and controlled by a thermocouple probe inserted into the heating block.

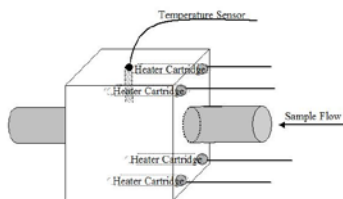


**Figure 2.2: Schematic of the heated inlet used for modifying the CIMS instrument for aerosol measurements. The thermally denuded system had four heater cartridges, inside a 1"x1"x1" stainless steel block. The stainless steel block encompasses a 0.5" ID stainless steel tube**

High temperatures are used to vaporize the atmospheric aerosols to their core molecules; thus enabling the chemical reaction to take place with the CIMS reagent ion ( $\text{NO}_3^-$ ). During the aerosol sulfuric acid measurements, the heating block temperature

was held constant at  $360^{\circ}\text{C} \pm 3^{\circ}\text{C}$ . The flow inside the sample flow tube was considered laminar as the velocities in the flow tube were around 66 cm/s and the Reynold's number was calculated to be 552 for a flow rate of 5 slpm, using the following equation:

$$R_e = (\rho v D) \mu^{-1} \quad (2.3)$$

Where  $R_e$  is the Reynold's number,  $\rho$  is density of air at 1 atm and  $20^{\circ}\text{C}$ ,  $v$  is the velocity of the sample flow,  $D$  is the diameter of the tube and  $\mu$  is the dynamic viscosity of air. Although the Reynold's number indicates that the flow is laminar, it is important to note that this may not have been entirely true due to the convective flows caused by the heating of the tube. The possible non-laminar nature of the flow would have resulted in the loss of  $\text{H}_2\text{SO}_4$  molecules to the walls of the tube. This problem was addressed by applying calibrations to these measurements under the same conditions as the ambient measurements, so that any loss to the walls was accounted for in the calculations.

The sampled ambient air was directed to the CIMS heater inlet at a flow of about 5-6 slpm. The reagent ion used for detection of sulfate was  $\text{NO}_3^-$ . The  $\text{H}_2\text{SO}_4$  in the air-flow participated in a proton exchange reaction with  $\text{NO}_3^-$ , as shown in Equation 1. The resulting signal from  $\text{HSO}_4^-$  ions is counted at 97 amu.

### 2.2.2. PILS-IC Setup

*Weber et al.* (2001) and *Orsini et al.* (2003), explain the principles of the operation of the PILS in great detail. Briefly, ambient particulates are collected into a small stream of high purity water, by mixing the ambient aerosol sample flow with a smaller flow of steam water. The resulting supersaturated environment causes the

particles to grow into droplets. In the setup used here, which is similar to that of *Peltier et al.* (2007b), the droplets are collected for further analysis by a Metrohm IC (Switzerland) Ion Chromatography (IC) system. Any interference from ambient gaseous compounds was eliminated by the use of glass honeycomb denuders in the sample line. The denuders are coated with citric acid and sodium carbonate. The limit of detection of the PILS-IC system for this setup was  $2 \text{ ug m}^{-3}$  for sulfate and about  $10 \text{ ug m}^{-3}$  for other organic aerosol components, such as oxalate.

### **2.2.3. Calibration Setup**

The aerosol  $\text{H}_2\text{SO}_4$  measurements were calibrated using known aerosol sulfate concentrations that were generated using an aerosol atomizer. At 35 psi, dry, ultra-pure nitrogen gas (AirGas, Kennesaw, GA.) was passed through a  $10^{-3}\%$  by mass solution of ammonium sulfate ( $(\text{NH}_4)_2\text{SO}_4$ ) in ultra-pure water. The DI water was acquired from a Barnstead nanopure water purifier system (Thermo Scientific, Weltham, MA). A model 3075/3076 aerosol atomizer (TSI, Shoreview, MN) was utilized for the production of the aerosols. The flow of air and aerosols out of the nebulizer was directed to a model 3062 diffusion dryer (TSI, Shoreview, MN) and then passed through a model 3077 aerosol neutralizer (TSI, Shoreview, MN). The calibration setup is presented in Figure 2.3.



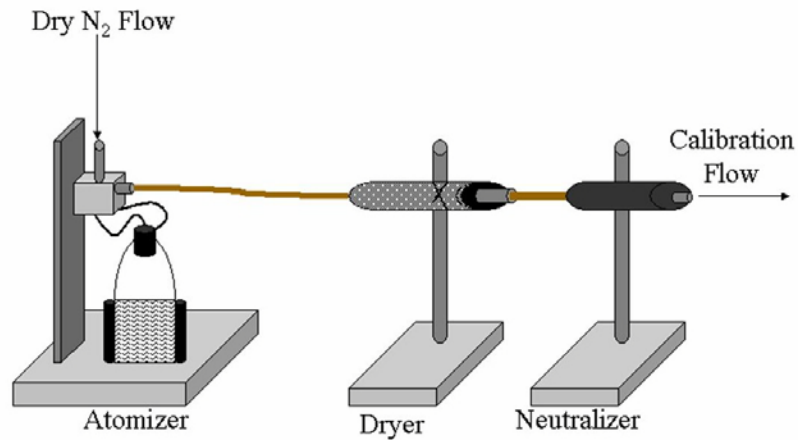


**Figure 2.3: Calibration setup for generation of sulfate aerosol for the aerosol CIMS system**

A flow splitter (TSI, Shoreview, MN) was then used to direct the flow of the sample to the PILS and CIMS, simultaneously. The sample flow out of the nebulizer was about 4 slpm; however the PILS and CIMS required flows of 16 slpm and 6 slpm, respectively. As external pumps were used to direct the sample flow to both CIMS and PILS, a HEPA filter (Gelman, Ann Arbor, MA) in combination with an inlet (over the sample line, before the thermal denuded inlet) was used to provide the needed excess flow to the systems. This resulted in the dilution of the aerosol flow from the aerosol generation system. The dilution was taken into account in the calculations of the sulfate concentrations in the PILS and CIMS systems. Background measurements were carried out for this system using an inline manual valve that directed the ambient flow through a HEPA filter, placed before the instrument inlet.

## **2.3. Results**

Many different laboratory tests were conducted to characterize the aerosol CIMS system for the measurement of sulfuric acid and its potential for the measurement of other organic aerosol components. Also, the aerosol CIMS was used for the measurement of sulfate aerosol concentrations in ambient air from Atlanta, GA. Some of the data collected from this study were compared with PILS. Some of the results from these laboratory and ambient studies are presented here.

### **2.3.1. System Information and Calibration**

As described previously, a heating block was used as a thermal denuder for the modification of the CIMS system for aerosol sulfate measurements. Sulfate aerosols were produced using the aerosol generation system and  $10^{-3}$ % w/w ammonium sulfate solution. A range of temperatures were investigated to find the optimal temperature for the vaporization of the sulfate aerosols into the gas phase for measurement with CIMS. The results of the thermal profile of the heater and the CIMS system for the ammonium sulfate solution are shown in Figure 2.4. This figure shows that sulfate aerosol vaporization starts at around 235° C and becomes optimal at around 360° C.

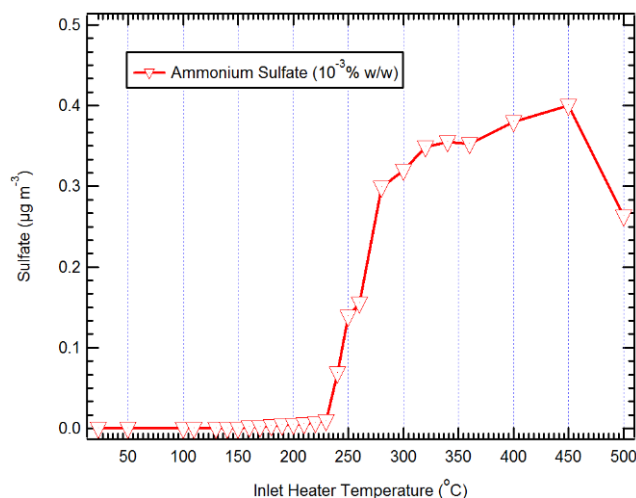


**Figure 2.4: Thermal profile of ammoniums sulfate at different temperatures (of the heater) for the CIMS system. The aerosol generation system was used to produce sulfate aerosols and the optimum temperature was around 360° C**

The optimal temperature for collection of data for aerosol sulfate measurements was 360° C. This was the temperature used for the study of sulfate aerosol with the CIMS. With this setup, this system is capable of making 1 Hz measurements of sulfate aerosols, with a sensitivity of 10 Hz/µg m<sup>-3</sup>. Based on comparisons with the PILS-IC system the LOD of the aerosol CIMS for sulfate measurements is about 0.01 ppt.

As noted before, a HEPA filter was used (with a manual valve) for background measurements. The following figure (Figure 2.5) presents a sample of Atlanta, GA ambient air mass spectrum. This spectrum was recorded using the CIMS system, with the thermal denuder heater temperature at 360° C. A signal for both aerosol and gas-phase sulfuric acid was observed at 97 amu. The signal from the filtered ambient air (i.e. HEPA filter was used to provide background levels for sulfate aerosol) is also included in Figure 2.5. As illustrated, some of the signal at 97 amu is due to the presence of gas

phase sulfuric acid in the sample flow. The use of a HEPA filter in-line for ambient measurements eliminated this source of interference. The signal for  $\text{HSO}_4^-$  (corresponding to aerosol sulfate) is clearly at 97 amu.

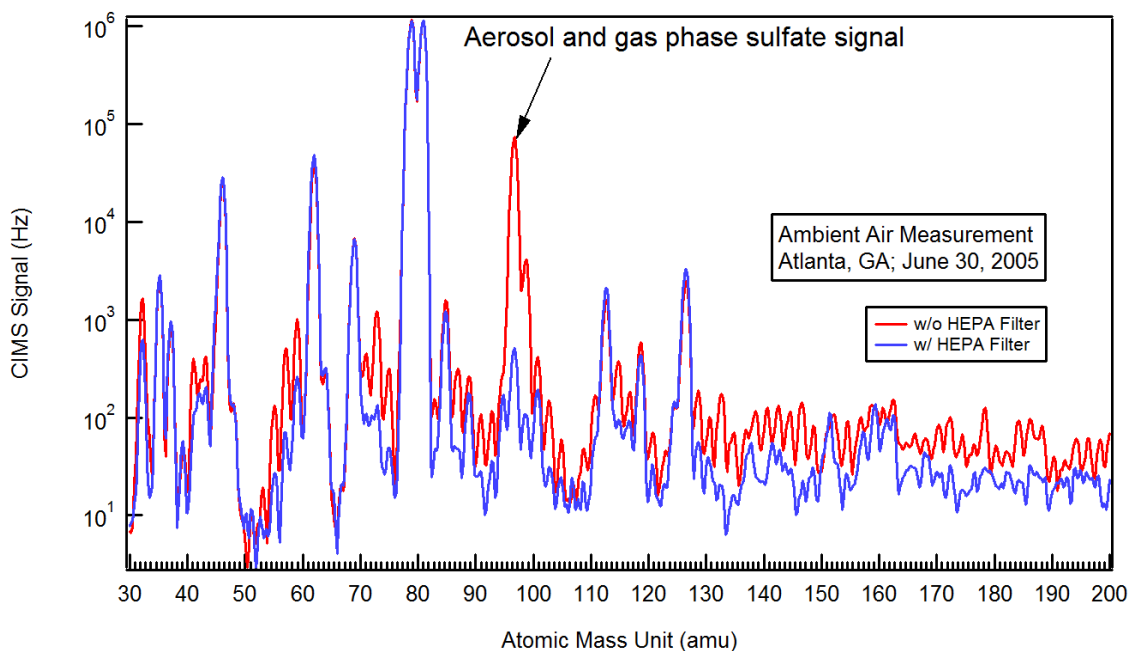


**Figure 2.5:** Mass spectrum of ambient air from Atlanta, GA, measured by the aerosol CIMS system. The temperature of the inlet heater was set at 360° C. The red trace on the graph is a spectrum of ambient air and the blue trace is a spectrum of ambient air with a HEPA filter inline.

### 2.3.2. Ambient Measurements

On March 22, 2005 ambient data on particulate sulfate concentrations from Atlanta, GA were collected with the aerosol CIMS system. As before, a HEPA filter was used for background measurements. Signal counts were collected at 64 and 97 amu.

Figure 2.6 shows a period when data was collected for the signal at 97 amu, where the CIMS signal for sulfate is observed. Background levels and ambient measurements are highlighted in this figure (Figure 2.6).

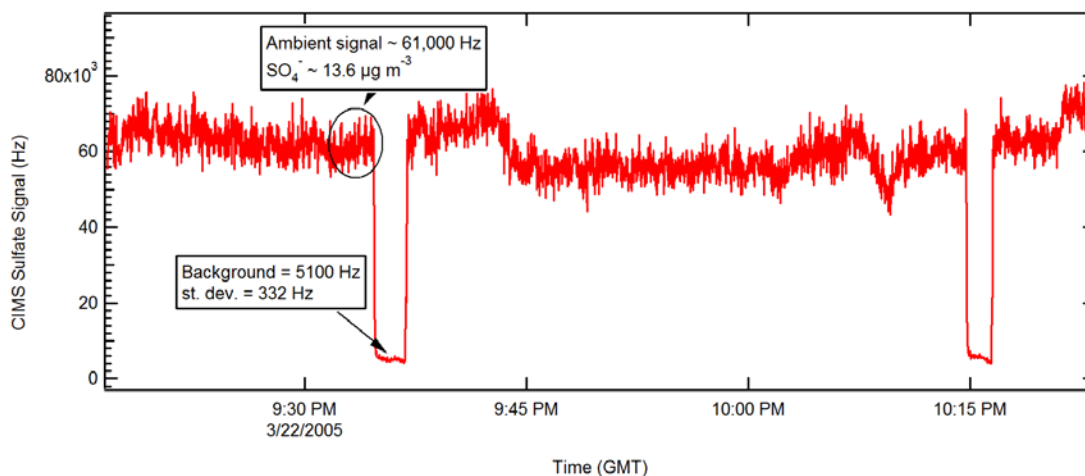


**Figure 2.6: Signal count for 97 amu, using the aerosol CIMS. Background measurements highlighted in this figure were performed by directing the sample flow through an inline HEPA filter.**

As shown in Figure 2.6, the aerosol CIMS system has a very fast response time to background measurements. Ambient measurements with this CIMS setup were performed at the same time as the PILS-IC, where ambient air was collected from the same source for both instruments, and distributed between the systems using a flow splitter. Figure 2.7 presents the correlation of the sulfate concentration data collected by both of these methods for ambient sampling. The data presented in this Figure were

collected on March 28<sup>th</sup>, 2005 in Atlanta, GA. Background checks were performed by directing the ambient airflow through a HEPA filter, with the use of a manual valve. The  $r^2$  value for the comparison of Aerosol CIMS and PILS-IC system was 0.96 and shows great agreement between the measurements of the two systems.

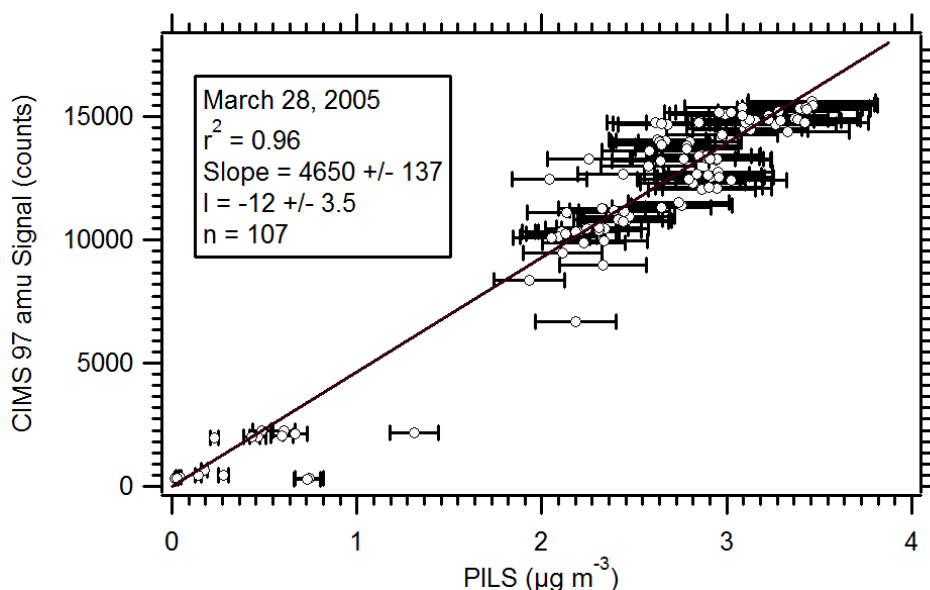


**Figure 2.7: Results of comparison of PILS-IC and aerosol CIMS sulfate measurements for ambient air collected on March 28, 2005 in Atlanta, GA. The error bars are  $1\sigma$  of the uncertainty of the PILS-IC system.**

Finally, to assess the potential use of this system for future measurements of organic aerosol components, using the thermal denuder inlet, the mass spectrum of oxalate was recorded. A solution of 100 pptv oxalic acid (in DI water) was used to produce oxalate aerosols. The aerosol generation scheme described in previous sections

was used here, also the heated inlet described before was used (the temperature of the heater was set at 200° C). The data collected from the aerosol CIMS system for oxalate aerosol is shown in Figure 2.8.

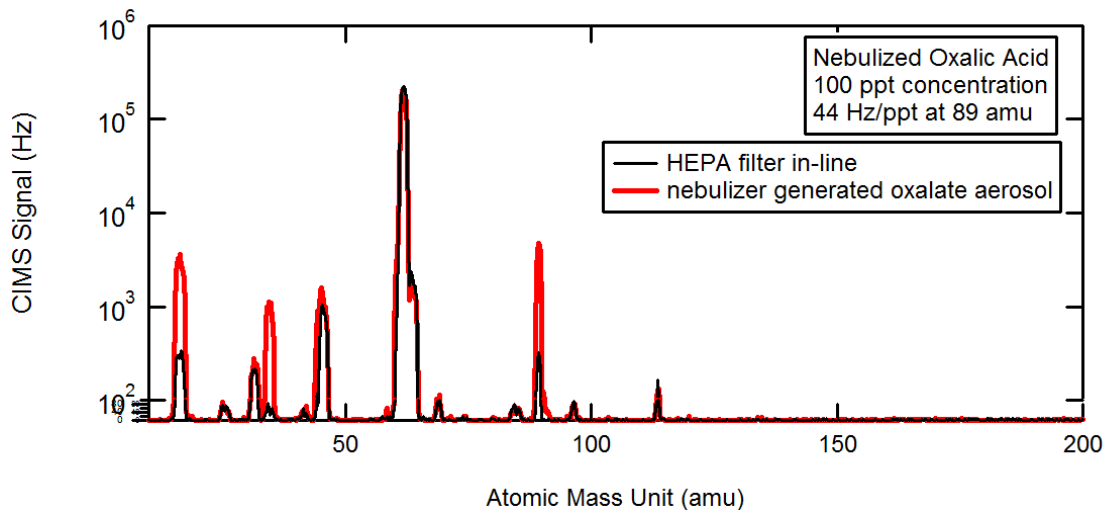


**Figure 2.8:** Mass spectrum of oxalate aerosol (in red) compared with the spectrum of filtered air (in black) is presented in this figure.

The mass spectrum from Figure 2.8 shows that the aerosol CIMS system can be used for measurements of aerosol oxalate in ambient air. Three distinct signals from the oxalate solution are observed at 16, 34 and 89 amu.

## 2.4. Conclusions

The results of sulfate measurements from aerosol CIMS agreed well with that of PILS-IC. In this chapter, the setup and use of a modified aerosol CIMS system for the measurement of aerosol sulfate has been described. This aerosol CIMS setup was proven

to be an effective and sensitive method of measurement of aerosol sulfate. The system can be utilized in laboratory kinetic mechanism experiments or airborne measurements where high sensitivity and fast time response are very important for successful data collection results. Also, with the activation or de-activation of the thermal denuder on the inlet of this system, it can be used to measure aerosol or gaseous sulfuric acid, alternatively.

Additionally, it was shown that the aerosol CIMS system has the potential to be used for the measurement of some aerosol organic acids such as oxalate. Further experiments for the setup and specifications of such system (CIMS for organic acid measurements) would be useful in the future.



## CHAPTER 3

### ARCTAS-2008

#### 3.1. Introduction

Biomass burning events include anthropogenic burning, such as bio-fuel or prescribed burning, and natural fires. Emissions from either type of burning are a significant source for a wide range of atmospheric trace gases and aerosol particles that can have important impacts on biogeochemical cycles, air quality, human health, and direct and indirect effects on the climate through influencing the global radiation budget [Bein *et al.*, 2008; Crutzen *et al.*, 1979; Crutzen and Andreae, 1990; Guyon *et al.*, 2003; Yamasoe *et al.*, 2000]. Because these emissions can persist in the atmosphere for weeks, they may be transported over great distances and have both regional and global impacts [Allen *et al.*, 2004; Duan *et al.*, 2004; Scholes and Andreae, 2000; Dickerson *et al.*, 2002; Honrath *et al.*, 2004; LeCanut *et al.*, 1996; Engling *et al.*, 2006; Fu *et al.*, 2009]. The frequency and intensity of biomass burning incidents and their effects are expected to be amplified in the future due to anticipated increases in global temperatures and alterations in precipitation patterns resulting from climate change [Guinot *et al.*, 2007; Narukawa *et al.*, 1999; Penner *et al.*, 1994; Reddy and Boucher, 2004].

In recent years, many studies have been conducted to clarify the emissions and physicochemical evolution of various trace gases and aerosols from fires (e.g., [Andreae *et al.*, 2001; Decesari *et al.*, 2006]). Using a variety of sampling methods, both laboratory and direct studies of biomass burning have characterized fire emissions in differing environments with various fuels and under diverse burning and meteorological conditions (e.g., [Andreae and Merlet, 2001 and references therein; Cao *et al.*, 2008;

*Haywood et al., 2003; Abel et al., 2003; Iinuma et al., 2007; Lacaux et al., 1995; Ludwig et al., 2003; Schmidl et al., 2008*]). The emission ratio, where the emission of a species of interest is divided by a co-emitted, non-reactive species (e.g., CO or CO<sub>2</sub>), of gases and particles released from fires is one important parameter used to represent fire emissions in model simulations [*Helas et al., 1995; Andreae et al., 2001; Andreae and Merlet, 2001; LeCanut et al., 1996*]. The term emission ratio is used when near the fire, whereas normalized excess mixing ratios are used to describe conditions after the plume has aged [*Yokelson et al., 2009*].

Studying both the direct emissions from fires through measurements close to the burning site, and comparisons with more aged smoke from the same fire to infer chemical evolution, can improve our understanding of the effects of fires on regional and global scales [*Dusek et al., 2005; Falkovich et al., 2005; Formenti et al., 2003; Hoyle et al., 2007*]. The gaseous emissions from biomass burning sources undergo a range of chemical and physical transformations over time ([*Johnson and Miyanishi, 2001*] and references therein). When compared to a relatively non-reactive co-emitted tracer, such as CO, primary gaseous and particulate emissions may be expected to be depleted as the plume ages due to photochemical or physical processes (e.g., differences in deposition mechanisms); whereas secondary trace gases and aerosols may be expected to increase, relative to CO, due to the production of new particle mass. However, many of the secondary gases have reduced vapor pressures and can partition to the aerosol phase resulting instead in the increase of secondary aerosols with plume age and depletion of gas phase components. It has also been proposed [*Grieshop et al., 2009a and 2009b*] that the evaporation of primary aerosol components in the diluting smoke plume may produce

compounds that can subsequently be photo-chemically converted to lower vapor pressure products that also contribute to secondary aerosol mass at the expense of primary aerosol emissions.

In addition to primary aerosol particle emissions from biomass burning, both inorganic and organic secondary aerosol compounds can be produced as smoke plumes age. *Jaffrezo et al.* (1998), using fine aerosol potassium as a biomass burning tracer, found elevated concentrations of secondary compounds such as oxalate and sulfate in central Greenland, which they believed were due to the transport of aged biomass burning plumes from northern Canada. Production of sulfate and nitrate has also been reported in studies of aged biomass burning plumes [*Bein et al., 2008; Formenti et al., 2003*].

There are conflicting research results regarding secondary organic aerosol (SOA) formation following the initial emissions of gases and aerosols from fires. Although laboratory studies suggest secondary organic aerosol formation in biomass-burning plumes should readily occur [*Grieshop et al., 2009a*] the results from ambient data are less clear. Some studies report evidence of SOA formation [*Bein et al., 2008; Clarke et al., 2007; DeCarlo et al., 2008; Engling et al., 2006; Kang et al., 2004; Lee et al., 2005; Lee et al., 2008*]. However, in other cases no or little evidence for SOA formation has been observed in an aging smoke plume [*Capes et al., 2009; DeCarlo et al., 2010*].

The wide range of observations reported in ambient smoke plumes is due to a number of reasons. First, emissions of both gaseous and particulate species can vary widely due to many factors, such as the type of fuel (duff, pine, etc) [*Koppmann et al., 1997*], fuel condition (wet/dry) [*Johnson and Miyonishi, 2001*], meteorological conditions in the burning region and down wind (cloudy/clear sky/RH) [*Hoffa et al.,*

1999], fire temperature [Cofer *et al.*, 1996], combustion phase of the fire [Gao *et al.*, 2003] and the location and distance where the data are collected from the fires [Reid *et al.*, 2005; Trentmann *et al.*, 2003]. Compounding the complexity of the emissions is the mixing of plumes from various regions or even the variability within the region of burning itself, resulting in the mixing of species of various chemical ages that may have burned under different combustion conditions. This mixing can further complicate studies of biomass burning plumes if there are fire emissions, throughout the region where the plumes are being investigated, making emission characterization difficult. Given that organic species comprise most of the smoke aerosol mass, this large variability in emissions from fires can make extracting evidence for SOA formation in a plume difficult [De Gouw and Jimenez, 2009]. The host of physical and chemical processes in the plumes can also further complicate the analysis of changes as the plumes age. For example, coagulation, evaporation of primary species and formation of secondary species may lead to the growth of particles into and out of instrument measurement size ranges.

Fires studied under controlled conditions, such as micro-combustion or the use of pyrolysis devices [Stankiewicz *et al.*, 1998], and introducing smoke into environmental chambers [Johnson and Miyanishi, 2001 and references therein] can eliminate many of these uncertainties. However, this simplifies the complexity of real fires and most experiments cannot simulate the chemical aging of the plumes over extended time periods in a manner similar to what occurs in the atmosphere.

A wide range of smoke plumes and ambient fires were studied as part of the ARCTAS (Arctic Research of the Composition of the Troposphere from Aircraft and

Satellites) study undertaken by the National Aeronautics and Space Administration (NASA). *Jacob et al.* (2010) provide detailed information on the various phases of the study and range of platforms and instrumentation deployed. This paper compares and contrasts measurements of all biomass-burning plumes intercepted by the NASA DC-8 research aircraft during the three phases of the ARCTAS experiment: ARCTAS-A, based out of Fairbanks, Alaska, U.S.A., from April 3 to 19, 2008; ARCTAS-B, based out of Cold Lake, Alberta, Canada; from June 29 to July 13, 2008; and ARCTAS-CARB, based out of Palmdale, California, U.S.A.; from June 18 to 24, 2008. The locations and types of biomass burning smoke plumes recorded during these three phases are shown in Figure 3.1.

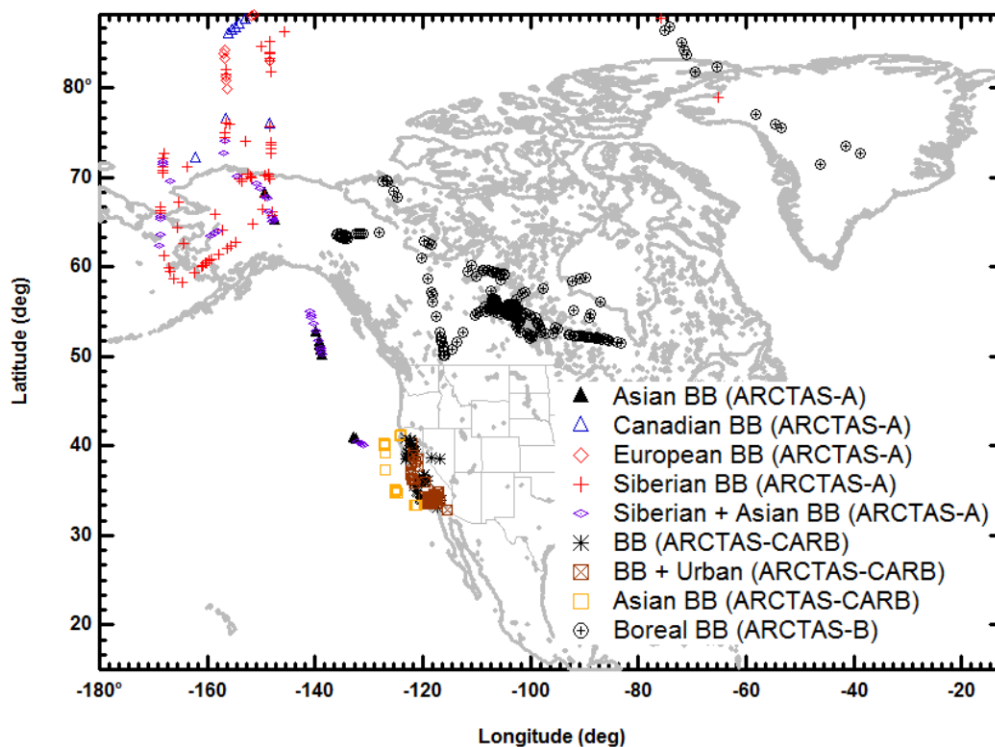


**Figure 3.1: Location of selected biomass burning plumes recorded during the ARCTAS-2008 experiment aboard the DC-8 aircraft. The plumes are identified by source categories**

A statistical summary of plume emission ratios or normalized excess mixing ratios (for species of interest  $X$ ,  $\Delta X/\Delta CO$ ) based on the DC-8 ARCTAS data is provided through contrasting various smoke emissions by broadly separating the plumes into categories according to their source and age (where available). The most extensive analysis of fires in this study was during ARCTAS-B, where smoke plumes from numerous Boreal forest fires were intercepted and aircraft missions were undertaken, specifically to investigate the evolution of smoke from large fires. The ARCTAS-B data set is discussed first to investigate evolution of plumes with age and to provide a basis for comparison with all other plumes intercepted during ARCTAS. During the ARCTAS-

CARB phase of the study, where measurements focused on California emissions, extensive wild fires burning during this period provide a contrast to the Boreal fires of ARCTAS-B, both in the type of material burned and the variety of other atmospheric species present in the burning region (i.e. pristine versus anthropogenic-influenced Californian plumes). In addition, smoke from fires that had been transported great distances and were serendipitously intercepted at various times during the three phases of this study, but most often in the high Arctic during ARCTAS-A, are also included in the analysis. These plumes are compared to the other fire emissions, acknowledging however, that they represent very different classes of plumes due to their origins and the different processes that may have affected them during long transport times (e.g., precipitation scavenging).

## 3.2. Methods

### 3.2.1. Aircraft Measurements

*Jacob et al.* (2010), have provided a complete list of all chemical and physical measurements made aboard the NASA DC-8 during ARCTAS. In this analyses the following aircraft data were used: carbon monoxide (CO), carbon dioxide (CO<sub>2</sub>), acetonitrile (AN), hydrogen cyanide (HCN), toluene (TU), benzene (BZ), oxides of nitrogen (NO<sub>x</sub> and NO<sub>y</sub>), ozone (O<sub>3</sub>), peroxy acetyl nitrate (PAN), methane (CH<sub>4</sub>), PM<sub>1</sub> (particulate matter with aerodynamic diameter less than 1µm) water soluble organic carbon (WSOC), nominally PM<sub>0.7</sub> aerosol chemical components including sulfate (SO<sub>4</sub><sup>2-</sup>), nitrate (NO<sub>3</sub><sup>-</sup>), ammonium (NH<sub>4</sub><sup>+</sup>), organic aerosol (OA), PM<sub>0.4</sub> black carbon mass (BC-Mass) and meteorological data and aircraft position measurements (such as latitude, longitude and altitude). A list of the instruments for each measurement and the

corresponding instrument description references and data collection rate are provided in Table 3.1.

**Table 3.1: Measurements from ARCTAS-2008 aboard the NASA DC-8 aircraft used for the analyses presented in this chapter**

Measurement	Abbreviation	Data Collection Rate	References
Carbon Monoxide Methane	CO CH <sub>4</sub>	1 sec	Sachse et al., 1987; Diskin et al., 2002
Carbon Dioxide	CO <sub>2</sub>	1 sec	Vay et al., 2003
Acetonitrile Toluene Benzene	C <sub>2</sub> H <sub>3</sub> N (AN) C <sub>6</sub> H <sub>5</sub> CH <sub>3</sub> (TU) C <sub>6</sub> H <sub>6</sub> (BZ)	0.5 sec	Wisthaler et al., 2002
Hydrogen Cyanide	HCN	0.5 sec	Crouse et al., 2006; 2009
Oxides of Nitrogen Ozone	NO NO <sub>2</sub> NO <sub>y</sub> O <sub>3</sub>	10 sec	Weinheimer et al., 1994
Peroxyacetyl Nitrate	PAN	10 sec	Slusher et al., 2004
Aerosol Components (Sulfate, Nitrate, Ammonium, Organics)	Aerosol (SO <sub>4</sub> <sup>2-</sup> , NO <sub>3</sub> <sup>-</sup> , NH <sub>4</sub> <sup>+</sup> , Org)	1 sec 10 sec	DeCarlo et al., 2008
Black Carbon Mass	BC_Mass	10 sec	Moteki and Kondo, 2007; 2008
Water Soluble Organic Carbon	WSOC	3 sec	Sullivan et al., 2006

### 3.2.2. Plume Analysis

To synchronize data used in the analysis, timing of all data was checked and adjusted, if necessary, to match that of ambient water vapor (H<sub>2</sub>O<sub>v</sub>) concentrations.



Differences can arise due to errors or drift in individual instrument clocks, lag times in sample transport from inlet to detector, and instrument response time. The data were then averaged to a continuous 10-second timeline to obtain a uniform time-base.

The two main trace gases emitted from biomass burning are CO and CO<sub>2</sub> [Crutzen *et al.*, 1979]. To identify all burning smoke plumes in the ARCTAS data set, all flights were checked for CO and CO<sub>2</sub> peaks. Acetonitrile (AN) and HCN were then used as specific biomass burning tracers to determine if CO and CO<sub>2</sub> enhancements (i.e. CO and CO<sub>2</sub> peaks) were mainly due to biomass burning. If the r values for CO and AN or CO and HCN was higher than 0.6 during the period of enhanced CO and CO<sub>2</sub>, the data (peak) were designated as biomass burning. From this data set, the peaks were initially categorized as ARCTAS-A, ARCTAS-B and ARCTAS-CARB. Further analyses were performed on these peaks to identify the source of the smoke (location of the fire, where available), the approximate transit time from the fire to the measurement, and evaluation of other emissions in the region (e.g., urban) to assess possible mixing of smoke during transport.

### **3.2.3. Identification of Fire Sources**

For all the plumes identified, plume trajectory from fire to measurement point and an estimate of transport age of the identified fire plume, were determined through a combination of back and forward trajectory analyses. Hybrid Single-Particle Lagrangian Integrated Trajectory (Hysplit) analyses (<http://www.arl.noaa.gov/ready/hysplit4.html>) were conducted within each smoke plume, at 10 second intervals, starting from the location where the aircraft first intercepted the plume. These back trajectories were extended to up to 10 days prior to the measurement. The back trajectory analyses (for

each point) were repeated for 3 different altitudes (the altitude where the plume was intercepted +/- 20% of the measurement altitude). Using the Fire Information for Resource Management System (FIRMS) [*Davies et al., 2009; Giglio et al., 2003; Justice et al., 2002*] website, (in cases where the location of the fires were available from this website, mostly during ARCTAS-B and ARCTAS-CARB), a combination of FLEXPART [*Stohl et al., 2005*] and Hysplit were used to predict the plume's trajectory.

#### FLEXPART

([http://www.esrl.noaa.gov/csd/metproducts/flexpart/flexpart\\_interactive/flexpart\\_custom.html](http://www.esrl.noaa.gov/csd/metproducts/flexpart/flexpart_interactive/flexpart_custom.html)) dispersion model runs for up to 6 days were used to locate the potential path of the plume from the fires to their intersection with the DC-8 flight path for each isolated peak. When both analyses (FLEXPART and HYSPLIT) were available, the results were compared and if the general direction of the plume did not agree, the wind direction and speed at the location of the data collection were checked for further verification. These two methods provided similar results in all 498 plumes, with the exception of three cases. As the wind direction and speed did not agree closely with either result in these three cases, these three were excluded from this analysis. The data from 495 biomass burning plumes are presented here.

For the plumes that were intercepted very near specific fires (ARCTAS-B), based on visual verification from the aircraft video files and FIRMS data; wind direction and wind speed, from the aircraft meteorological data, and the location of the fire and plume were used for a better estimation of the transport age. The uncertainties associated with this calculation depend on various factors. The errors associated with the measurements of the meteorological variables (i.e. wind speed and wind direction) were added to the

uncertainties in FIRMS fire data location reports. The uncertainties of transport age for ARCTAS-B were calculated to be approximately 10%. However, it is important to note that this value is less when closer to the fires (as visual verification is possible) and it increases further away from the biomass burning sources as our inability for visual verification increases the level of uncertainty.

In some cases, especially in the ARCTAS-CARB portion of the experiment, the fire plumes intercepted were either from air masses that had been emitted within or advected over somewhat rural regions with minor anthropogenic influence, whereas other plumes were transported over regions heavily impacted by anthropogenic emissions (i.e. urban emissions). These two types of cases were separated by inspecting and comparing the trajectories of the smoke plumes and trajectories of the urban emissions. If these trajectories intersected prior to the measurement, these plumes were categorized into a different class (ARCTAS-CARB BB + Urban).

Overall, 495 aircraft intersects with biomass burning plumes from ARCTAS-A, ARCTAS-B and ARCTAS-CARB were isolated from the seventeen DC-8 flights performed during this study. The plumes were separated into nine different categories based on source and mixing with urban emissions. For some fires, there were multiple transects through what appeared to be the same smoke plume at different times and downwind distances (e.g., Boreal forest fires in Canada, ARCTAS-B). The evolution of these plumes are investigated in detail first, and they are grouped into one general category (e.g., Boreal fires) for overall comparisons with plumes from other sources. A list and description of each plume category is presented in Table 3.2.

**Table 3.2: Abbreviations and descriptions of plume categories selected during the ARCTAS-2008 study**

<b>Plume Abbreviations</b>	<b>Plume Description</b>
<u><i>BB CARB</i></u>	Biomass burning plumes from California wildfires
<u><i>BB CARB + Urban</i></u>	Mixed California urban plumes and biomass burning plumes from California wildfires
<u><i>Asian BB (CARB)</i></u>	Mixed Asian biomass burning plumes and biomass burning plumes from California wildfires
<u><i>Siberian BB (ARCTAS-A)</i></u>	Siberian biomass burning plumes over the Arctic
<u><i>Asian BB (ARCTAS-A)</i></u>	Asian biomass burning plumes over the Arctic
<u><i>European BB (ARCTAS-A)</i></u>	Mixed European urban plumes and biomass burning plumes over the Arctic
<u><i>Canadian BB (ARCTAS-A)</i></u>	Canadian biomass burning plumes over the Arctic
<u><i>Siberian + Asian BB (ARCTAS-A)</i></u>	Mixed Asian and Siberian biomass burning plumes over the Arctic
<u><i>Boreal forest fire BB ARCTAS-B</i></u>	Biomass burning plumes from Canadian wildfires

The location of each plume discussed in this paper is shown in Figure 3.1. The data presented in this figure are from all 495 plumes and the type and category of each plume are displayed in the Figure 3.1 legend.

### **3.2.4. Data Processing and Analysis**

For each smoke plume identified, a normalized excess mixing ratio was determined relative to CO (i.e.,  $\Delta X/\Delta \text{CO}$ ) for all gaseous and aerosol components of interest (see Table 3.1 for a list of variables used in this analysis). CO has been previously used as an inert tracer for biomass burning and other emissions [e.g., *Sullivan*

*et al., 2006; Yokelson et al., 2008*]. All biomass-burning events emit CO and its slow chemical loss relative to time scales investigated here makes CO an appropriate compound to use as an inert tracer (lifetime of CO in the atmosphere ranges between 1-4 months [*Seinfeld and Pandis, 1998*]). Normalized excess mixing ratios were determined in two ways; from the slope of a linear regression fit, or by using the mean plume concentration (area under the curve of concentration values versus time within the plume) and subtraction of background concentrations. The two methods generally agreed when the component of interest (X) and CO were well correlated ( $r > 0.6$ ). When the correlation coefficient was smaller ( $r < 0.6$ ), the area under the curve was used to determine the ratio. In this case the enhancement in the concentration of each species ( $\Delta X$ ) and CO ( $\Delta CO$ ) were calculated by subtracting the in-plume enhancement of the data (i.e. the area under the peak) from the background values of X and CO, respectively. The background values considered for this analysis were the concentration of the species of interest measured immediately outside of the plume under consideration.

Averaging the data for each species over a 10 second time period minimizes some differences between instrument response times (i.e. reduces time smearing). However, this was still a concern when data were collected close to the fires where plumes could be extremely narrow, resulting from short plume widths and fast aircraft speed (the typical range of speed for the NASA DC-8 was 500-850 km h<sup>-1</sup> for an altitude range of 1.5-12 km). For species (such as WSOC) susceptible to time smearing, the correlation was generally poor and so the area under the peak was used in order to further reduce the effects of instrument response time.

Once the plumes were identified,  $\Delta X/\Delta CO$  values were calculated. Then, the sources and approximate plume ages were used to categorize the plumes and the statistics of each species ( $\Delta X/\Delta CO$ ) were determined. The transport time and development of the identified fires from Canadian Boreal fires were compared for evidence of possible evolution of the chemical properties as the smoke aged (Figures 3.2a to 3.2o). A statistical analysis is used to compare different species in all ARCTAS smoke plumes for an overview of fire emission properties from different sources.

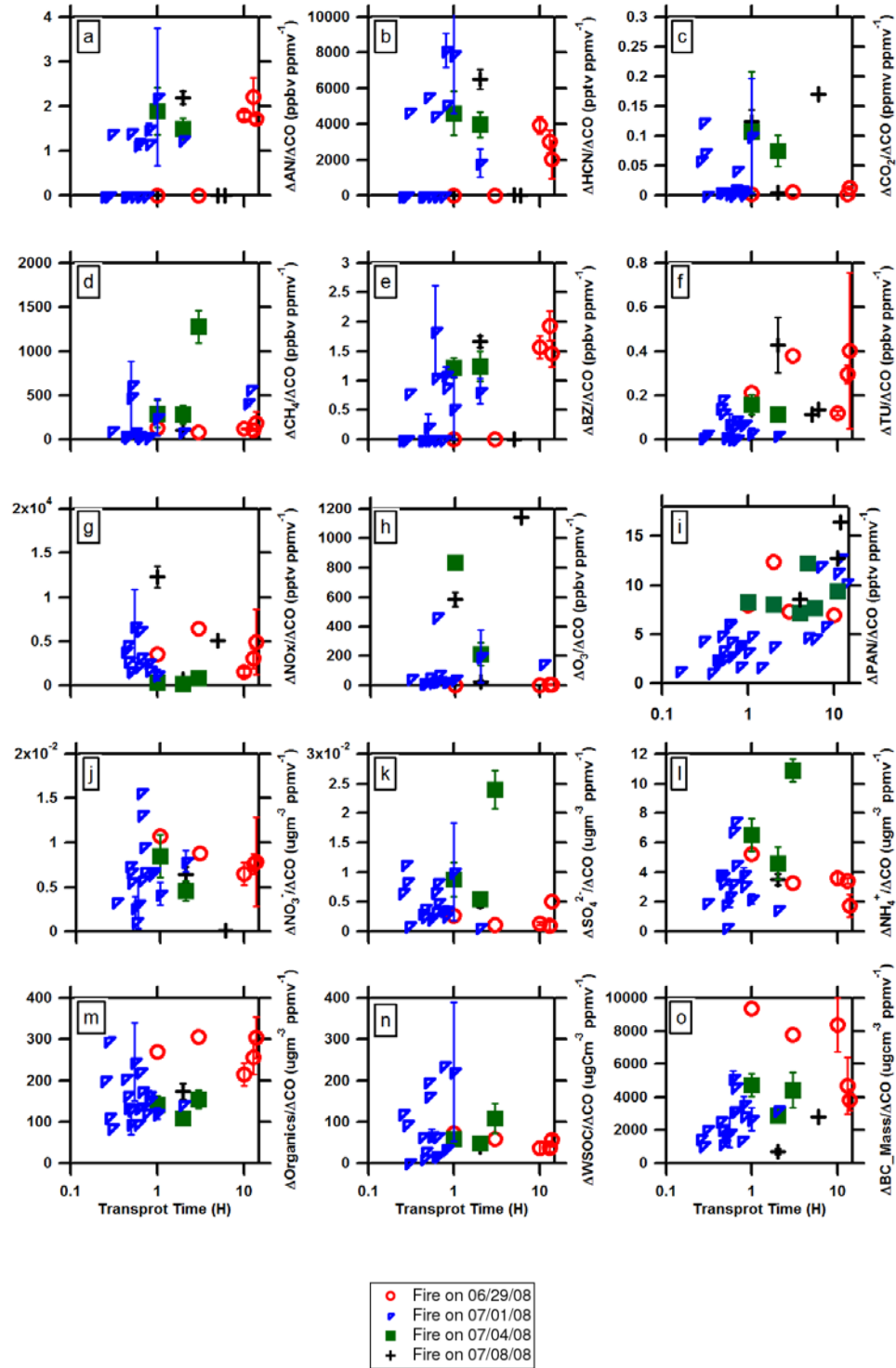


**Figure 3.2: Evolution of emission ratios for trace-gas and aerosol chemical components in four large boreal forest fires detected during ARCTAS-B. Specific fires are identified by date on which they were intercepted (month/day/year). For cases where transport times were within  $\pm 10\%$  for a fire measured on a given day, the mean normalized excess mixing ratio is given and the data range shown as error bar of  $\pm 1$  standard deviation**

### **3.3. Analysis Complications and Simplifications**

#### **3.3.1. Detailed Segregation vs. Counting Statistics**

The 495 plumes analyzed in this study were segregated by fire location, (which is likely related to the type of material burned) and mixing with other emissions (e.g., urban + biomass burning). The result of this categorization is that some groups are comprised of fewer plumes, making the statistical analysis weak. However, the advantage of better comparison between different plumes is thought to override this shortcoming. The number of plumes in each grouping for each species is listed in the figures (Figure 5a to 5o).

#### **3.3.2. Transport Age vs. Photochemical Age**

In the analysis of plume age for the Canadian biomass burning plumes, transport age is calculated (i.e. time elapsed from when emitted to when measured), which is different from the photochemical age of the plume. These two times may differ due to the time of day when the smoke was emitted and when the plume was intercepted by the aircraft, (e.g., early or late in the day, etc), or the meteorological conditions in the region (cloudy/clear sky). No suitable species emitted in the fires were measured in the time resolution used in this analysis for estimating photochemical age; so only transport age is considered. This adds some degree of ambiguity when comparing plumes of various ages for evidence of chemical evolution.

#### **3.3.3. Mixing of Various Emissions into Single Smoke Plumes**

Identifying the source of a plume, either visually when close to the fire or based on back trajectories, and assuming this source is representative of a specific fire, is



somewhat uncertain for a number of reasons. First, even within a single region of burning there could be significant differences in material burned and burning conditions. This was visually observed in the Boreal fires (ARCTAS-B) as emissions of white and black smoke mixing within a single plume. Second, as the plume moves away from the fire, other smaller nearby fires may add fresh emissions to the plume, mixing in smoke of different ages and possibly emission characteristics. Evidence of such events was observed in the Boreal fires of ARCTAS-B, also. Because of the averaging approach used in this analysis, these issues add uncertainty and likely some scatter to the calculated normalized excess mixing ratios.

#### **3.3.4. Different Loss Processes of Species Relative to CO**

Accounting for dilution of both trace gas and aerosol particle emissions by normalizing to CO assumes that dilution is the main loss process leading to the loss of primary emissions as the plume moves away from the fire. This is not the case if the species in the plume experience significant dry or wet deposition losses. For example, hydrophilic trace gases or particles are likely to be much more efficiently lost in wet scavenging events compared to CO or other hydrophobic species. Model studies have also shown that normalized excess mixing ratios calculated for diluting plumes can depend on background concentrations [Mckeen *et al.*, 1996]. This effect is most prominent when the difference between in-plume and background concentrations is low, either due to a very diffuse plume and/or for species with high background concentrations (e.g., CO<sub>2</sub>). Both of these effects are not considered here, but should mostly affect the more aged plumes.

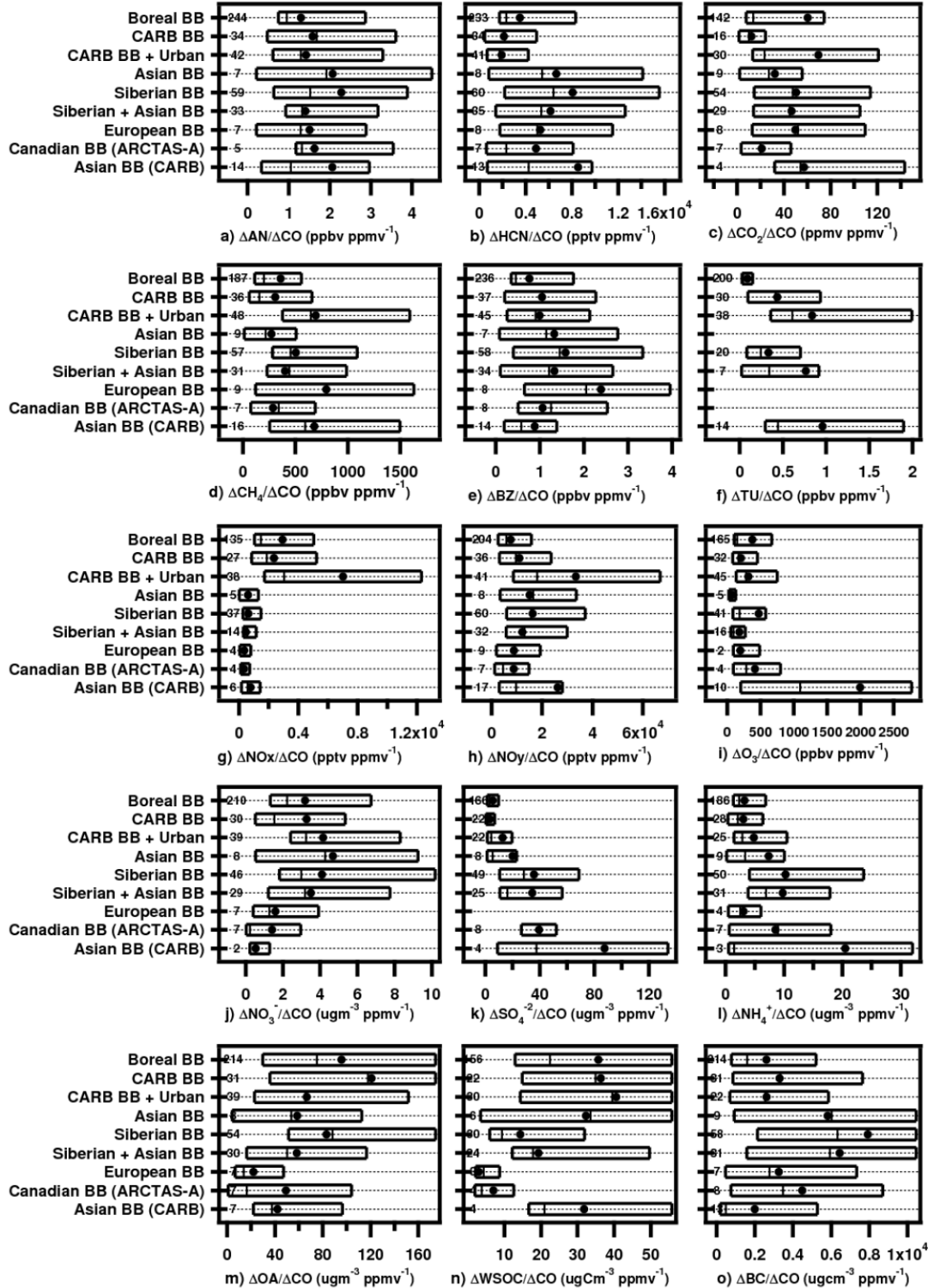
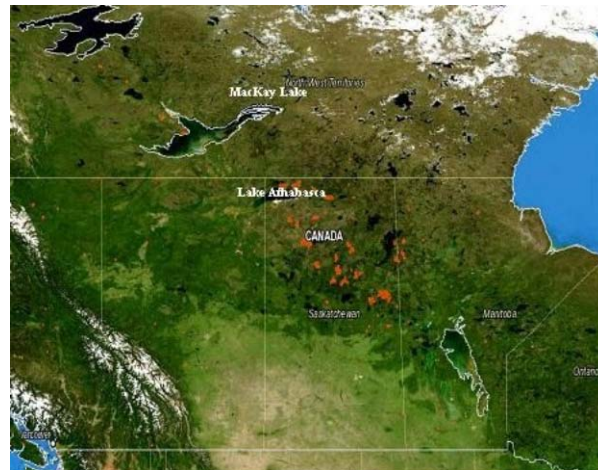


Figure 3.3: Comparison of Median (25th and 75th %-ile and mean) for various trace gas and aerosol components in all biomass burning plumes intercepted by the NASA DC-8 during ARCTAS-A, ARCTAS-B and ARCTAS-CARB. Numbers inside the graphs represent the number of points present in each category

## 3.4. Results

### 3.4.1. Canadian Boreal Forest Fires

During the second phase of ARCTAS, smoke plumes from many active Boreal fires in Northwestern Canada were investigated. Figure 3.4 shows the locations of all active fires in this region during ARCTAS-B. The most substantial fires were located near Lake Athabasca (59.27, -109.45) and Mackay Lake (63.94, -111.16) and were extensively sampled during flights on July 1 and 4, 2008, respectively. The average altitude where the Boreal plumes of ARCTAS-B were intercepted was approximately  $3600 \pm 2700$  m (asl) and ranged between 700 m (asl) close to the fires, to about 3000 m (asl) further downwind.



**Figure 3.4: A cumulative representation of observed boreal fires during the period of June 29 to July 10, 2008 (ARCTAS-B), from FIRMS website**

To investigate the evolution of various gaseous species and secondary aerosol formation in Boreal fires as a function of plume age, in detail, smoke plumes from four distinct ARCTAS-B fires were investigated. These fires were encountered during four different dates (06/29/08, 07/01/08, 07/04/08 and 07/08/08). Figures 3.2a to 3.2o show the normalized excess mixing ratios (i.e.  $\Delta X/\Delta CO$ ) for each of these fires as a function of plume age; with time scales varying from less than approximately 30 minutes since emission, to plumes with estimated transport times of 10 hours encountered some distance down wind of the fires.

Figures 3.2a and 3.2b show changes in AN and HCN concentrations relative to CO versus transport age, in these Boreal fire plumes. There tend to be two groups of data; there are plumes with low levels of AN and HCN (especially for the plumes encountered on 07/01/08) and ones with higher levels of HCN and AN relative to CO. In either case, transport age did not seem to have a significant affect on the concentrations of these species, consistent with the long lifetimes of these tow compounds in the atmosphere. The high and low values encountered from the same fire, or between different fires, may be indicative of differences in emissions, even within the same fire (i.e. the edge of fire may have a lower temperature and thus different emissions than the center of the fire) [e.g., *Maleknia et al., 2009*]. This may be more pronounced in larger fires such as the one encountered on 07/01/08. Similar trends are observed for CO<sub>2</sub> and CH<sub>4</sub> (Figures 3.2c and 3.2d), which are also stable compounds on these time scales, thus indicating variability in fire emissions.

Benzene and toluene enhancements relative to CO ranged from 0.01 to 2.2 ppbv ppmv<sup>-1</sup> and 0.001 to 0.5 ppbv ppmv<sup>-1</sup>, respectively (Figures 3.2e and 3.2f). The trend of

changes in the normalized emission mixing ratios (NEMR) of these two compounds is similar to the other stable species. The variation in benzene NEMR is most similar to AN.

There was also no clear trend in the evolution of  $\text{NO}_x$  and  $\text{O}_3$  relative to CO (Figures 3.2g and 3.2h). However, peroxyacetyl nitrate (PAN) concentrations increased as the plumes aged (Figure 3.2i). Elevated concentrations of PAN may explain the lack of net  $\text{O}_3$  production in the aged plumes. The production of  $\text{O}_3$  in biomass burning plumes is limited by the availability of  $\text{NO}_x$ . The increase in the NEMR of PAN shows evidence of  $\text{NO}_x$  conversion to PAN which has a lifetime of weeks in the lower temperatures in the Arctic [Finlayson-Pitts and Pitts, 1999], thus even though no net  $\text{O}_3$  production is observed within the timeline of the aging of the plumes discussed here (i.e. 10 hours), it is possible that further downwind of the fires due to the thermal decomposition and photolysis of PAN more  $\text{NO}_x$  is made available and  $\text{O}_3$  is produced. Mauzerall *et al.*, (1998) observed similar enhancements of PAN in the biomass burning plumes over the tropical South Atlantic; additionally, they observed conversion of PAN to  $\text{HNO}_3$  in the course of a week. Concentrations of ozone relative to CO were mostly low, with a few plume intercepts occurring on three of the four days where ratios were high. These infrequent high ozone episodes were not associated with unusually high enhancements of other species, either trace gas or aerosol chemical components.

Inorganic aerosol components (nitrate, sulfate and ammonium; Figures 3.2j, 3.2k and 3.2l, respectively) also show no clear trend. Nitrate relative to CO is fairly uniform after approximately 0.6 hrs; prior to that it is somewhat lower. Sulfate does not show this trend and ammonium, although more scattered, is somewhat similar to nitrate. This is expected since ammonium is likely to be associated mostly with the aerosol nitrate and

sulfate and so should reflect the combined trends of both these inorganic species. For sulfate, high values recorded near the fires on 07/01/08 contribute a great deal to the scatter in the early stages of the plume transport, and reduce the validity of a clear increasing trend. This could be due to differences in smoke emissions from different areas (locations) of the same fire, as seen from the HCN and AN data in Figures 3.2a and 3.2b. The same numbers of data points are not available for nitrate and ammonium from 0.2 to 0.4 hours as sulfate, and this may have contributed to the more suggestive trend for these species.

The concentrations of organic aerosol and WSOC are shown in Figures 3.2m and 3.2n. Again, no trend is observed; which may be due to the high degree of scatter, including values near the fires on 07/01/08. The lack of evidence for SOA formation relative to CO in these fires may be due to a number of factors in addition to variability in emissions. For example, variability in secondary formation processes due to dependence on a host of other factors (T, RH) and the fact that a significant fraction of OA and WSOC are composed of primary emissions (e.g., carbohydrates). The NEMR values for WSOC show more variability when compared to OA. Differences in measurement methods may account for some of this variability, or that WSOC is comprised of a smaller subset of compounds, and these may be more variable in nature. One example would be SOA; if more highly variable, WSOC would be expected to also fluctuate more than OA. Additionally, the increasing trend in PAN NEMR provides evidence for lack of available  $\text{NO}_x$  species. This can hamper the production of  $\text{O}_3$  (Figure 3.2h) and thus result in lower concentrations of the hydroxyl radical (OH). The lack of high concentrations of oxidizing species (i.e.  $\text{O}_3$  and OH) can cause a delay in the oxidation of VOC-s as they

are emitted by the fires, which in turn can affect their solubility and thus the production of SOA. *Cubison et al.*, (2010) have shown that the organic aerosols become more oxidized as they age in these fires. This can be explained through the possible self reaction of compounds such as methylglyoxal and glyoxal in the aqueous phase as the aerosol droplet evaporates [De Haan et al., 2009b] after the initial emissions of primary organic aerosols from the fires.

Black carbon NEMR values ( $\Delta\text{BC\_Mass}/\Delta\text{CO}$ ) varied between roughly 2000 and 10000  $\mu\text{g cm}^{-3} \text{ppmv}^{-1}$  among these four fires (Figure 3.2o). Although as a primary emission, no increasing trend with age is expected, of all the species investigated, BC shows a trend.

Plume temperature and RH were investigated for possible trends.

Temperatures of all the plumes were similar with a standard deviation of 10°K and the RH varied by 12% in plumes. No significant correlations between RH and/or temperature with the changes in NEMR of any of the species investigated here were observed. Overall, the results show that for these fires, processes leading to changes in mass concentrations were minor relative to variability in emissions.

### **3.4.2. Comparison of NEMRs for All Biomass Burning Categories**

In the following analysis, results from all fires encountered during the ARCTAS missions are compared. This includes the Boreal fires recorded in Northern Canada during ARCTAS-B and discussed above, smoke plumes from springtime measurements in the Arctic (ARCTAS-A), and plumes encountered over California (ARCTAS-CARB). Although recorded in the high Arctic, practically all plumes from ARCTAS-A were from fires from other regions that had undergone long range transport. For ARCTAS-CARB,

most of the plumes originated from local fires, however there were a few cases of smoke transported from other regions. ARCTAS-B was exclusively from Boreal fires in the region of the measurements.

During ARCTAS-A, flights were conducted over the Arctic from April 3 to 19 2008. Air masses over the Arctic appeared to be broadly influenced by biomass burning emissions [Fisher *et al.*, 2010]. This was evident in the elevated HCN levels recorded throughout the ARCTAS-A study period. Frequent biomass burning plumes were encountered over a wide region, as shown in Figure 1, and generally at altitudes of  $\sim 5200 \pm 800$  meters asl. Using HYSPLIT and FLEXPART, these biomass-burning plumes were separated into five categories based on their origin of emission. Most of the emissions were from Southern Russia (Siberian), Western China (Asian) or a mixture of both (Siberian-Asian), with a few plumes traced back to European fires. European plumes were also likely influenced by some urban emissions from cities near the burning areas. The final type of plume encountered in this region originated from a few fires in Canada (Canadian-BB-ARCTAS-A). Note that the number of plumes from each category is included on the bar graphs (Figures 3.3a to 3.3o).

Fire emissions over and around the Los Angeles Basin were investigated during four NASA DC-8 flights on 18, 20, 22 and 24 of June 2008. Also, at the end of Canada (ARCTAS-B) - to - California transit flight (13 July 2008), some California fire plumes were intercepted and are included in this analysis. The location of all California plumes are shown in Figure 1, and the location of all fires burning in California and the Western U.S. during the ARCTAS-CARB sampling period are shown in Figure 3.5. The average



altitude of the plumes encountered for the Californian fires studied were  $1500 \pm 700$  meters asl.

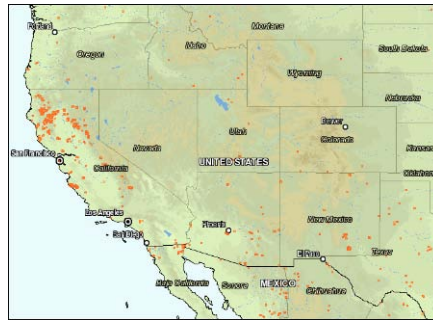


**Figure 3.5: A cumulative representation of the fires in California from 18 June 24 June 2008**

The California fire plumes were further separated into plumes that were influenced by urban emissions and ones that were not. Note that even for the plumes that are categorized as not influenced by urban emissions, there was always evidence for some urban influence (especially for the aged plumes); however, this influence was not as significant as the group defined here as urban-influenced. This separation is consistent with trends in urban tracers. For example, the coefficient of variation ( $r^2$ ) between CO and toluene for biomass burning plumes with urban emission influence was 0.62, whereas biomass burning plumes, which were categorized as not significantly mixed with urban emissions, had coefficients of variation of 0.27. According to HYSPLIT back trajectories, these plumes traveled over areas that were less directly influenced by the

large urban centers near the data collection area (e.g., Los Angeles, Sacramento, San Francisco and San Diego).

Analysis of variance (ANOVA) with Tukey's multiple range test was used to compare the significance of the differences between the means of all species in different categories. ANOVA has been previously used in many environmental and atmospheric studies to evaluate the variance of mean between multiple categories of samples (e.g., [Zhang *et al.* 1994; Gustin *et al.*, 1996; Viskari *et al.*, 2000]). The results from this analysis are shown in Table 3.3. Based on  $\alpha=0.05$ , all compounds show a significant difference between the means of different categories except AN, where  $p=0.23 \geq 0.05$  and WSOC where  $p=0.42 \geq 0.05$ . These differences and similarities are further discussed in the following sections.

**Table 3.3: Results of ANOVA analysis for the differences in means of different species in categorized plumes**

Chemical or Aerosol Species	P Value
AN	0.23
BZ	1.4 E -5
CH <sub>4</sub>	3.4 E -7
CO <sub>2</sub>	0.017
HCN	3.1 E -10
NH <sub>4</sub> <sup>+</sup>	4.0 E -17
NO <sub>x</sub>	4.2 E -6
NO <sub>y</sub>	1.9 E -20
NO <sub>3</sub> <sup>-</sup>	2.2 E -9
O <sub>3</sub>	8.9 E -11
Organic Aerosols	9.1 E -13
SO <sub>4</sub> <sup>2-</sup>	1.8 E -16
TU	0.014
WSOC	0.42

Figures 3.3a through 3.3o compare the normalized excess mixing ratios (NEMR) between all plumes and the results discussed next.

3.4.2.1.  $\Delta AN/\Delta CO$  and  $\Delta HCN/\Delta CO$  (Figures 3.3a and 3.3b)

Acetonitrile (AN) and hydrogen cyanide (HCN) are used as biomass burning markers and so expected to vary little with plume age, and ideally not vary widely between types of fires. Figure 3.3a shows the range of AN NEMR and Figure 3.3b presents the range of NEMR for HCN in each plume category. The overall range for AN was approximately 0.1-5 ppbv ppmv<sup>-1</sup> (relative to CO). *Grieshop et al. (2009a)*, recorded  $\Delta AN/\Delta CO$  levels

of 0.1-0.8 ppbv ppmv<sup>-1</sup> in biomass burning simulated chamber studies. *Warneke et al.* (2008) reported an average of 3.1 ppbv ppmv<sup>-1</sup> for agricultural, 2.1 ppbv ppmv<sup>-1</sup> for fires from Lake Baikal and 2.4 ppbv ppmv<sup>-1</sup> from Canadian Boreal forest fires. These values are consistent with the range of the median values for all the fires that were encountered during ARCTAS (1-2 ppbv ppmv<sup>-1</sup>).  $\Delta\text{HCN}/\Delta\text{CO}$  data were more variable than  $\Delta\text{AN}/\Delta\text{CO}$ , with significantly lower values for the California fire plumes with mean and medians near 2 pptv ppmv<sup>-1</sup> compared to ranges of 5 to 9 2 pptv ppmv<sup>-1</sup> for all other plume categories. This may also be due to the possible presence of other sources of HCN in the Asian and Siberian plumes.

#### 3.4.2.2. $\Delta\text{CO}_2/\Delta\text{CO}$ and $\Delta\text{CH}_4/\Delta\text{CO}$ (Figures 3.3c and 3.3d)

$\Delta\text{CO}_2/\Delta\text{CO}$  ratios were typically less than roughly 50 to 60 ppmv ppmv<sup>-1</sup>, but in some cases the distributions were skewed towards higher ratios, such as the Boreal fires of ARCTAS-B. The highest  $\Delta\text{CO}_2/\Delta\text{CO}$  ratios were recorded in Asian biomass burning plumes. Normalized excess mixing ratios of methane span a large range from near zero to roughly 1800 ppbv ppmv<sup>-1</sup> with generally higher values in the biomass burning plumes that were influenced by urban emissions (e.g., ARCTAS-CARB-Urban, European BB and Asian BB (ARCTAS-CARB)).

#### 3.4.2.3. $\Delta\text{BZ}/\Delta\text{CO}$ and $\Delta\text{TU}/\Delta\text{CO}$ (Figures 3.3e and 3.3f)

The  $\Delta\text{BZ}/\Delta\text{CO}$  levels in all the plumes were very similar (means typically between 1 and 1.5 pptv ppbv<sup>-1</sup>) except for the plumes that originated from Europe. These plumes contained about twice as much  $\Delta\text{BZ}/\Delta\text{CO}$ . Overall,  $\Delta\text{BZ}/\Delta\text{CO}$  ratios in this study

were similar to those of *Grieshop et al.* (2009a) (0.1-4.3 ppbv ppmv<sup>-1</sup>) and *Warneke et al.* (2008) (1.1-1.3 pptv ppbv<sup>-1</sup>).

Toluene normalized excess mixing ratios were generally less than roughly 1 ppbv ppmv<sup>-1</sup>. *Grieshop et al.* (2009a) reported a range of 0-1.1 ppbv ppmv<sup>-1</sup> of  $\Delta\text{TU}/\Delta\text{CO}$  in their laboratory studies. *Warneke et al.* (2008) reported 0.15 pptv ppbv<sup>-1</sup> of  $\Delta\text{TU}/\Delta\text{CO}$  for agricultural fires and 0.2 pptv ppbv<sup>-1</sup> of  $\Delta\text{TU}/\Delta\text{CO}$  for fires near Lake Baikal and Canada. The largest increase in  $\Delta\text{TU}/\Delta\text{CO}$  levels were in the ARCTAS-CARB biomass burning plumes that were mixed with urban ones. This may be due to the mixing of vehicle exhaust emissions with the biomass burning plumes from the urban areas. Typical urban normalized excess mixing ratios for  $\Delta\text{TU}/\Delta\text{CO}$  are 0.81 – 3.07 ppbv ppmv<sup>-1</sup> [*de Guow and Warneke, 2007*] considerably higher than what was recorded in the pure fires. *Muhle et al.* (2007) also report elevated levels (~ 2 ppb) of toluene in ambient air masses that were influence by forest fires in California. The Asian biomass burning plumes that were intercepted near the coast of California also showed slightly higher ratios of  $\Delta\text{TU}/\Delta\text{CO}$ , which may be due to the mixing of these plumes with urban or ship emissions in this area [*Wang et al., 2006*]. For  $\Delta\text{TU}/\Delta\text{CO}$  a number of plume categories are not shown because data were not available for all plume intersects.

#### 3.4.2.4. $\Delta\text{NO}_x/\Delta\text{CO}$ , $\Delta\text{NO}_y/\Delta\text{CO}$ and $\Delta\text{O}_3/\Delta\text{CO}$ (Figures 3.3g, 3.3h and 3.3i)

$\Delta\text{NO}_x/\Delta\text{CO}$  levels were clearly highest in the Boreal and California fires (ARCTAS-B and ARCTAS-CARB) compared to all others that were associated with long-range transport.  $\text{NO}_x$  is expected to be depleted relative to CO as the smoke plumes age and as  $\text{NO}_x$  is converted to other compounds (e.g., PAN) over time, thus this may just

reflect differences in plume ages (although no age trends were observed for times scales less than roughly 10 hours, discussed in previous sections). As the Siberian, European and Asian plumes were subject to long-range transport, the low levels of  $\text{NO}_x$  in these plumes are to be expected.

In contrast,  $\Delta\text{NO}_y/\Delta\text{CO}$  was fairly similar in all plumes. The ARCTAS-CARB BB mixed with urban emissions had a few  $\text{NO}_x$  and  $\text{NO}_y$  concentrations relative to CO that were much higher than all other categories, skewing these distributions to much higher ratios.

For  $\Delta\text{O}_3/\Delta\text{CO}$  ratios, a number of trends were observed. In the California biomass-burning plumes that were mixed with urban emissions, ozone ratios were often (but not always) higher than the biomass plumes not mixed with urban emissions. Some studies have reported greatly enhanced  $\text{O}_3$  when fire and urban emissions interact [*Lee et al., 2008*]; there was no strong evidence for that in this data set. Asian BB (ARCTAS-CARB) plumes encountered near the coast of California often had significantly higher  $\text{O}_3$  ratios, possibly due to mixing with nearby ship plumes, as confirmed by the toluene data. *Chen and Griffin (2005)* also reported the observation of  $\text{O}_3$  enhancement in this area, due to ship plumes, in an earlier aircraft study.

#### 3.4.2.5. $\Delta\text{NO}_3^-/\Delta\text{CO}$ , $\Delta\text{SO}_4^{2-}/\Delta\text{CO}$ and $\Delta\text{NH}_4^+/\Delta\text{CO}$ (Figures 3.3j, 3.3k and 3.3l)

Highest  $\text{NO}_3^-$  levels relative to CO were generally observed in ARCTAS-CARB biomass burning plumes that were mixed with urban emissions. The lowest levels were recorded in Asian BB along the coast of California, the region of highest  $\text{O}_3$  NEMR levels.  $\text{NO}_3^-$  normalized excess mixing ratios were similar in the Asian, Siberian, and mixed Asian-Siberian plumes, but often lower in the European and Canadian fires

observed in the Arctic during ARCTAS-A (the Asian-CARB fires consisted of only two plumes and so are not considered). Relative to CO, fine particle nitrate loss due to volatility or precipitation scavenging during transport may account for some of the lower ratios in the long-range transport categories. Generally the overall trends between source categories were somewhat similar for  $\Delta\text{NO}_y/\Delta\text{CO}$  and  $\Delta\text{NO}_3^-/\Delta\text{CO}$ , whereas  $\Delta\text{NO}_x/\Delta\text{CO}$  was different.

For sulfate, lowest ratios relative to CO for all plume sources were observed in the Boreal fires and California fires (not influenced by urban sources). Curiously, the Canadian fires recorded in ARCTAS-A had significantly higher levels of sulfate relative to CO. Some studies have shown emission of  $\text{SO}_2$  from biomass burning sources (e.g., Smith et al., 2001). Huey et al. (2010) report higher emissions of  $\text{SO}_2$  in the Canadian Boreal fires which may account for the higher sulfate levels after the plumes have been processed for some time. The most obvious feature of the sulfate data is the much higher normalized excess mixing ratios in plumes subjected to long range transport. Note that this is the opposite trend to that of  $\Delta\text{NO}_3^-/\Delta\text{CO}$ . Contributions from anthropogenic  $\text{SO}_2$  emissions in the regions of the fires may be one reason. Fine particle sulfate production in Asian anthropogenic plumes advecting to North America is well documented (e.g., [van Donkelaar et al., 2008; Peltier et al., 2007a]) and thought to be due to the conversion of a large reservoir of  $\text{SO}_2$  to non-volatile sulfate aerosol, which is not significantly depleted by any precipitation scavenging on route. For this study, highest sulfate normalized excess mixing ratios were observed in the Asian plumes intercepted near the coast of California, possibly in part due to influence by ship emissions along the

California coast. *Capaldo et al.* (1999) reported that as ships are the dominant source of SO<sub>2</sub> in this area they might contribute significantly to the production of sulfate aerosols.

$\Delta\text{NH}_4^+/\Delta\text{CO}$  levels were similar in Boreal and California fire plumes and higher in the California fire plumes that were influenced by urban emissions. For the plumes subject to long-range transport,  $\Delta\text{NH}_4^+/\Delta\text{CO}$  variability between sources followed that of  $\Delta\text{SO}_4^{2-}/\Delta\text{CO}$ , as expected.

#### 3.4.2.6. $\Delta\text{OA}/\Delta\text{CO}$ and $\Delta\text{WSOC}/\Delta\text{CO}$ (Figures 3.3m and 3.3n)

Organic species are the largest chemical components in fine particulate matter in smoke, and secondary formation may significantly enhance aerosol mass with plume age, however, no evidence for this was observed in the ARCTAS-B Boreal fire plumes. The emission data have wide and overlapping variability in each transport age group, likely due to the issues discussed in previous sections. Also, the low NO<sub>x</sub> regime (as evidenced by the increasing PAN NEMR) may have contributed to the lack of SOA formation.

The Boreal and California fire plumes had similar levels of OA and WSOC. However, for the California biomass burning plumes that were influenced by urban emissions, there were slightly higher levels of WSOC NEMR and on average lower levels of OA NEMR when compared to the non-urban influenced and Boreal plumes. Often, the OA and WSOC normalized excess mixing ratios in plumes transported over larger distances were lower compared to smoke plumes encountered closer to the sources of fire (ARCTAS-B and CARB). In this regard, the behavior of these organic components is more similar to that of nitrate and not sulfate. It is also similar to the preferential loss of fine particle OA or WSOC relative to sulfate that has been observed in Asian plumes advected to North America [*van Donkelaar et al., 2008; Peltier et al.,*



2007a]. In those cases it was proposed that SOA was not regenerated in route, as sulfate could be, following precipitation-scavenging losses. Similar processes may be at work in these smoke plumes.

#### 3.4.2.7. $\Delta BC/\Delta CO$ (Figures 3.3o)

Higher levels of  $\Delta BC/\Delta CO$  are observed in most of the plumes that were subject to long-range transport during ARCTAS-A. In this case the highest levels are seen in Asian and Siberian plumes. Encountered during ARCTAS-A, these plumes, on average, contain twice as much  $\Delta BC/\Delta CO$  as the ARCTAS-B and ARCTAS-CARB plumes. This may be a result of biomass burning and anthropogenic emissions in the same general region rather than due to the differences from the fire emissions themselves.

### **3.5. Conclusions**

Data from over 495 biomass-burning plumes from the different phases of the ARCTAS-2008 study (ARCTAS-A, ARCTAS-B and ARCTAS-CARB) have been collected and analyzed. These plumes were separated into 9 different categories (Table 3.2), based on their location and origin. Many different measurements on the chemical and physical properties of these plumes were carried out on board the NASA DC-8 aircraft. 16 different chemical and aerosol compounds have been investigated and compared for each category of these plumes (Figures 3.3a to 3.3o). One of the goals of this chapter was to provide a general overview of the similarities and differences of the biomass burning plumes encountered during the ARCTAS-2008 experiment. The results of this analysis show that the NEMR values for AN are similar in all the categories. The

NEMR values for  $\text{CO}_2$ ,  $\text{CH}_4$ , TU,  $\text{NO}_3^-$  and  $\text{SO}_4^{2-}$  were higher in plumes from California fires that were influenced by urban emissions. Also,  $\text{SO}_4^{2-}$ ,  $\text{NO}_3^-$  and HCN NEMR levels were enhanced in plumes from Asian and Siberian fires that were subject to long-range transport.  $\Delta\text{NO}_x/\Delta\text{CO}$  levels were distinctly higher in plumes that were intersected closer to the sources of emissions (ARTAS-B and ARCTAS-CARB). Overall, biomass-burning plumes that were influenced by urban emissions during ARCTAS-CARB had enhanced levels of some gaseous and aerosol species ( $\text{CO}_2$ ,  $\text{CH}_4$ , TU,  $\text{NO}_x$ ,  $\text{NO}_y$ ,  $\text{NO}_3^-$ ,  $\text{SO}_4^{2-}$  and  $\text{NH}_4^+$ ) when compared to other plumes encountered close to the sources of emission (i.e. ARCTAS-B and ARTCA-CARB). And BC-Mass, and inorganic aerosol components were enhanced in Asian and Siberian fire plumes. Depletion of  $\text{NO}_x$  was clear in these plumes. It appears that for the plumes that were subject to long-range transport, the gaseous and aerosol components were similar. The same general trend was observed for plumes encountered near the emission sources. The only exceptions were the ARCTAS-CARB plumes that were influenced by urban emissions and Asian fire plumes that were intercepted off the coast of California.

Additionally, during ARCTAS-B, distinct fires were encountered and the data from the plumes emitted from these fires and the changes in the NEMRs of the 16 species with age were discussed in this chapter (Figure 3.2a to 3.2o). Overall, as expected when comparing normalized excess mixing ratios from many biomass-burning sources, the inherent variability in the emissions from various sources appears to be large relative to any changes that may occur due to chemical evolution. This may be especially true when evaluating the evolution of species such as OA and WSOC, which can be produced both as primary emissions from biomass burning sources and also enhanced with time due to

secondary production processes. No evidence of production of secondary aerosol species was observed in these fires. This may have been due to the lack of sufficient concentration of oxidizers (i.e.  $O_3$  and OH), which would hinder the oxidation of VOC-s that are essential for SOA production. Also, the possible enhancement of secondary species (e.g., nitrate) may have been obscured due to the high spatial variability in the emissions (i.e. the burning temperatures varied in large fires from the center to the edges of the fires, and multiple fires were contributing to the plumes present in one region). Also, the variability in the production of secondary compounds may have been due to the dependence of these processes to various other factors such as: photo-chemistry rates affected by cloud cover, temperature and RH, time of day, etc. For the organic aerosol compounds, a significant fraction of OA and WSOC are from primary emissions. These vary between different fires and also the addition of secondary species to the large primary emissions present in the plumes may not be discernable.

## CHAPTER 4

### WATER SOLUBLE ORGANIC AEROSOL LIGHT ABSORPTION

#### 4.1. Introduction

Organic and elemental carbon are a significant fraction of ambient fine aerosols and can have many chemical forms. Since comprehensive chemical speciation of the carbonaceous aerosol is not possible, [e.g., *Gelencser et al., 2000c; Kiss et al., 2001; Krivacsy et al., 2001; Gelencser et al., 2002; Gelencser et al., 2003, Myhre et al., 2004; Graber and Rudich, 2006; Salma et al., 2008; Baduel et al., 2009*], grouping these compounds by physical properties has proven an effective means of characterizing their sources, impacts and fate in the atmosphere. Based on thermal volatility, carbonaceous aerosols are often divided into two groups: elemental carbon (EC) and organic carbon (OC) [*Turpin et al., 1990; Salma et al., 2008*], with the delineation between the two dependant on the measurement method (e.g., thermal/optical transmission (TOT) versus thermal/optical reflectance (TOR)) [*Chow et al., 2004*]. EC is refractory and highly light absorbing, especially in the visible region of the electromagnetic spectrum [*Seinfeld and Pankow, 2003*]. It is also commonly measured based solely on light absorption properties, and in this case is referred to as black carbon (BC) [*Hansen and Novakov, 1990*]. Soot is also a term used to for light absorbing carbon. However, soot can include BC (graphitic component) and other adsorbed organic species [*Rosen et al., 1980*] that may or may not absorb light. These small carbonaceous particles containing EC are directly emitted to the atmosphere from all combustion processes [*Horvath, 1993a; Bergstrom et al., 2002; Seinfeld and Pankow, 2003*]. Limited oxygen or low combustion temperatures lead to incomplete conversion of fuel to carbon oxides and the production

of EC or BC. EC and BC are mainly composed of chain agglomerates of small, almost spherical, carbon particles that can evolve into branched or straight chains. EC and BC are often internally mixed with other components from combustion. For example, different combustion sources and processes can produce up to 10% moles of hydrogen as well as some other trace elements. Significant quantities of organic carbon can also combine with EC or BC during cooling of combustion emissions [Seinfeld and Pandis, 1998].

Organic carbon (OC) includes a vast array of chemical species that can have both primary and secondary sources. OC has been divided into a number of sub-groups, such as pure hydrocarbon organic aerosol (HOA) versus oxygenated organic aerosol (OOA) [Zhang *et al.*, 2005]. This categorization tends to follow the classification of water-insoluble organic carbon (WIOC) and water-soluble organic carbon (WSOC), respectively. HOA and WIOC have been found to be mainly from primary emissions, which includes combustion of both fossil and biomass fuels [e.g., Kanakidou *et al.*, 2005 and references therein; Zhang *et al.*, 2007]. OOA and WSOC can have both primary and secondary sources, with primary emissions mainly from biomass burning (with small contributions from fossil fuel burning) [e.g., Kawamura *et al.* 1985; Pandis *et al.* 1991; Khwaja, 1995; Forstner *et al.* 1997a and 1997b; Seinfeld and Pandis, 1998; Kanakidou *et al.*, 2004 and references therein; Edney *et al.*, 2005; Kroll *et al.*, 2005a and 2005b; Sullivan *et al.*, 2006; Zhang *et al.*, 2007; Paredes-Miranda *et al.*, 2009], and gas-to-particle conversion processes in which volatile organic compounds (VOCs) are oxidized to semi-volatile forms that partition to the aerosol phase (i.e. SOA formation) [e.g., Anderson-Skold and Simpson, 2001; Sullivan *et al.*, 2006; Volkamer *et al.*, 2006].

WSOC has been further divided by its other bulk physical and chemical properties [e.g., *Decesari et al., 2000; Mayol-Bracero et al., 2002*]. One of the more common sub-classifications has been based on Solid Phase Extraction techniques that tend to segregate WSOC into more hydrophilic (soluble) versus more hydrophobic (less soluble) components [e.g., *Varga et al., 2001; Krivacsy et al., 2000; Andracchio et al., 2002; Duarte and Duarte, 2005; Duarte et al., 2005; Sullivan et al., 2006*]. More hydrophobic components have been found to have properties that include, but are not limited to, higher molecular weight, ability to cause surface tension depression and light absorption characteristics, and are referred to as Humic-like substances (HULIS) [*Graber and Rudich, 2006*].

BC has been recognized and extensively studied as the strongest light-absorbing component of aerosols, especially in the visible and near Infrared region (400 to 700 nm wavelength range) [e.g., *Rosen et al., 1980; Horvath, 1993a; Horvath, 1993b; Bond et al., 1999; Lindberg et al., 1999; Clarke et al 2007; Marley et al., 2009*]. The wavelengths where BC has been studied range from 400 to 700 nm [*Horvath., 1993a and references therein*]. *Bergstrom et al.* (2002) studied the light absorbing properties of BC at 400 nm. *Alexander et al.* (2008) and *Rosen et al.* (1980) studied the light absorbing properties of soot (BC) at 550 nm and 630 nm. *Marley et al.* (2001) studied the absorption of light from UV to infrared by freshly emitted BC and found that it decreases concomitantly with wavelength.

In addition to BC, mineral dust and some organic aerosol components also absorb light [*Yang et al., 2009*]. As a group, light absorbing organic aerosols, have been referred to as Brown Carbon [*Andreae and Gelencser, 2006; Yang et al., 2009*] since they are

composed of compounds that are highly absorbing near the UV region of the electromagnetic spectrum. This includes polycyclic aromatic hydrocarbons (PAHs), the nitrate derivatives of PAHs [Marley *et al.*, 2009 and references therein], and HULIS. These species are strong light absorbers in the range of 200 to 400 nm [e.g., Krivacsy *et al.*, 2000; Kiss *et al.*, 2001; Krivacsy *et al.*, 2001; Varga *et al.*, 2001; Andracchio *et al.*, 2002; Gelencser *et al.*, 2003; Decesari *et al.*, 2006; Hoffer *et al.*, 2006; Gimbert *et al.*, 2007; Alexander *et al.*, 2008; Salma *et al.*, 2008; Baduel *et al.*, 2009; Martins *et al.*, 2009; Shapiro *et al.*, 2009].

Light absorbing organic compounds have been found in different atmospheric media from different sources. For example, Went (1966) found yellow, brown and black aggregates in snow and rainwater, when studying condensation nuclei. Mukai and Ambe (1986) observed brown colored soluble material in atmospheric particles at a rural site in Japan that was mainly impacted by local combustion sources. Havers *et al.* (1998) found compounds that absorb light at the same wavelength as brown carbon in mineral dust particles. Bond *et al.* (1999) report light absorbing compounds (brown) from residential coal burning samples. Many studies have focused on HULIS and its optical properties at rural [Gelencser *et al.*, 2000a; Duarte *et al.*, 2005; Gao *et al.*, 2006] and urban sampling sites [Dinar *et al.*, 2006a; Gao *et al.*, 2006; Baduel *et al.*, 2009], and the properties associated with fog and cloud samples [Facchini *et al.*, 1999; Gelencser *et al.*, 2000b; Krivacsy *et al.*, 2000; Andracchio *et al.*, 2002].

A variety of studies have investigated sources of brown carbon. Incomplete combustion, especially when associated with biomass burning, has been found to be a significant source of brown carbon [Mayol-Bracero *et al.*, 2002; Gelencser *et al.*, 2003; Dinar *et al.*,

2006a; Hoffer et al., 2006; Iiuma et al 2007; Baduel et al., 2009]. Brown carbon can also be formed in the atmosphere through chemical reactions [e.g., Mayol-Bracero et al., 2002; Baduel et al., 2009]. Heterogeneous reactions of biogenic volatile organic compounds (VOCs) such as isoprene in the presence of sulfuric acid [Limbeck et al., 2003] have been shown to produce brown carbon. In a more general sense, a variety of studies show that light-absorbing organic carbon species can be produced from biogenic VOC oxidation products and their subsequent polymerization [Andreae and Crutzen, 1997; Hoffer et al., 2004]. Photo-oxidation products of anthropogenic VOCs can also produce brown carbon [Duarte et al., 2005]. More specifically, Gomez-Gonzalez et al. (2008), Noziere et al. (2009) and Shapiro et al. (2009) observed the formation of light absorbing material from reactions of glyoxal in acidic ammonium sulfate solutions. The reaction of glyoxyl with amino acids [De Haan et al., 2009a], methyl amines [De Haan et al., 2009b] and glyoxyl and methyl glyoxyl self reactions [De Haan et al., 2009c] have been proven to produce secondary organic compounds that absorb light near the same wavelength as brown carbon. Glyoxal is an oxidation product of both anthropogenic and biogenic VOCs. Gelencser et al. (2003) and Gimbert et al. (2007) observed formation of HULIS from Fenton reactions in aqueous solutions from hydroxyacid precursors. Noziere et al. (2005) found that the acid catalyzed aldol condensation reactions of aldehydes and ketones can produce light absorbing compound in aqueous solutions. Other possible pathways for production of brown carbon in the atmosphere are polyacidic species from lignin breakdown [Mayol-Bracero et al., 2002, Baduel et al., 2009] and from the recombination of low molecular weight primary emissions after secondary condensation reactions [Mayol-Bracero et al., 2002].



Studying the sources and fate of brown carbon in the atmosphere is important for a variety of reasons. The presence of brown carbon can cause an overestimation of BC or EC based on currently used measurement methods [Andreae and Gelencser, 2006]. Underestimating the absorption of light by atmospheric aerosols in the UV region may impact photolysis rate calculations, especially for those near UV [Martins *et al.*, 2009] and influence climate predictions [Bernard *et al.*, 2008; Alexander *et al.*, 2008].

Finally, it is noted that brown carbon and HULIS have often become synonymous [e.g., Lukacs *et al.*, 2007], but HULIS may constitute only a portion of the light absorbing carbonaceous compounds. For example, Yang *et al.* (2009) showed that brown carbon includes not only HULIS, but also poly aromatic hydrocarbons (PAH-s) and lignin. Sun *et al.* (2007) found that the light absorption due to brown carbon is greater than that of only HULIS. In this paper no link is made between HULIS and Brown Carbon.

## **4.2. Methods**

The light absorbing properties of water-soluble components of PM<sub>2.5</sub> aerosols and their relationship with WSOC were investigated in this work. The data were generated from two sources; archived Teflon filters collected at various sites throughout the Southeastern U.S. in 2007, and from an online measurement system deployed from July to September of 2009, in Atlanta, GA. In both cases, light absorbing properties of water extracts containing dissolved aerosol components were measured with the same UV-VIS Spectrophotometer.

### **4.2.1. Light Absorption Measurements**

Light absorbing properties of water-soluble aerosol components were measured with a UV-VIS Spectrophotometer and Long-Path Absorption Cell. Liquid samples

either from FRM filter extracts or the online system (Particle Into Liquid Sampler, PILS) were injected via syringe pumps into a 100-cm path length Liquid Waveguide Capillary Cell (LWCC-2100, World Precision Instrument, Sarasota, FL), with an internal volume of 250  $\mu\text{L}$ . A dual deuterium and tungsten halogen light source (DT-Mini-2, Ocean Optics, Dunedin, FL) and absorption spectrometer (USB4000 spectrometer, Ocean Optics, Dunedin, FL) were coupled to the wave-guide via fiber optic cables (QP400-2-SR, Ocean Optics, Dunedin, FL). Absorption spectra were recorded over a wavelength range of 200 to 800 nm with an Ocean Optics Spectra-Suite data acquisition software system (Ocean Optics, Dunedin, FL). This software was capable of collecting data as both complete spectra and/or absorption at individual wavelengths (or an integration of absorption over specified wavelength ranges), simultaneously. For the filters, only complete spectra were collected. However, for the online setup complete spectra and absorption at 250, 325, 365, 400 and 700 nm were recorded. Complete absorption spectra data were integrated over 30 seconds at 0.2 nm resolution. A data analysis algorithm was developed using Igor Pro (Wavemetrics, Oswego, OR) to extract data at wavelengths of interest from the whole spectra, collected from the filters.

During operation, the system was rinsed with a 0.6N solution of HCl and Milli-Q (>10 M $\Omega$ ) DI water after each filter aliquot analysis, and every three days for the online system. Each cleaning of the system was followed by manual zeroing of the baseline using the Spectra-Suite software so that zero absorption was recorded at all wavelengths as the initial system baseline using milli-Q (>10 M $\Omega$ ) DI water.

#### **4.2.2. Filter Measurements**

Through a network of monitoring stations, the Georgia Department of Natural Resources (DNR) routinely measures ambient aerosol PM<sub>2.5</sub> mass at sites positioned throughout the state. This is accomplished by following a Federal Reference Method protocol [*Patachnick et al., 2001*] that involves collecting particles on 46.2 mm Teflon filters (Pall-Life Science, Ann Arbor, MI) using a fine particulate cyclone size selector and non-denuded sampler operating for 24 hours at a flow rate of 16.7 L min<sup>-1</sup>. At many sites, these filters are collected every six days, subsequently weighted to determine mass concentrations, archived, and eventually discarded. Other states in the region follow a similar protocol. In 2008, archived filters for the year of 2007 were obtained for a range of sites from the Georgia DNR, the South Carolina Department of Health and Environmental Control and the Alabama Department of Environmental Management and Jefferson Co. Department of Health. Sites were chosen to include a range of rural and urban locations spread throughout the Southeastern U.S. Figure 4.1 is a map of the 15 site locations.

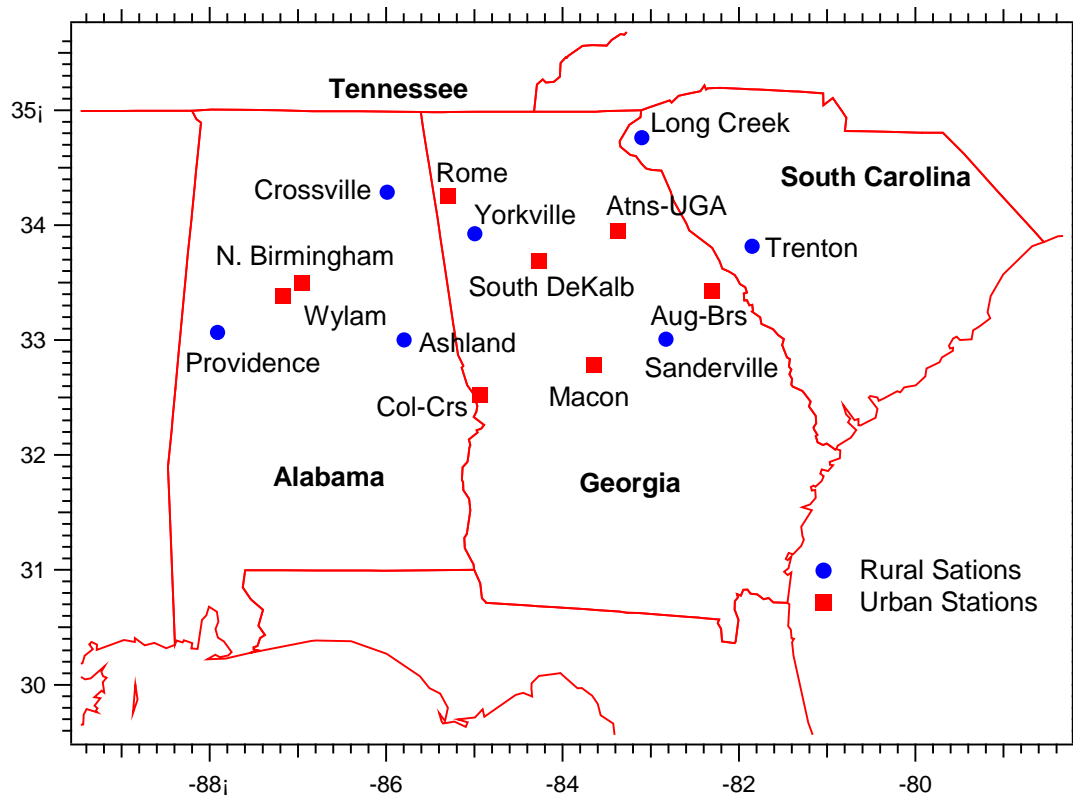


**Figure 4.1: The locations and designation (rural/urban) of FRM filter collection sites in Southeastern United States**

An every-sixth day sampling frequency in each site resulted in 60 filters per site and a total of 900 filters for analysis for the year 2007. Filters were shipped from the monitoring stations in coolers with blue ice and then immediately transferred to a freezer (nominally  $-10^{\circ}\text{C}$ ) where they were stored until analysis. Thus, these filters had been in storage at below freezing temperatures for approximately one year prior to the analysis. *Zhang et al.* (2010a) provide an overview of the overall study and methods used to extract and analyze these filters. A brief overview of some of these processes is presented here.

Filters were extracted in 30 mL of  $>18\text{ M}\Omega$  water (Barnstead Nanopure System, Thermo Scientific, Weltham, MA) in 30 mL amber Nalgene HDPE bottles with screw top lids. These bottles were triple rinsed in Milli-Q water by sonicating the bottle in an ultrasonic bath at room temperature for 30 minutes, before use. Liquid was extracted from the bottle with a 5 mL disposable (HDPE) syringe and transferred to another identical 30 mL amber bottle and filtered using a  $0.45\ \mu\text{m}$  PTFE disposable syringe filter. The bottles were stored in a fridge in the dark at  $4^\circ\text{C}$  until analysis. All analysis was typically completed within 2 to 3 days. Aliquots of sample were taken from the bottle for a series of analyses. A Dionex (Sunnyvale, CA) ion chromatography system (DX-500), LC25 Chromatography Oven, GP40 Gradient Pump and ED50 Electrochemical Detector was used for the measurement of a range of carbohydrates, including levoglucosan, a biomass-burning tracer [e.g., *Schkolnik and Rudich, 2006; Puxbaum et al., 2007*]. The filter aliquots were introduced to the system with an AS40 Auto sampler (Dionex, Sunnyvale, CA). To accomplish a complete speciation of carbohydrates of interest a Dionex CarboPac PA-1 column (an anion exchange column, used with pulsed amperometric detection) was used. The mobile phase eluent used for this system was made from 50% v/v sodium hydroxide (NaOH) stock solution. The solution was degassed by purging with ultra pure helium for 30 minutes before the beginning of daily measurements. A gradient mobile phase was used for the elution of the different carbohydrates. The gradient was as follows: 7.2 mM NaOH for the initial seven minutes, 7.2 mM NaOH ramp up to 72 mM NaOH from the 8<sup>th</sup> to the 25<sup>th</sup> minutes, 180 mM NaOH from 28<sup>th</sup> to 43<sup>rd</sup> minutes to clean the column and 7.2 mM NaOH from the 43<sup>rd</sup> to the 59<sup>th</sup> minute to achieve re-equilibrium of the column. The samples were loaded onto

the PA-1 column from a 100  $\mu\text{L}$  sample loop. Calibration of the IC system for the carbohydrates of interest was accomplished by making stock solutions from solid phase compounds in Milli-Q DI water. The stock solutions were stored in cool, dry conditions at nominally 4° C temperatures. Calibrations for the system were repeated three times during the study and in all cases the  $r^2$  values were typically greater than 0.99 and the variability of the slopes were approximately 2% to 25% for various compounds. Dionex Chromeleon CHM-1-IC was used to control the instruments and the integration of resulting peaks. Even though the PA-1 column provided the peak separation for many of the carbohydrates of interest, levoglucosan and arabitol were co-eluted [*Iiuma et al.*, 2009 and references therein]. The correction for the co-elution of arabitol and levoglucosan was accomplished by using mannitol, which has a strong linear correlation with arabitol [*Zhang et al.*, 2010b]. A more detailed discussion of the setup and methods of analysis are presented by Zhang et al. (2010a).

The water-soluble organic carbon (WSOC) concentrations were determined in 10 ml aliquots using a Sievers Total Organic Carbon (TOC) Analyzer (Model 900, GE Analytical Instruments; Boulder, CO.). The TOC concentrations were calculated by subtracting the measured total inorganic carbon (TIC) from the measured total carbon (TC). The TOC analyzer has two  $\text{CO}_2$  sensors. One is used for the measurement of  $\text{CO}_2$  released from the oxidation of both organic and inorganic compounds by using a 25% solution of ammonium sulfate (flow rate = 0.75  $\mu\text{L min}^{-1}$ ) and an ultraviolet reaction chamber (wavelengths of 254 and 184 nm). The other sensor is used to measure the  $\text{CO}_2$  released from the inorganic compounds only by oxidizing the sample merely using the ammonium sulfate solution. Both reactions are performed on samples with a pH of

approximately 2 or less, as the samples have been acidified by the addition of 6M phosphoric acid before the oxidation reactions take place. The CO<sub>2</sub> sensors operate by isolating the CO<sub>2</sub> through a selective membrane into a high purity water loop and measuring the concentrations of CO<sub>2</sub> using a conductometric detector (Carlson, 1980). The TOC analyzer was factory calibrated. The calibration was confirmed at the beginning and near the end of the measurements with a series of sucrose standards. Typical results of the calibration were as follows:  $r^2=0.9997$ ; Slope= $7.3E-1 \pm 1\%$ ; I=-120  $\mu\text{gC m}^{-3}$  and N=5. The laboratory calibrations were used in the data analysis.

For the absorption measurements, an automated multiport syringe (Klohn, LTD; Las Vegas, NV) was programmed to inject 1 mL of the sample into the LWCC. Complete absorption spectra were recorded 30 seconds after the injection of the aliquot. Following each measurement, the LWCC was flushed with 1 mL of a 0.6N solution of HCl and 3 mL of Milli-Q DI water.

Additional series of analyses were done to quantify a suite of inorganic ions; however, these data are not discussed here. A complete overview of the measurements and the results are presented by *Zhang et al.*, 2010a.

A series of field and laboratory blanks, and laboratory prepared standards were also analyzed during the study to eliminate interferences and assess measurement precision. In addition to the field blank filters, provided by the participating sites, for every 10<sup>th</sup> filter in the sample queue a water blank and a single standard (a range of standards were prepared) were analyzed. For all the data quality assurance results reported here the aqueous concentrations are converted to equivalent ambient concentration for ease and uniformity of comparison. The limit of detection (LOD) of

WSOC was calculated from the  $3\sigma$  (standard deviation) of the filter blanks, whereas the LODs for the carbohydrates were calculated from  $3\sigma$  of the noise of the typical baseline of the IC system. The LOD for WSOC was  $0.15 \mu\text{gC m}^{-3}$ , and ranged from 0.2 to  $0.6 \text{ ng m}^{-3}$  for the carbohydrates. The results for the field filter blanks and DI water blanks were all well below LOD of the carbohydrates. The concentrations of WSOC on the blank filters were very small (about 0.5%) and were thus negligible. Comparisons of concentrations from co-located filter measurements (measurement precision) were usually within 15%; specifically, 4% for WSOC, 13% for levoglucosan and 9% for light absorbance at 365 nm. Finally, measurement uncertainties were calculated using errors associated with volume measurements, calibration standards, filter blanks and precision values for each species. The uncertainty associated with the measurement of WSOC was 9% and 21% for levoglucosan.

#### **4.2.3. Online Measurements**

An automated online system was constructed to provide semi-continuous measurements of both the absorption spectra and carbon mass of water-soluble aerosol components (Figure 4.2).



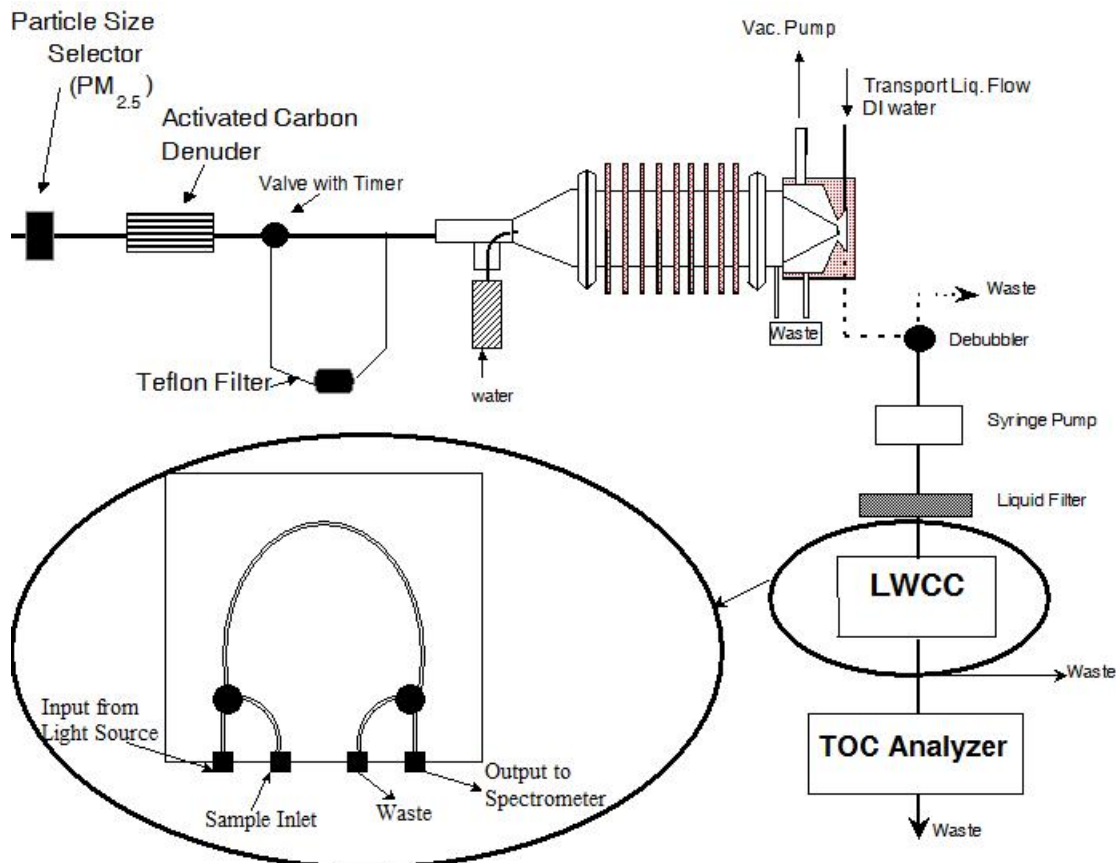


**Figure 4.2: Schematic of Online Light Absorption and WSOC measurement. The area highlighted and enlarged is the LWCC schematic, which presents the setup that was used for the filter measurements**

This was accomplished by adding a LWCC to an online system for measurement of water-soluble organic carbon (WSOC). A detailed description of the online WSOC measurement with a Particle-Into-Liquid Sampler (PILS) is described elsewhere [Sullivan *et al.*, 2004; Sullivan *et al.*, 2006; Peltier *et al.*, 2007b; Hennigan *et al.*, 2008]. Briefly, in this instrument (PILS) ambient particles are concentrated into a continuous flow of high purity water by a steam-condensation-droplet impaction collection system. Two syringe pumps with automated selection valves (Klohn, LTD.; Las Vegas, NV) continuously draw sample from the PILS through a debubbler to remove air and then

pump the liquid sample at a nominal rate of 0.3 mL/min through a 0.45  $\mu$ m PTFE disposable syringe filter followed by the LWCC and the TOC analyzer (discussed in the previous section). The TOC analyzer was operated in normal mode (non-turbo), drawing sample into the detector at a flow rate of 0.2 mL/min and recorded liquid carbon concentrations at a 6-minute duty cycle. Upstream of the PILS either a sharp cut cyclone (URG; Chapel Hill, NC) or a non-rotating multi-orifice impactor (MSP; Shoreview, MN) was used to exclusively sample PM<sub>2.5</sub> aerosols. Possible positive artifacts due to interfering gases such as VOC-s were reduced with an activated carbon denuder [Eatough *et al.*, 1993] and a pre-programmed automated valve that shunted sample through a Teflon filter (Pall-Life Science, Ann Arbor, MI) to provide an automated blank. Subtraction of this blank accounted for possible interferences due to collection and analysis of any water-soluble VOCs and contaminations in the ultra-pure water used in this system. The complete spectra were collected every five minutes and the data for selected wavelengths of interest (250, 365, 400 and 700 nm) were collected every 20 seconds. Background measurements were performed twice per day (4:30 and 18:30 local time) for 45 minutes, for the duration of the study. Ambient WSOC concentrations were determined by subtraction of the results of a linear interpolation between consecutive blank levels and the liquid TOC concentrations. These values were then converted to ambient WSOC concentrations using the following equation [Orsini *et al.*, 2003; Weber *et al.*, 2003; Sullivan *et al.*, 2004]:

$$C = (C_l Q_l R) / (Q_a) \quad (4.1)$$

where  $C$  is the ambient concentration of WSOC in  $\mu\text{g m}^{-3}$ ,  $C_1$  is the aqueous concentration of WSOC in  $\mu\text{g L}^{-1}$ ,  $Q_1$  is the liquid flow rate over the impactor in  $\text{mL min}^{-1}$ ,  $R$  is the sample dilution ratio (a constant value of  $X$  was assumed) and  $Q_a$  is the flow rate of air through the PILS in  $\text{L min}^{-1}$ . From previous studies, the uncertainty of this system has been estimated at 8% and the limit of detection (LOD)  $\sim 0.1 \mu\text{gC m}^{-3}$  for WSOC measurements [Sullivan *et al.*, 2004]. Figure 4.3 shows an example of non blank-corrected ( $C_1$ ) ambient WSOC and light absorption data at 365 and 700 nm using the online PILS-LWCC-WSOC system. Periods of dynamic blank measurements are evident in the Figure in both the WSOC and absorption at 365nm.

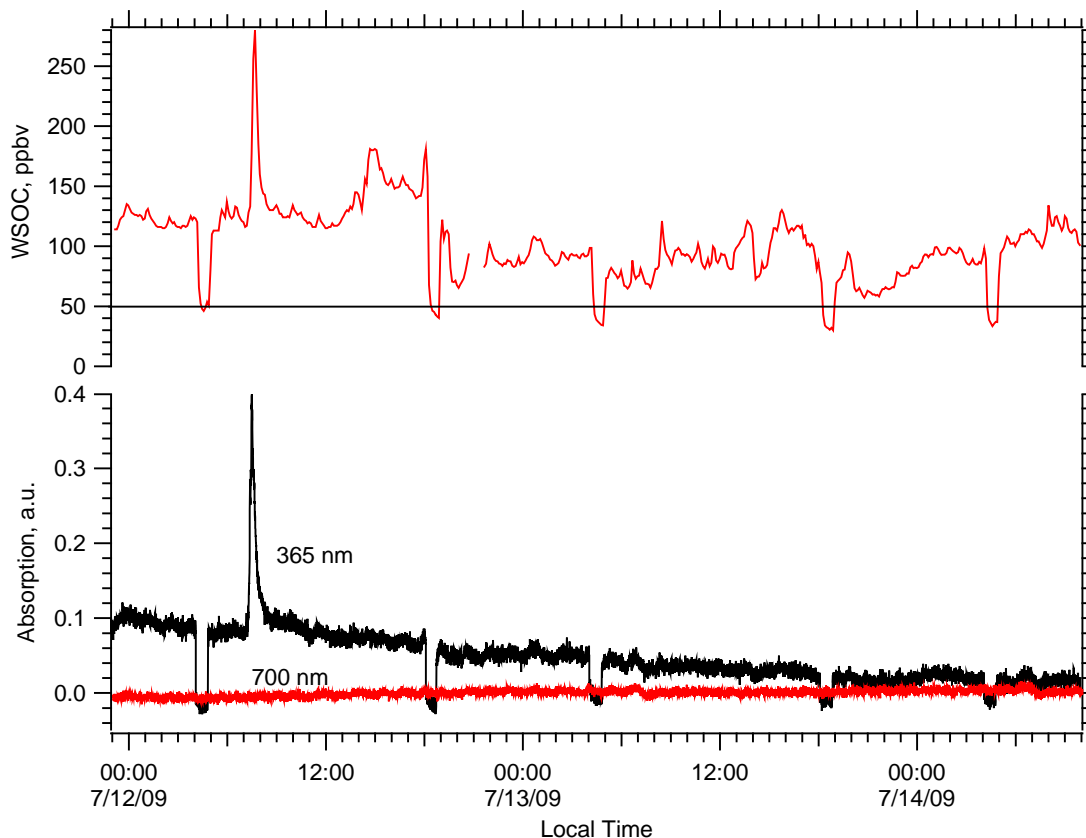


**Figure 4.3: Raw light absorption data from online measurements of light absorption in Atlanta, GA; July 2009**

From July to September of 2009, online water-soluble aerosol absorption measurements were performed in Atlanta, GA with this system. The site for this study was located in the Georgia Institute of Technology's Ford Environment Sciences and Technology air quality laboratory situated on the building's top floor approximately 20 to 40 m above ground level (depending on the side of the building) at approximately (33.78° and -84.40°). The station is a straight-line distance of roughly 840 m from a major interstate highway. A number of atmospheric chemistry studies have been published based on data from this site [e.g., *Hennigan et al., 2009*].

To assess any effect of adding an LWCC to the PILS-TOC system on WSOC measurements de-ionized water (18 MΩ) and different solutions of oxalate were used to check for positive and negative artifacts. Background carbon levels increased from a typical concentration of 25 ppbv to 50 ppbv. This background increase was accounted for in the blank corrections. The TOC response to oxalate solutions with the LWCC inline compared to offline did not change significantly ( $r^2 = 0.998$ , I=5.6 ppbv, S=1.07 ppbv and n=6), indicating no adverse effect on the WSOC concentrations by the LWCC system.

#### 4.2.4. Interpretation of Absorption Data

A UV-VIS Spectrophotometer and Long-Path Absorption Cell were used for the absorbance measurements presented here. This instrument setup uses the fundamentals of Beer-Lambert Law which states that “for monochromatic radiation, absorbance is directly proportional to the path length ( $l$ ) through the medium and concentration ( $C$ ) of the absorbing species” [Skoog *et al.*, 1998]. This relationship is shown in Equation (4.2):

$$A_{\lambda} = C \varepsilon l = l \sum (C_i \varepsilon_i) = -\log_{10}(I/I_0) \quad (4.2)$$

where,  $A_{\lambda}$  is the absorbance,  $I$  is the intensity of transmitted light and  $I_0$  is the intensity of incident light.  $\varepsilon$  is the molar absorptivity. Furthermore, the absorbance is the product of the concentration of the chromophores in the solution ( $C$ ), their molar or mass absorptivities ( $\varepsilon$ ) and the ( $l$ ) is the absorption path length.  $l$  is approximately 1 m in this setup ( $\pm 5\%$ ) [Belz *et al.*, 1999]. Thus,  $A_{\lambda}$  is linear with the sum of all chromophore concentrations, times their mass absorptivity.

Although the complete light absorption spectra were recorded from 200 to 800 nm, for simplicity the absorption values averaged between 360 to 370 nm, centered at 365 nm were used as a general measure of the absorption by light absorbing carbonaceous aerosols. This wavelength was chosen because it is far enough from the UV region of the electromagnetic spectrum to avoid interferences from compounds such as phthalate and oxalate [Myhre and Nielsen, 2004] and nitrate. Many studies have collected data over a wide range of wavelengths (from 190 to 1200 nm) [e.g., Kiss *et al.*, 2001; Duarte *et al.*, 2005; Shapiro *et al.*, 2009; Yang *et al.*, 2009] to evaluate the light absorbing properties of brown carbon or HULIS; however, the main range of wavelengths of interest has been from approximately 200 to 500 nm. For example, Varga *et al.* (2001) and Baduel *et al.* (2009) studied the absorption at 250 nm, Andracchio *et al.* (2002) at 254 nm and Decesari *et al.* (2006) at around 260 nm. Some have studied the absorption of carbonaceous compounds at higher wavelengths; for example, Gelencser *et al.* (2003) and Gimbert *et al.* (2007) observed light absorption at 400 nm. Some other studies chose a collection of wavelengths to analyze. Hoffer *et al.* (2006) studied absorption at 300 and 532 nm and Krivacsy *et al.* (2001) looked at a multitude of wavelengths, including 210, 280, and 350 nm.

Baseline drift during the extended periods when measurements were being conducted was accounted for by referencing all the measurements to the absorbance at 700 nm. Also, to account for the differences between the FRM-filter and PILS methods for sample collection and extraction into water (e.g., sample air flow rates, integration times, extent of dilution into water), absorption (in arbitrary units) was multiplied by a volume correction factor. All absorption data were determined by Equation 4.3:

$$\text{Abs (a.u. m}^{-3}\text{)} = (\text{Abs}_{365} - \text{Abs}_{700}) V_1 / (V_a V_{\text{LWCC}}) \quad (4.3)$$

Where  $\text{Abs}_{365}$  is the measured absorbance at 365 nm (mean between 360 and 370 nm),  $\text{Abs}_{700}$  the measured absorbance at 700 nm (mean between 695 and 705 nm),  $V_1$  is the volume of water the filter is extracted into (30 mL) or PILS liquid sample flow rate ( $0.3 \text{ mL min}^{-1}$ ),  $V_a$  the volume of sample air passed through the filter ( $24 \text{ hrs} \times 16.7 \text{ L min}^{-1} \times 0.06 \text{ min m}^3 \text{ hrs}^{-1} \text{ L}^{-1}$ ) or the PILS sample air flow rate ( $15 \text{ L min}^{-1}$ ), and  $V_{\text{LWCC}}$  the volume over which the absorbance measurement is made (LWCC internal volume of  $0.25 \mu\text{L}$ ). The resulting absorption at 365 nm is in units of arbitrary units per cubic meter of air ( $\text{a.u. m}^{-3}$ ).

It should be noted that inferring HULIS from light absorbance is highly uncertain due to the complex mix of the organic aerosols that likely contains a wide range of chromophoric species with varying absorptivities. Furthermore there are species that absorb in the UV-Vis region of EM but lack the typical HULIS structure (Yang et al., 2009). For example, xylose, a plant mono-sacharide released during biomass burning [Simoneit, 2002; Iiuma et al., 2007], but not likely considered HULIS by most separation methods, was one of the carbohydrates in the FRM-filter extracts which was highly correlated with absorbance at 365 nm, especially for filters that were influenced by biomass burning plumes ( $r^2=0.78$ , Slope=5.4,  $I=0.007$  and  $N=285$ ).

### 4.3. Results

#### 4.3.1. Absorbance Data

An example of absorption spectra recorded from filter extracts is shown in Figure 4.4. The online measurements produced similar spectra.

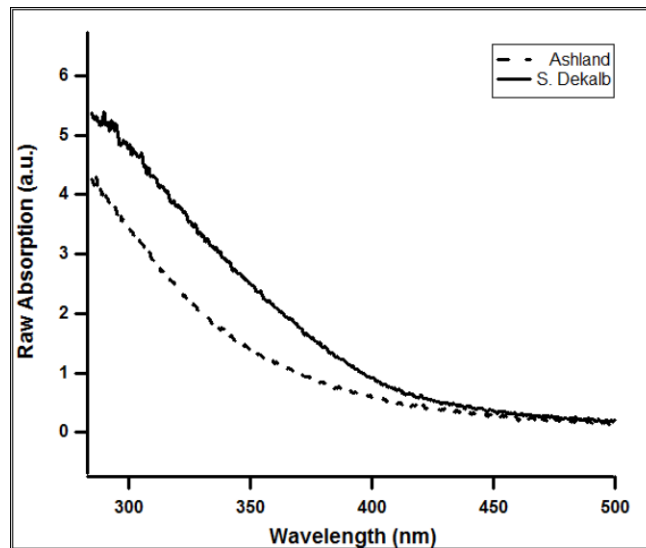


**Figure 4.4: Examples of absorption spectra from FRM filters collected at two sites during 2007**

The shape is similar to what has been measured for HULIS [Gelencser *et al.*, 2003; Gimbert *et al.*, 2007; Hoffer *et al.*, 2006]. The general shape of the ambient aerosol spectra, especially for the filters that were affected by biomass burning plumes, were similar to spectra of humic acid and fulvic acid isolated from different surface water sources; such as those from landfill runoff [Kang *et al.*, 2002], in lake waters [Oliveira *et al.*, 2006], ocean water [Esteves *et al.*, 2009], and Mediterranean soil samples [Munoz *et al.*, 2009].



The wavelength dependence of absorption is often fit with a power law in the form:

$$\alpha_{\text{abs}} = K \times \lambda^{-A'} \quad (4.4)$$

Where  $\alpha_{\text{abs}}$  is the aerosol mass absorption efficiency, typically expressed in  $\text{m}^2/\text{g}$ ,  $K$  is a constant independent of the wavelength of light ( $\lambda$ ) and is related to aerosol concentration.  $A'$  is the Angstrom exponent for absorption. In urban environments where light absorption is dominated by soot,  $A'$  is found to be close to 1 [Andreae *et al.*, 2006], whereas values of 2 and higher are observed in biomass burning [Kirchstetter *et al.*, 2004], with highest values found in smoldering combustion [Lawless *et al.*, 2004] and water-soluble HULIS (see Andreae *et al.* (2006) for a review).

The results of the fit of the filter data to the power equation (Equation 4.4) are discussed below. The data are segregated by biomass burning influence (biomass burning influence was delineated by a levoglucosan concentration of  $50 \text{ ng m}^{-3}$ ) or location. A range of wavelengths were chosen for this analysis. The range was selected based on the linearity of the fit of  $\log(\text{absorbance})$  and  $\log(\text{wavelength})$ , which was varied for the different categories of filters (i.e. rural and urban). The power fit was applied to 330-430 nm range as this was the area that was linear for all the filter samples. Hoffer *et al.* (2006) note that the fit tends to over-estimate absorption for wavelengths below 350nm. This is also the range where the absorption of light (UV) is highest by brown carbon with the least interference from other non-carbonaceous soluble compounds. The fit results showed a range of  $A'$  from 6.5 to 8 for all the filters collected in this study.

These results ( $A'$  values) are somewhat similar to those of *Hoffer et al.* (2006) for HULIS extracted from biomass burning samples collected in the Amazon basin. Using absorption measured at two wavelengths to estimate the Angstrom exponent, *Hoffer et al.* (2006) obtained Angstrom exponents of 6.4 and 6.8 for day and night, respectively. Biomass burning or non-biomass burning rural or urban samples all had similar mean Angstrom exponents. These biomass burning Angstrom exponents are somewhat lower than *Hoffer et al.* (2006), and may be related to our measurement of WSOC absorption and not just that of HULIS.

Spectral absorbances have also been used to infer the degree of sample aromaticity (e.g., *Krivacsy et al.*, 2008). In their studies, *Krivacsy et al.* (2008) divided the value of absorption at 250 nm with the value of absorption at 365 nm (E2/E3). There is an inverse correlation between E2/E3 with the levels of aromaticity of the collected samples [*Peuravuori and Pihlaja, 1997; Krivacsy et al., 2008*]. Applied to the FRM filter data, this ratio was substantially lower in biomass burning aerosols (E2/E3 = 4.6) compared to non-biomass burning filter samples (9.5), consistent with significantly higher levels of aromaticity in the biomass burning samples. However, for non-biomass burning conditions (levoglucosan < 50 ng/m<sup>3</sup>) filters from rural sites had lower ratios (6.2) compared to filters collected at urban sites (8.6), indicating higher levels of aromaticity in rural fine particles. Overall, the highest degree of aromaticity (lowest ratio) observed for the filters that were influenced by biomass burning plumes is consistent with the highly aromatic nature of biomass burning smoke and with the results observed by *Krivacsy et al.* (2008). However, results from our analysis should be used cautiously as we did not isolate the organic component and other light absorbing

compounds, such as aerosol nitrate, which is known to absorb at 250 nm and may influence these results. This may account for the unexpectedly higher aromaticity at the rural sites.

#### **4.3.2. FRM Filter Results**

As in other studies, the FRM filter data showed that biomass burning was a significant source for brown carbon. Figure 4.5 shows the monthly averages of levoglucosan, light absorption at 365 nm ( $Abs_{365}$ ) and WSOC for all sites.

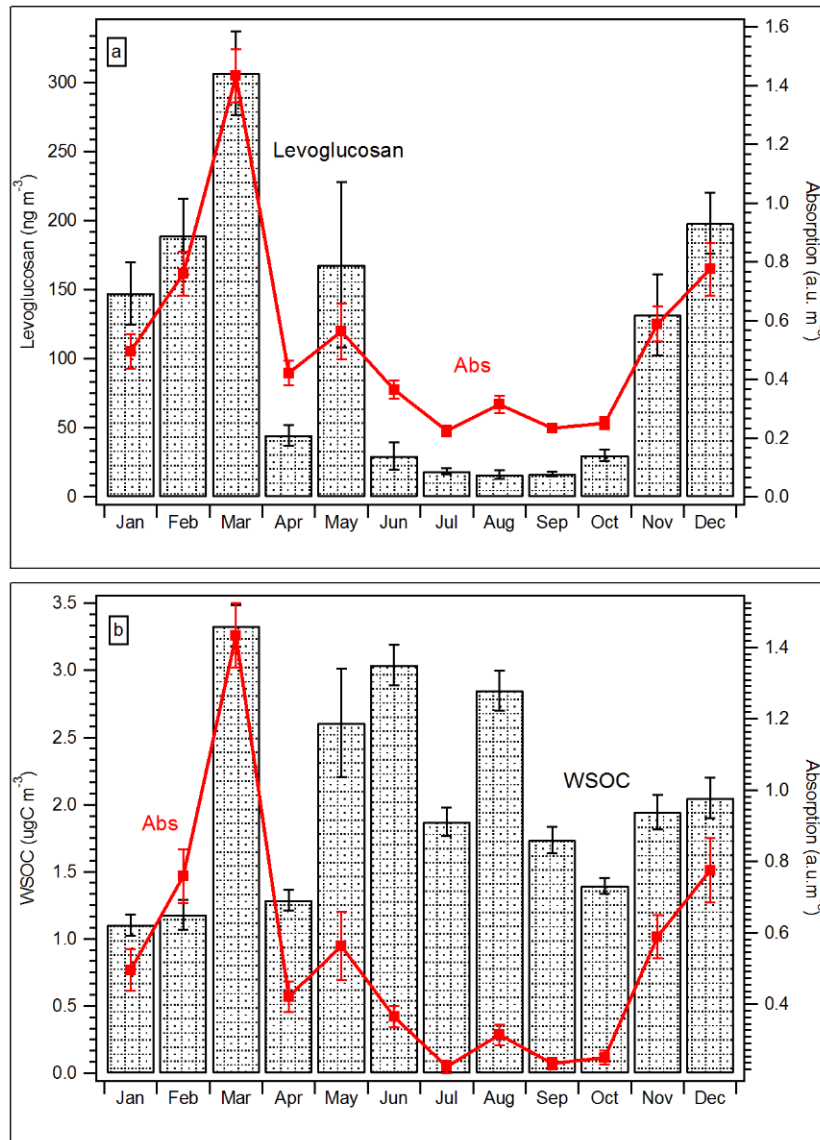


**Figure 4.5: Monthly average concentration for all sites for 2007. Variability is shown as the standard error. The number of filters averaged for each month is roughly 75**

*Zhang et al.* (2010b) present a detailed analysis of levoglucosan as a biomass-burning tracer, the seasonal variability of these species, and the sources of WSOC during this study. As indicated by levoglucosan concentrations, the highest contributions from biomass burning were observed in the cool months, November through March. In 2007 extensive burning episodes over a broad region of Southern Georgia resulted in smoke impacts over much of the Southeast (Georgia Department of Natural Resources, Environmental Protection Division), and account for the high levoglucosan concentrations in May 2007. Figure 4.5a clearly shows the same seasonal trend for biomass burning emissions (as indicated by levoglucosan concentrations) and Abs<sub>365</sub> for the Southeastern U.S. During the colder months Abs<sub>365</sub> and levoglucosan at individual sampling sites were highly correlated, both at urban and rural locations. Figures 6a and 6b show that for cold months (J, F, M, A, O, N, D) the slopes at these two sites are somewhat similar, and this trend is observed in other sites also. The relationship between Abs<sub>365</sub> and levoglucosan in all sites are as follows: for cold months  $r_c=0.8$ ;  $Slope_c=0.0017 \pm 0.0007$ ;  $I_c=0.2 \pm 0.2$  a.u./ng m<sup>-3</sup> and for the warm months (M, J, J, A)  $r_w=0.7$ ;  $Slope_w=0.002 \pm 0.002$ ;  $I_w=0.2 \pm 0.1$  a.u./ng m<sup>-3</sup>. When levoglucosan was greater than 50 ng m<sup>-3</sup> for the 15 sites, (mostly cold months, Figure 4.5), on average, roughly 80% of the Abs<sub>365</sub> could be explained by levoglucosan (i.e., mean  $r^2=0.81$ ), whereas only 10% could be explained by levoglucosan, when levoglucosan was less than 50 ng m<sup>-3</sup> ( $r^2=0.12$ ).

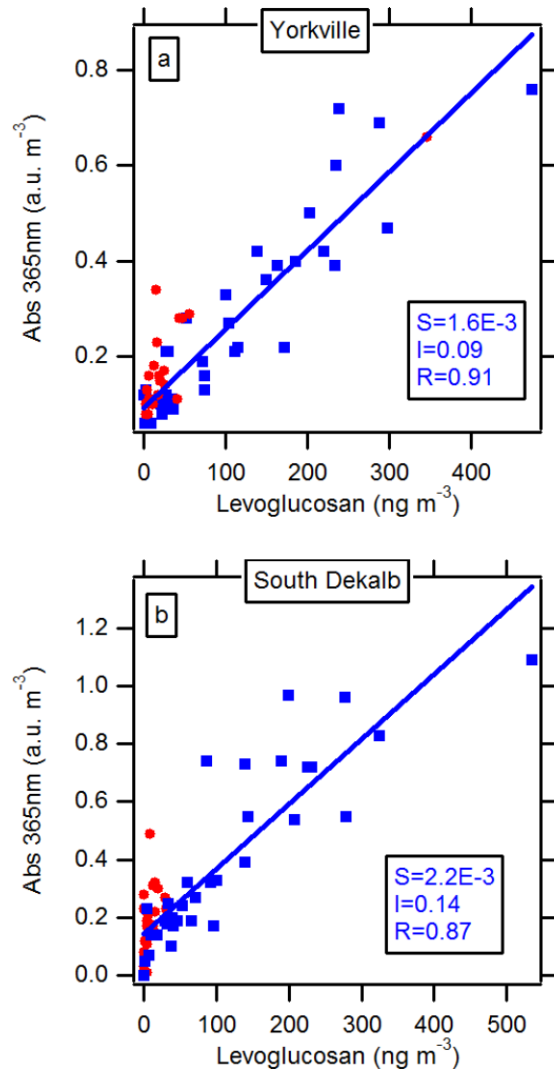


**Figure 4.6:** . Correlations between Abs<sub>365</sub> and levoglucosan at a representative rural (6a.Yorkville) and urban (6b. South Dekalb) site. The data for the cooler months (J, F, M, A, O, N, D) are presented in blue and the data for the warmer months (M, J, J, A, S) are shown in red. The regression fit is only for the cooler month's data

The data show that during the warmer season levoglucosan is much lower, as is  $Abs_{365}$  (see Figure 4.5b); however, WSOC remains high, presumably due to another source that produces a significantly lower proportion of WSOC-chromophoric compounds. Zhang *et al.* (2010a) and other studies indicate that this summer source is secondary organic aerosol formation, especially from biogenic sources [e.g., Gelencser *et al.*, 2002; Duarte *et al.*, 2005; Baduel *et al.*, 2009]. The bifurcation of the WSOC data by biomass/non-biomass burning is demonstrated in Figure 4.7. This Figure shows a clear difference in the fraction of light-absorbing species to total WSOC (i.e., slopes of  $Abs_{365}$  vs. WSOC) and thus divides the data into two distinct categories by levoglucosan concentrations, which results from two differing WSOC sources.

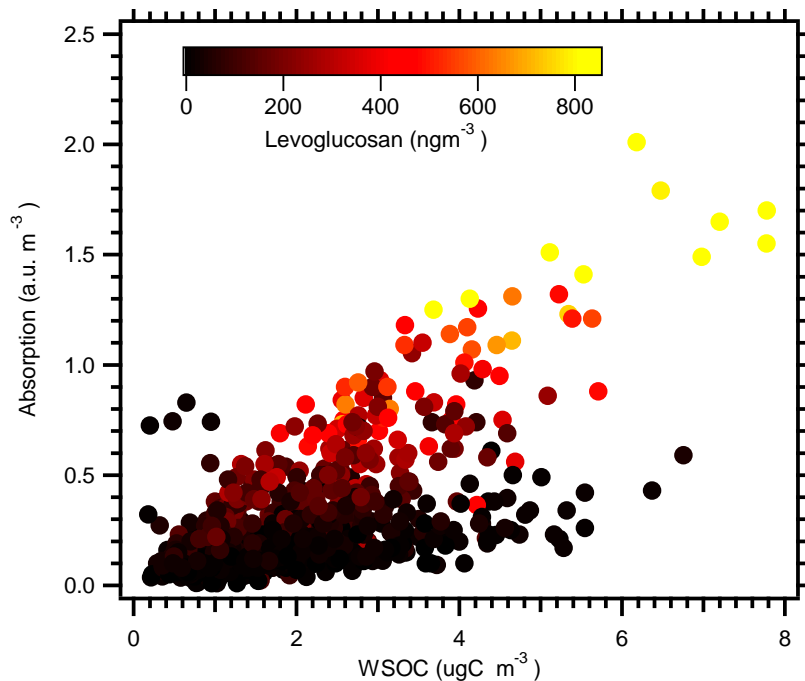


**Figure 4.7: Comparison of Absorption vs. WSOC for all filter data. The data points have been color coded based on levoglucosan values. Light colors indicate high concentrations of levoglucosan (i.e. filters influenced by biomass burning plumes) and dark colors show low levels of levoglucosan (i.e. filters that were less affected by biomass burning plumes)**

The FRM-filter data were separated into biomass burning and non-biomass burning-influenced periods using levoglucosan concentrations of  $50 \text{ ng m}^{-3}$  as the delineating value. A levoglucosan value of  $50 \text{ ng m}^{-3}$  is arbitrary; however, a relatively low value (for urban and rural areas) was chosen to more rigorously exclude all biomass-burning contributions since one of the goals of this work was to investigate non-biomass burning sources of light-absorbing WSOC. Winter and summer mean levoglucosan concentrations were  $170$  and  $19 \text{ ng m}^{-3}$ , respectively [Zhang *et al.*, 2010a]. Background concentrations in Europe have been reported to be in the range of  $5$  to  $52 \text{ ng m}^{-3}$  [Puxbaum *et al.*, 2007]. The data were further segregated into urban and rural sites (see Figure 4.1), and the results of the comparison of WSOC and  $\text{Abs}_{365}$  are summarized in Table 4.2.



**Table 4.1: Summary of linear regression results for 24-hr FRM filter Abs(365) versus WSOC concentration for each site, separated by high and low levels of levoglucosan (>50 ng/m<sup>3</sup> and <50 ng/m<sup>3</sup>, respectively). The mean result exclude the LCRK site and the non-biomass burning also excluded the ATH site, which all had very low correlations**

	<b>Biomass Burning</b>		<b>Non-Biomass Burning</b>	
	<b>r</b>	<b>Slope (Abs/μgC)</b>	<b>r</b>	<b>Slope (Abs/μgC)</b>
<b>URBAN SITES</b>				
ATH	0.86	0.23	0.33	0.015
AUG-BRS	0.84	0.25	0.79	0.043
COL-CRS	0.88	0.18	0.72	0.030
N BHM	0.93	0.17	0.71	0.071
MACON	0.89	0.25	0.83	0.058
ROME	0.77	0.15	0.70	0.039
S. DEKALB	0.83	0.20	0.77	0.065
WYL	0.87	0.20	0.77	0.082
Mean ± Stdev		0.20 ± 0.04		0.056 ± 0.018
Std/Mean		20%		32%
<b>RURAL SITES</b>				
ASH	0.78	0.21	0.65	0.063
CROSS	0.70	0.16	0.71	0.067
LCRK	0.23	0.05	0.25	0.057
PROV	0.88	0.21	0.56	0.042
SND	0.91	0.22	0.73	0.047
TRE	0.92	0.21	0.74	0.041
YKL	0.78	0.14	0.75	0.038
Mean ± Stdev		0.19 ± 0.03		0.052 ± 0.012
Std/Mean		16%		23%

For most sites there is a high correlation (r) between Abs<sub>365</sub> and WSOC concentrations, with correlation coefficients typically greater than 0.8 and generally higher correlations for the biomass burning filters. The data for non-biomass burning influenced filters from two sites (Long Creek and Athens) had poor correlations due to

the presence of some high WSOC values that do not show a corresponding increase in the levoglucosan concentrations and the results from these two sites are not included in the following analysis.  $Abs_{365}$  relative to WSOC (e.g., slopes) at various monitoring stations demonstrate: 1) For a given category (biomass-burning or non-biomass-burning) the extent of  $Abs_{365}$  per WSOC mass was fairly consistent between all sites (urban and rural), with similar mean slopes for urban versus rural sites of  $\sim 0.2 \text{ a.u. } \mu\text{g C}^{-1} \pm 20\%$  (relative standard deviation) for biomass-burning influenced filters and mean slope of  $\sim 0.05 \text{ a.u. } \mu\text{gC}^{-1} \pm 30\%$  for non-biomass-burning filters. 2) The extent of  $Abs_{365}$  per WSOC mass (slopes) are approximately a factor of 3.5 times higher in the biomass burning emissions versus the non-biomass-burning. These results suggest wide-spread spatial uniformity in the chemical characteristics (in terms of fractions of water-soluble light absorbing organic species), both when air masses were influenced by biomass burning and when they were not. It is noted however, that the results from the FRM filters likely do not include any semi-volatile species due to the sampling method and length of time the filters were kept in storage. *Zhang et al.* (2010a) investigate the extent of semi-volatile contributions to WSOC mass for this study. Thus, these results represent the more stable and aged components of the ambient aerosol. The online measurements should be less susceptible to artifacts and can also be used to investigate the more rapid variability of  $Abs_{365}$  relative to WSOC.

To evaluate the statistical significance of the differences between  $Abs_{365}/WSOC$ , a p-value test with  $\alpha=0.01$  was applied to the filters from all the sites, in pairs. Only the filters in N. Birmingham showed a clear difference with  $p<0.01$  (with the exception of N.

Birmingham and S. Dekalb where  $p=0.84$ ). All other site pairings showed  $p>0.01$ , which indicates that the  $\text{Abs}_{365}/\text{WSOC}$  values were not significantly different in these sites.

#### 4.3.3. Online Measurement Results

Continuous light absorbance and WSOC measurements were collected in Atlanta, GA, from July to September 2009 on the Georgia Institute of Technology Campus to investigate the sources or process that lead to the production of non-biomass burning brown carbon.

The summer 2009 data using the online system produced results that were similar to the FRM-filter non-biomass burning (for the months of July, August and September for the South Dekalb sampling site) of 2007. For 2009, the daily averages for the online data were calculated and the slope of  $\text{Abs}_{365}$  to WSOC was  $0.052 \text{ a.u. } \mu\text{g C}^{-1}$ , (Figure 4.8); similar to the value for 2007 at  $\sim 0.054 \text{ abs } \mu\text{g C}^{-1}$ . During the summer months for these two years, in addition to similar  $\text{Abs}_{365}/\text{WSOC}$  ratios, WSOC concentrations were similar. For 2009  $\text{WSOC} = 2.9 \pm 0.9 \mu\text{gC m}^{-3}$  versus for 2007 the Georgia EPD sites average was  $2.2 \pm 0.6 \mu\text{gC m}^{-3}$ . Despite these similarities,  $\text{PM}_{2.5}$  mass in 2009 on average was significantly lower at  $12 \pm 8 \mu\text{g m}^{-3}$  compared to  $20 \pm 11 \mu\text{g m}^{-3}$  in 2007.

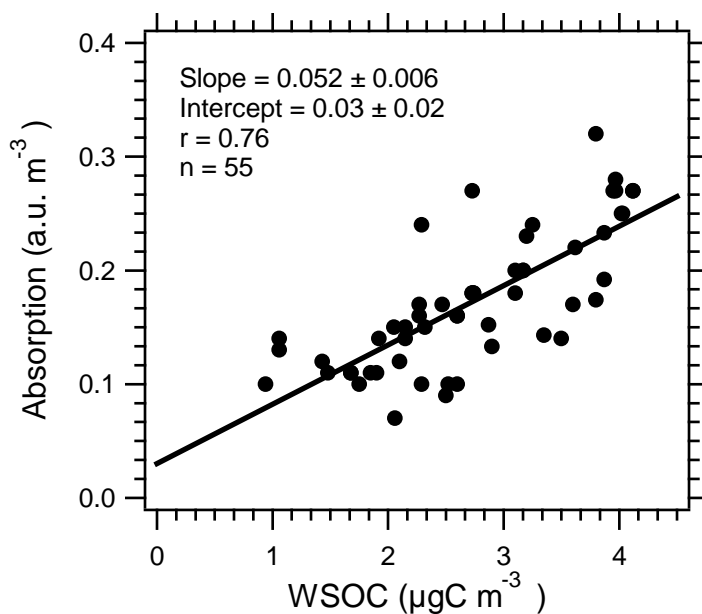


**Figure 4.8: Comparison of daily averages of online measurements of light absorption and WSOC in Atlanta, GA (July – September 2009)**

Patterns in diurnal variability of  $\text{Abs}_{365}$  relative to WSOC and other emissions can provide insight into sources of light-absorbing species. Figure 4.9 shows the mean diurnal trends for all online  $\text{Abs}_{365}$ , WSOC, CO, and ozone, all binned into hourly averages. The CO and ozone data are from the year 2008, averaged over the months of July to September from the Southern Aerosol Research Characterization Study (SEARCH) monitoring site, located at Jefferson Street station, Atlanta, GA ( $33.78^\circ$ ,  $84.41^\circ$ ), since these measurements were not included in our study and we are only interested in typical diurnal trends for these two species.

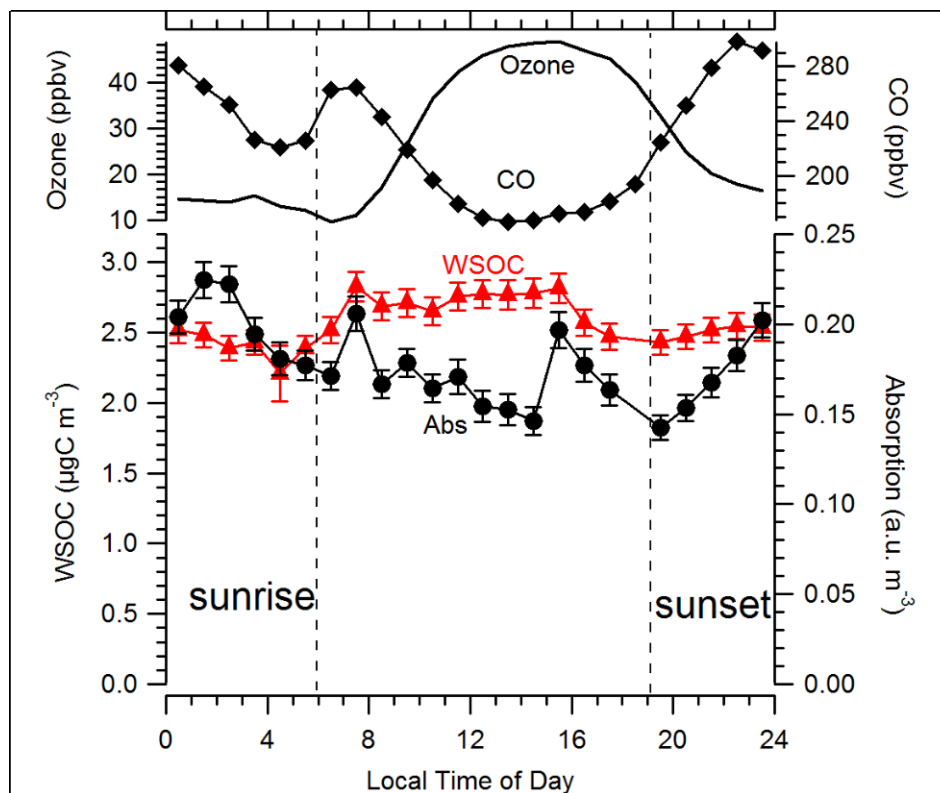


**Figure 4.9: Hourly means of Ozone, CO, WSOC and light absorption from online measurements in Atlanta, GA. Ozone and CO data are from SEARCH monitoring site at Jefferson street, Atlanta, GA (2008) and included for only general comparison purposes. WSOC and Abs are from July-Sep 2009. Variability in the hourly averages is the standard error, where n=120 for each hourly average.**

Abs<sub>365</sub> and WSOC both show comparatively small diurnal variability relative to a high background, which is typical of the regional characteristic of trace gases and aerosols in the Southeastern U.S. [Zhang *et al.*, 2010a]. For WSOC there is a clear daytime increase of roughly 20% (an increase of 0.5  $\mu\text{gC m}^{-3}$ ) over the typical nighttime concentration of approximately 2.4  $\mu\text{gC m}^{-3}$ , which is attributed to photochemical SOA production linked to urban emissions, since this increase was not observed at a rural site (Yorkville, GA) ~ 70 km from central Atlanta, GA (see Zhang *et al.* 2010a for more

details). A similar daytime WSOC increase has been observed at other urban sites, such as Mexico City [Hennigan *et al.*, 2008]. A small WSOC peak was observed at ~ 7:00 (local time) at the same time as a peak in CO and both are likely due to primary vehicle emissions resulting from morning rush hour traffic combined with low boundary layer heights in the early morning. A similar peak was not observed in WSOC or CO during the afternoon rush hour, likely due to much higher afternoon boundary layer heights resulting in significant dilution of the afternoon emissions.

In contrast to WSOC, light absorbance diurnal trend was different. First, the daytime increase in WSOC was not observed in Abs<sub>365</sub>, instead Abs<sub>365</sub> levels actually decreased during the day, suggesting that relatively freshly formed water-soluble WSOC (e.g., SOA) contains few chromophores. At the time of morning rush hour there is a significant increase in light absorbance levels corresponding to the slight increase in WSOC. This indicates that the fresh, likely primary WSOC from vehicle emissions was composed of significant light absorbing compounds, possibly mainly from aromatic species [Salma *et al.*, 2008]. At this time, the estimated increase in Abs<sub>365</sub> to the increase in WSOC (i.e.,  $\Delta\text{Abs}_{365}/\Delta\text{WSOC}$ ) was ~0.2 a.u.  $\mu\text{g C}^{-1}$ , similar to the levels in biomass burning plumes. A similar light absorbance peak is observed in the afternoon at 14:00 to 20:00 hrs local time, but in this case with no corresponding WSOC or CO increase; thus this does not appear to be linked to primary WSOC emissions, in contrast to the morning rush hour. This peak appears to be real, as it was observed for 80% of the sampling days. The afternoon minimum in both Abs<sub>365</sub> and WSOC occurs near the time of the afternoon blank for these data (18:30 to 19:15), however, the blank measurements are not thought to be the cause since they would not effect the trend prior to the blank, during which both

Abs<sub>365</sub> and WSOC were decreasing, nor the general trends hours later. The source of the afternoon Abs<sub>365</sub> peak is not clear, but may be related to some form of chemical conversion of WSOC to more light absorbing compounds, such as formation of oligomers [*Havers et al., 1998; Graham et al., 2002; Graber and Rudich, 2006* and references therein] or oxidation of secondary compounds by OH in the aqueous phase [e.g., *Gelencser et al., 2003; Duarte et al., 2005*]. The chemical conversion would explain the lack of increase in WSOC. Laboratory studies show that the typical time for formation of oligomers from low molecular weight carbonyls is less than 25 hours [*De Haan et al., 2009b*]. This peak does not follow solar intensity, and hence OH concentrations, which peak near noon; however, it does occur in late afternoon when ozone concentrations are still high. Alternatively, this peak could also be due to increases in fresh WSOC with highly efficient light absorbers, which contribute a very small amount to the overall WSOC concentrations, but significantly increase the overall WSOC light absorption properties.

At night, Abs<sub>365</sub> increased again following sunset and reached a peak near 2:00 to 3:00, and then declined. The trend during morning rush hour and night are somewhat similar to CO measured in Atlanta in 2008 and so could be linked to primary emissions and diurnal trends in boundary layer height. The nighttime increases, however, could be linked to the production of secondary organic nitrates through nitrate radical chemistry, especially with biogenic emissions [*Spittler et al., 2006; Brown et al., 2009; Rollins et al., 2009*], but the lack of concurrent WSOC concentration increase indicate that it would have to be a minor component of WSOC mass. The ratio of Abs<sub>365</sub> to WSOC is roughly 21% higher at night compared to daytime levels. However, because the concentrating

effect of low nighttime inversion height and diluting effect of daytime boundary layer expansion were not accounted for here; in terms of production rates, the daytime processes are much more important, suggesting that overall, much of the urban contribution to fresh WSOC are species that are not highly light absorbing. More data at other sites and additional years of online data are needed to further confirm or refute these trends. Also, measurements in closer proximity to the possible sources of light absorbing WSOC compounds would provide a better emission estimate.

A similar fit to that of Equation 4.4 was applied to the online data in the 330-430 nm range. The spectra were separated into hourly bins and averaged, then fit using Equation 4.4. The resulting  $A'$  values were very similar for each hour, with a median value of  $6.8 \pm 0.8$ .

#### **4.4. Conclusions**

Seasonal data from the FRM filters confirm that biomass burning is overall the most significant source of water soluble light absorbing species, due to the much higher fraction of chromophoric species per water-soluble carbon mass compared to other sources (~ 3.5 times higher than non-biomass burning). This may be due to the more oxygenated nature of the emissions from biomass burning sources [*Decesari et al., 2006*]. The contribution of biomass burning is significant throughout the Southeastern U.S. during the winter months, based on levoglucosan concentrations. These factors result in brown carbon concentrations being generally highest during this period. In urban environments, primary vehicle emissions appear to also produce similar levels of light absorbing species relative to soluble carbon mass as biomass burning, but the amount of primary WSOC appears to be relatively small making this a minor source of brown



carbon. In contrast, freshly formed secondary WSOC shows no evidence of producing chromophoric species. These compounds, in turn, would produce an even lower fraction of light absorbing species in secondary WSOC. However, a consistent chromophoric component to WSOC was observed throughout the Southeast that was not correlated with biomass burning tracers (e.g., levoglucosan). This suggests that there is an additional source for the light absorbing species. This may be from SOA not involving urban emissions, such as SOA formation from biogenic VOCs in rural regions, and/or chemical aging of SOA formed in rural or urban regions [e.g., *Gelencser et al., 2002; Duarte et al., 2005; Baduel et al., 2009*]. An analysis of this data set by *Zhang et al. (2010b)* supports the view of a linkage between aged secondary organic aerosol and light absorbing species in WSOC, where a principle component analysis produces a SOA factor that contains WSOC, oxalate (a known ubiquitous SOA product) and light absorbing species. Relative to combustion sources [*Sun et al, 2007*], this was a weaker source for light absorbing species and accounts for the much lower levels of brown carbon relative to WSOC during the summer.

The relatively uniform spatial distribution of  $Ab_{365}/WSOC$  ratio based on the 24-hour FRM filters for biomass-burning and non-biomass burning impacted filters suggests that the light absorbing components are wide-spread, fairly uniformly distributed, and a consistent fractions of WSOC (although much higher for biomass burning). Some of this uniformity may be due to the limitations associated with the filter data, a combination of both highly time averaged data and bias towards sampling only the more stable water-soluble aerosol components [*Subramanian et al., 2004; Watson et al., 2009*]. The light absorbing nature of the WSOC likely does depend on the type of fuel burned and the

nature of the fire, but this is not detected in our data. If  $\text{Abs}_{365}/\text{WSOC}$  emissions vary, our data may indicate that aging somehow leads to a more consistent ratio. Also, the very different sources and processes that lead to the production of light absorbing carbonaceous species in the atmosphere, clearly show that lumping all water-soluble light absorbing compounds as HULIS may not be the correct approach to studying these compounds.

This study demonstrates the utility of online  $\text{Abs}_{365}$ -WSOC measurement for investigating aerosol chemistry. Extending the measurements to various plumes at different stages of aging, combined with other detailed chemical analysis could provide significant new insights into chemical processing of aerosols. Longer-term data sets than what were presented here would also provide more robust conclusions on the sources and processes leading to the production of brown carbon. Collection of data on the light-absorbing properties (i.e. absorption of light at the ultra violet region of the electromagnetic spectrum) of water-insoluble organic compounds in the atmosphere would also provide a more complete picture.

## **CHAPTER 5**

### **FUTURE WORK**

The mechanisms leading to the formation of secondary organic aerosol (SOA) are an important piece in the overall puzzle of the affect of aerosols on climate change. The physical and chemical characteristics of SOA, when first produced, from different sources, and as it ages, can provide useful information regarding the nature of the compounds and reactions involved in its production. The most common sources of SOA , anthropogenic and natural, are urban emissions, biomass burning and biogenic emissions. Organic and aquatic chemists have been working on analyzing the nature of water soluble organic compounds and the possible reaction pathways (in liquid phase) that they may undergo for many years. Many impressive and useful databases on these organic compounds as they relate to aquatic chemistry are available. However, the need for a database on the physical properties (e.g., light absorption, hygroscopicity, etc.) on the chemicals that have been found in different samples collected from various ambient sources is felt in the atmospheric chemistry research arena. These chemicals should be cataloged, and where the physical properties information is available, referenced and where not, measured and cataloged. Such a database will be invaluable to the atmospheric chemistry community and will be the basis of unifying the various information sources that has been published on these compounds.

The PILS-LWCC-WSOC system can be used, in combination with some filter measurements, to shed light on the chemical properties of aerosols as they are released into the atmosphere as primary compounds and as they age into secondary complexes. Such data collected from different regions, under various meteorological conditions and

over extended periods of time would be helpful in addressing SOA production mechanisms. It is important to note that this system only collects information on bulk WSOC material and is unable to address specific compound separations. However, as valuable as speciation of compounds may be, there are very many different compounds that can be found in WSOC. Thus, addressing the WSOC as a bulk property has the advantage of simplifying a myriad of compounds into a group and concentrating on the mechanisms that may be viable for the production of SOA, based on the bulk properties of WSOC.

Operating this system (for the collection of ambient measurements) alongside a CIMS system that has been modified to measure aerosol oxalic acid can provide even more useful information on the nature of SOA formation and aging. Further tests will need to be conducted to better quantify this system (CIMS for aerosol oxalic acid) for the measurement of various organic components of aerosols. Oxalic acid has been recognized as an important compound in the formation of SOA, generally as an end product of aqueous phase oxidation products [*Seinfeld et al., 2001; Carlton et al., 2006; Carlton et al., 2007*]. Simultaneous data collection of the light absorption properties of water soluble aerosols, which is related to their chemical structure (Chapter 4), the mass of WSOC and aerosol phase oxalic acid will provide information on the different processes involved in the production of SOA.

The biomass burning data and characteristics of plumes used here can be further integrated into other research studies that have similar information on biomass burning and/or urban plumes. An extensive database where WSOC, CO, OA, meteorological data and transport time of plumes are available can be used to compare plumes of different

origins, but with similar age. Also, in the ARCTAS-2008 data archive information about numerous chemical and aerosol species have been presented. The main reason that the data were not included here was the choice of 10s averaging time that has been used for this analysis. This excluded many other measurements that were collected on longer time-scales. Reducing the resolution of the data will decrease the number of plumes and diminish the statistical value of the analysis; however, the addition of data from many other species and the information gained from analyzing and comparing the data would overshadow this problem, especially since the high resolution analysis of possible compounds in the plumes has already been presented (Chapter 3).

And finally, future measurements of biomass burning plumes where bulk organic and inorganic aerosol composition, WSOC and light absorption properties of water soluble and insoluble aerosol are collected would further advance our knowledge of the processes that contribute to the production of POA and SOA in fires.

## CHAPTER 6

### CONCLUSIONS

Secondary organic aerosols (SOA-s) in the atmosphere, comprise a large fraction of atmospheric aerosols. However, the chemical and physical processes and mechanisms that lead to the formation of SOA are still not well understood. Information on emissions from various sources, such as urban and biomass burning, and the fate of the primary emissions as air-masses are transported downwind, can be very useful in clarifying some of the processes involved in the formation of SOA. Furthermore, data collection on various characteristics of OA, such as light absorption properties, could be useful in understanding the various groups of chemical compound involved in the different stages of SOA production.

The results presented in this thesis showed that a negative ion chemical ionization mass spectrometer (CIMS), can be modified by the addition of a thermally denuded inlet to measure aerosol phase sulfuric acid. This system can also be used to measure other aerosol phase organic acids.

Biomass burning is a significant source of aerosol and gaseous emissions. *Stocks et al.* (2004) have discussed the potential for increased occurrences of forest fires with an increase in global temperatures. Thus, information on emissions from different fires and the fate of these emissions as they are transported to regions away from the location of original emission is important. Data from many biomass burning sources were compared in Chapter 3. Some primary and secondary compounds had different normalized excess mixing ratios (NEMR) when emitted from different types of fires. For example, HCN was higher in fires that were emitted from Asian and Siberian forest fires, in contrast to

the California and Canadian Boreal fires. Also, the levels of some compounds, such as ( $\text{CO}_2$ ,  $\text{CH}_4$ , TU, aerosol  $\text{NO}_3^-$  and  $\text{SO}_4^{2-}$ ) were elevated in biomass burning plumes that were influenced by urban emissions. When comparing gaseous emissions, the levels of primary emissions such as  $\text{NO}_x$  were higher for plumes that were encountered closer to the fires than the ones that were subject to long range transport. Black carbon mass and some inorganic aerosol component ( $\text{NO}_3^-$  and  $\text{SO}_4^{2-}$ ) concentrations were higher in the air-masses that were transported long distances away from the location of original emission. During the second part of the ARCTAS-2008 field measurement experiment, emissions from Canadian Boreal forest fires were evaluated based on the transport time of the plumes from the location of four known fires. The NEMR for different gaseous and aerosol species showed scatter in the data, in the plumes, for each fire and when comparing the different fires with each other. No clear indication of formation of secondary aerosol or gaseous species was observed. Any enhancements may have been obscured due to the high spatial variability in the emissions (i.e. the burning temperatures varied in large fires from the center to the edges of the fires, as visually observed from the color of the smokes from the fires; also, multiple fires may have been contributing to the plumes present in one region). Additionally, the variability in the production of secondary compounds may have been due to the dependence of these processes to various other factors such as: photo-chemistry rates affected by cloud cover, temperature and RH, time of day, etc. These factors may have been dissimilar for various fires, on different days. In biomass burning emissions, a significant fraction of OA and WSOC are from primary emissions. The addition of a much smaller amount of secondary

species to the large primary emissions (e.g., OA and WSOC) present in the plumes may have not been discernible.

Filter data collected from FRM sites in the Southeastern U.S. showed that biomass burning is the most dominant source of water soluble light absorbing carbonaceous aerosol in this region. In fact, biomass burning emissions contain about 3.5 times higher water soluble light absorbing compounds per mass of WSOC. In urban emissions (especially vehicular exhaust), primary WSOC appears to be less dominant but the emissions contain high levels of water soluble light absorbing carbonaceous aerosols per mass of WSOC. Also, the spatial distribution of light absorbing material in the Southeastern U.S. appears to be uniform. Although this may have been due to limitations of the filter data collection system (i.e. highly averaged and biased towards less volatile water soluble aerosol compounds).

It was also demonstrated that humic like substances (HULIS) are not the only type of light absorbing material present in aerosols. There are other organic compounds, such as xylose, that are not categorized as HULIS and yet clearly absorb light in the same region.

And finally, the data from a study in Atlanta, GA showed that the online PILS-LWCC-WSOC system might be used for measurements of light absorbing properties of aerosols and WSOC.



## REFERENCES

- Abel, S. J., et al. "Evolution of Biomass Burning Aerosol Properties from an Agricultural Fire in Southern Africa." *Geophysical Research Letters* 30 15 (2003)
- Alexander, D. T. L., P. A. Crozier, and J. R. Anderson. "Brown Carbon Spheres in East Asian Outflow and Their Optical Properties." *Science* 321 5890 (2008): 833-36
- Allen, A. G., A. A. Cardoso, and G. O. da Rocha. "Influence of Sugar Cane Burning on Aerosol Soluble Ion Composition in Southeastern Brazil." *Atmospheric Environment* 38 30 (2004): 5025-38
- Andersson-Skold, Y., and D. Simpson. "Secondary Organic Aerosol Formation in Northern Europe: A Model Study." *Journal of Geophysical Research-Atmospheres* 106 D7 (2001): 7357-74
- Andracchio, A., et al. "A New Approach for the Fractionation of Water-Soluble Organic Carbon in Atmospheric Aerosols and Cloud Drops." *Atmospheric Environment* 36 32 (2002): 5097-107
- Andreae, M. O., et al. "Transport of Biomass Burning Smoke to the Upper Troposphere by Deep Convection in the Equatorial Region." *Geophysical Research Letters* 28 6 (2001): 951-54
- Andreae, M. O., and P. J. Crutzen. "Atmospheric Aerosols: Biogeochemical Sources and Role in Atmospheric Chemistry." *Science* 276 5315 (1997): 1052-58
- Andreae, M. O., and A. Gelencser. "Black Carbon or Brown Carbon? The Nature of Light-Absorbing Carbonaceous Aerosols." *Atmospheric Chemistry and Physics* 6 (2006): 3131-48
- Andreae, M. O., and P. Merlet. "Emission of Trace Gases and Aerosols from Biomass Burning." *Global Biogeochemical Cycles* 15 4 (2001): 955-66
- Andrews, E., and S. M. Larson. "Effect of Surfactant Layers on the Size Changes of Aerosol-Particles as a Function of Relative-Humidity." *Environmental Science & Technology* 27 5 (1993): 857-65
- Arnold, F., et al. "Stratospheric Aerosol Sulfuric Acid: First Direct in Situ Measurements Using a Novel Balloon-Based Mass Spectrometer Apparatus." *Journal of Atmospheric Chemistry* 30 1 (1998): 3-10
- Artaxo, P., et al. "Aerosol Characteristics and Sources for the Amazon Basin During the Wet Season." *Journal of Geophysical Research-Atmospheres* 95 D10 (1990): 16971-85

- Asa-Awuku, A., et al. "Investigation of Molar Volume and Surfactant Characteristics of Water-Soluble Organic Compounds in Biomass Burning Aerosol." *Atmospheric Chemistry and Physics* 8 4 (2008): 799-812
- Atkinson, R. "Atmospheric Chemistry of VOC-s and Knox." *Atmospheric Environment* 34 12-14 (2000): 2063-101
- Baduel, C., D. Voisin, and J. L. Jaffrezo. "Comparison of Analytical Methods for Humic Like Substances (HULIS) Measurements in Atmospheric Particles." *Atmospheric Chemistry and Physics* 9 16 (2009): 5949-62
- Bein, K. J., et al. "Interactions between Boreal Wildfire and Urban Emissions." *Journal of Geophysical Research-Atmospheres* 113 D7 (2008)
- Belz, M., et al. "Linearity and Effective Optical Pathlength of Liquid Waveguide Capillary Cells." *SPIEIE Conference on Internal Standardization and Calibration Architectures for Chemical Sensors, Boston Massachusetts* 3856 (1999): 271-281
- Bergstrom, R. W., P. B. Russell, and P. Hignett. "Wavelength Dependence of the Absorption of Black Carbon Particles: Predictions and Results from the Tarfox Experiment and Implications for the Aerosol Single Scattering Albedo." *Journal of the Atmospheric Sciences* 59 3 (2002): 567-77
- Bernard, L., and N. Ostlander. "Assessing Climate Change Vulnerability in the Arctic Using Geographic Information Services in Spatial Data Infrastructures." *Climatic Change* 87 1-2 (2008): 263-81
- Berresheim, H., et al. "Chemical Ionization Mass Spectrometer for Long-Term Measurements of Atmospheric Oh and H<sub>2</sub>so<sub>4</sub>." *International Journal of Mass Spectrometry* 202 1-3 (2000): 91-109
- Bond, T. C., et al. "Light Absorption by Primary Particle Emissions from a Lignite Burning Plant." *Environmental Science & Technology* 33 21 (1999): 3887-91
- Brimblecombe, P., and C. Bowler. "The History of Air-Pollution in York, England." *Journal of the Air & Waste Management Association* 42 12 (1992): 1562-66
- Brown, S. S., et al. "Nocturnal Isoprene Oxidation over the Northeast United States in Summer and Its Impact on Reactive Nitrogen Partitioning and Secondary Organic Aerosol." *Atmospheric Chemistry and Physics* 9 9 (2009): 3027-42
- Cao, G. L., et al. "Investigation on Emission Factors of Particulate Matter and Gaseous Pollutants from Crop Residue Burning." *Journal of Environmental Sciences-China* 20 1 (2008): 50-55

- Capaldo, K., et al. "Effects of Ship Emissions on Sulphur Cycling and radiative Climate Forcing Over the Ocean." *Nature* 400 6746 (1999): 743-6
- Capes, G., et al. "Secondary Organic Aerosol from Biogenic Vocs over West Africa During Amma." *Atmospheric Chemistry and Physics* 9 12 (2009): 3841-50
- Carlton, A. G., et al. "Link between Isoprene and Secondary Organic Aerosol (SOA): Pyruvic Acid Oxidation Yields Low Volatility Organic Acids in Clouds." *Geophysical Research Letters* 33 6 (2006)
- Carlton, A. G., et al. "Atmospheric Oxalic Acid and SOA Production from Glyoxal: Results of Aqueous Photooxidation Experiments." *Atmospheric Environment* 41 35 (2007): 7588-602
- Charlson, R. J., et al. "Climate Forcing by Anthropogenic Aerosols." *Science* 255 5043 (1992): 423-30
- Chen, J. J., and R. J. Griffin. "Modeling Secondary Organic Aerosol Formation from Oxidation of Alpha-Pinene, Beta-Pinene, and D-Limonene." *Atmospheric Environment* 39 40 (2005): 7731-44
- Chow, J. C., et al. "Equivalence of Elemental Carbon by Thermal/Optical Reflectance and Transmittance with Different Temperature Protocols." *Environmental Science & Technology* 38 16 (2004): 4414-22
- Claeys, M., et al. "Formation of Secondary Organic Aerosols through Photooxidation of Isoprene." *Science* 303 5661 (2004a): 1173-76
- Claeys, M., et al. "Formation of Secondary Organic Aerosols from Isoprene and Its Gas-Phase Oxidation Products through Reaction with Hydrogen Peroxide." *Atmospheric Environment* 38 25 (2004b): 4093-98
- Clarke, A., et al. "Biomass Burning and Pollution Aerosol over North America: Organic Components and Their Influence on Spectral Optical Properties and Humidification Response." *Journal of Geophysical Research-Atmospheres* 112 D12 (2007)
- Clemittshaw, K. C. "A Review of Instrumentation and Measurement Techniques for Ground-Based and Airborne Field Studies of Gas-Phase Tropospheric Chemistry." *Critical Reviews in Environmental Science and Technology* 34 1 (2004): 1-108
- Cofer, W. R., et al. "Source Compositions of Trace Gases Released During African Savanna Fires." *Journal of Geophysical Research-Atmospheres* 101 D19 (1996): 23597-602

- Crounse, J., et al. "Measurement of Gas-Phase Hydroperoxides by Chemical Ionization Mass Spectrometry." *Analytical Chemistry* 79 (2006): 6726-32
- Crounse, J., et al. "Biomass Burning and Urban Air Pollution Over the Central Mexican Plateau." *Atmospheric Chemistry and Physics* 9 14 (2009): 4929-44
- Crutzen, P. J., and M. O. Andreae. "Biomass Burning in the Tropics - Impact on Atmospheric Chemistry and Biogeochemical Cycles." *Science* 250 4988 (1990): 1669-78
- Crutzen, P. J., et al. "Biomass Burning as a Source of Atmospheric Gases Co, H<sub>2</sub>, N<sub>2</sub>O, No, Ch<sub>3</sub>cl and Cos." *Nature* 282 5736 (1979): 253-56
- Cubison, M., et al. "A Lagrangian Case Study of the Evolution of Aerosol Composition from a Boreal Fire Plume During the ARCTAS Campaign." *In Preparation* (2010)
- Curtius, J., and F. Arnold. "Measurement of Aerosol Sulfuric Acid 1. Experimental Setup, Characterization, and Calibration of a Novel Mass Spectrometric System." *Journal of Geophysical Research-Atmospheres* 106 D23 (2001): 31965-74
- Curtius, J., et al. "First Direct Sulfuric Acid Detection in the Exhaust Plume of a Jet Aircraft in Flight." *Geophysical Research Letters* 25 6 (1998): 923-26
- Davies, D. K., et al. "Fire Information for Resource Management System: Archiving and Distributing Modis Active Fire Data." *IEEE Transactions on Geoscience and Remote Sensing* 47 1 (2009): 72-79
- DeCarlo, P. F., et al. "Investigation of the Sources and Processing of organic Aerosol Over the Central Mexican Plateau from Aircraft Measurements During MILAGRO." *Atmospheric Chemistry and Physics Discussions* 10 (2010): 2445-2502
- DeCarlo, P. F., et al. "Fast Airborne Aerosol Size and Chemistry Measurements Above Mexico City and Central Mexico During the MILAGRO Campaign." *Atmospheric Chemistry and Physics* 8 14 (2008): 4027-48
- De Gouw, J., and J. L. Jimenez. "Organic Aerosols in the Earth's Atmosphere." *Environmental Science & Technology* 43 20 (2009): 7614-18
- De Gouw, J., and C. Warneke. "Measurements of Volatile Organic Compounds in the Earths Atmosphere Using Proton-Transfer-Reaction Mass Spectrometry." *Mass Spectrometry Reviews* 26 2 (2007): 223-57
- De Gouw, J. A., et al. "Budget of Organic Carbon in a Polluted Atmosphere: Results from the New England Air Quality Study in 2002." *Journal of Geophysical*

*Research-Atmospheres* 110 D16 (2005)

- De Haan, D. O., et al. "Secondary Organic Aerosol-Forming Reactions of Glyoxal with Amino Acids." *Environmental Science & Technology* 43 8 (2009a): 2818-24
- De Haan, D. O., et al. "Secondary Organic Aerosol Formation by Self-Reactions of Methylglyoxal and Glyoxal in Evaporating Droplets." *Environmental Science & Technology* 43 21 (2009b): 8184-90
- De Haan, D. O., M. A. Tolbert, and J. L. Jimenez. "Atmospheric Condensed-Phase Reactions of Glyoxal with Methylamine." *Geophysical Research Letters* 36 (2009c) DOI: L11819 10.1029/2009gl037441
- Decesari, S., et al. "Characterization of Water-Soluble Organic Compounds in Atmospheric Aerosol: A New Approach." *Journal of Geophysical Research-Atmospheres* 105 D1 (2000): 1481-89
- Decesari, S., et al. "Characterization of the Organic Composition of Aerosols from Rondonia, Brazil, During the Lba-Smocc 2002 Experiment and Its Representation through Model Compounds." *Atmospheric Chemistry and Physics* 6 (2006): 375-402
- Dickerson, R. R., et al. "Analysis of Black Carbon and Carbon Monoxide Observed over the Indian Ocean: Implications for Emissions and Photochemistry." *Journal of Geophysical Research-Atmospheres* 107 D19 (2002)
- Dinar, E., T. F. Mentel, and Y. Rudich. "The Density of Humic Acids and Humic Like Substances (HULIS) from Fresh and Aged Wood Burning and Pollution Aerosol Particles." *Atmospheric Chemistry and Physics* 6 (2006a): 5213-24
- Diskin, G. S., et al. "Open Path Airborne Tunable Diode laser Hygrometer." *In Diode Lasers and Applications in Atmospheric Sensing, SPIE Proceedings* 4817, (2002): 196-204
- Donahue, N. M., A. L. Robinson, and S. N. Pandis. "Atmospheric Organic Particulate Matter: From Smoke to Secondary Organic Aerosol." *Atmospheric Environment* 43 1 (2009): 94-106
- Duan, F. K., et al. "Identification and Estimate of Biomass Burning Contribution to the Urban Aerosol Organic Carbon Concentrations in Beijing." *Atmospheric Environment* 38 9 (2004): 1275-82
- Duarte, Rmbo, and A. C. Duarte. "Application of Non-Ionic Solid Sorbents (XAD Resins) for the Isolation and Fractionation of Water-Soluble Organic Compounds from Atmospheric Aerosols." *Journal of Atmospheric Chemistry* 51 1 (2005): 79-93

- Duarte, Rmbo, et al. "Spectroscopic Study of the Water-Soluble Organic Matter Isolated from Atmospheric Aerosols Collected under Different Atmospheric Conditions." *Analytica Chimica Acta* 530 1 (2005): 7-14
- Dusek, U., et al. "'Missing' Cloud Condensation Nuclei in Peat Smoke." *Geophysical Research Letters* 32 11 (2005)
- Edney, E. O., et al. "Formation of 2-Methyl Tetrols and 2-Methylglyceric Acid in Secondary Organic Aerosol from Laboratory Irradiated Isoprene/Nox/So<sub>2</sub>/Air Mixtures and Their Detection in Ambient Pm<sub>2.5</sub> Samples Collected in the Eastern United States." *Atmospheric Environment* 39 29 (2005): 5281-89
- Eisele, F. L., and D. J. Tanner. "Ion-Assisted Tropospheric Oh Measurements." *Journal of Geophysical Research-Atmospheres* 96 D5 (1991): 9295-308
- Eisele, F. L., and D. J. Tanner. "Measurement of the Gas-Phase Concentration of H<sub>2</sub>so<sub>4</sub> and Methane Sulfonic-Acid and Estimates of H<sub>2</sub>so<sub>4</sub> Production and Loss in the Atmosphere." *Journal of Geophysical Research-Atmospheres* 98 D5 (1993): 9001-10
- Eisele, F. L., et al. "Measurements and Steady State Calculations of Oh Concentrations at Mauna Loa Observatory." *Journal of Geophysical Research-Atmospheres* 101 D9 (1996): 14665-79
- Engelhart, G. J., et al. "CCN Activity and Droplet Growth Kinetics of Fresh and Aged Monoterpene Secondary Organic Aerosol." *Atmospheric Chemistry and Physics* 8 14 (2008): 3937-49
- Engling, G., et al. "Composition of the Fine Organic Aerosol in Yosemite National Park During the 2002 Yosemite Aerosol Characterization Study." *Atmospheric Environment* 40 16 (2006): 2959-72
- Ervens, B., and S. M. Kreidenweis. "SOA Formation by Biogenic and Carbonyl Compounds: Data Evaluation and Application." *Environmental Science & Technology* 41 11 (2007): 3904-10
- Esteves, V. I., M. Otero, and A. C. Duarte. "Comparative Characterization of Humic Substances from the Open Ocean, Estuarine Water and Fresh Water." *Organic Geochemistry* 40 9 (2009): 942-50
- Eatough, D. J., et al. "A Multiple-System, Multichannel Diffusion Denuder Sampler for the Determination of Fine Particulate Organic Material in the atmosphere." *Atmospheric Environment Part A-General Topics* 27 8 (1993): 1213-19
- Facchini, M. C., et al. "Partitioning of the Organic Aerosol Component between Fog

- Droplets and Interstitial Air." *Journal of Geophysical Research-Atmospheres* 104 D21 (1999): 26821-32
- Falkovich, A. H., et al. "Low Molecular Weight Organic Acids in Aerosol Particles from Rondonia, Brazil, During the Biomass-Burning, Transition and Wet Periods." *Atmospheric Chemistry and Physics* 5 (2005): 781-97
- Fehsenfeld, F. C., et al. "Ground-Based Intercomparison of Nitric Acid Measurement Techniques." *Journal of Geophysical Research-Atmospheres* 103 D3 (1998): 3343-53
- Fine, P. M., et al. "Chemical Characterization of Fine Particle Emissions from Fireplace Combustion of Woods Grown in the Northeastern United States." *Environmental Science and Technology* 35 13 (2001): 2665-2675
- Finlayson-Pitts, B. J. and J. N. Pitts Jr. "Chemistry of the Upper and Lower Atmosphere: Theory, Experiments and Applications." *Academic Press, California* (1999)
- Fisher J.A., et al. "Source Attribution and Interannual Variability of Arctic Pollution in Spring Constrained by Aircraft (ARCTAS, ARCPAC) and Satellite (AIRS) Observations of Carbon Monoxide" *Atmospheric Chemistry and Physics* 10 (2010): 977-996
- Formenti, P., et al. "Inorganic and Carbonaceous Aerosols During the Southern African Regional Science Initiative (Safari 2000) Experiment: Chemical Characteristics, Physical Properties, and Emission Data for Smoke from African Biomass Burning." *Journal of Geophysical Research-Atmospheres* 108 D13 (2003)
- Forstner, H. J. L., et al.. "Molecular Speciation of Secondary Organic Aerosol from Photooxidation of the Higher Alkenes: 1-Octene and 1-Decene." *Atmospheric Environment* 31 13 (1997a): 1953-64
- Forstner, H. J. L., et al. "Secondary Organic Aerosol from the Photooxidation of Aromatic Hydrocarbons: Molecular Composition." *Environmental Science & Technology* 31 5 (1997b): 1345-58
- Fu, P. Q., et al. "Photochemical and Other Sources of Organic Compounds in the Canadian High Arctic Aerosol Pollution During Winter-Spring." *Environmental Science & Technology* 43 2 (2009): 286-92
- Fuzzi, S., et al. "A Simplified Model of the Water Soluble Organic Component of Atmospheric Aerosols." *Geophysical Research Letters* 28 21 (2001): 4079-82
- Gao, S., et al. "Water-Soluble Organic Components in Aerosols Associated with Savanna Fires in Southern Africa: Identification, Evolution, and Distribution." *Journal of Geophysical Research-Atmospheres* 108 D13 (2003)

- Gao, S., et al. "Characterization of Polar Organic Components in Fine Aerosols in the Southeastern United States: Identity, Origin, and Evolution." *Journal of Geophysical Research-Atmospheres* 111 D14 (2006)
- Gelencser, A., et al. "Thermal Behaviour of Carbonaceous Aerosol from a Continental Background Site." *Atmospheric Environment* 34 5 (2000a): 823-31
- Gelencser, A., et al. "Voltammetric Evidence for the Presence of Humic-Like Substances in Fog Water." *Atmospheric Research* 54 2-3 (2000b): 157-65
- Gelencser, A., et al. "On the Possible Origin of Humic Matter in Fine Continental Aerosol." *Journal of Geophysical Research-Atmospheres* 107 D12 (2002)
- Gelencser, A., et al. "In-Situ Formation of Light-Absorbing Organic Matter in Cloud Water." *Journal of Atmospheric Chemistry* 45 1 (2003): 25-33
- Gelencser, A., et al. "Structural Characterization of Organic Matter in Fine Tropospheric Aerosol by Pyrolysis-Gas Chromatography-Mass Spectrometry." *Journal of Atmospheric Chemistry* 37 2 (2000c): 173-83
- Giglio, L., et al. "An Enhanced Contextual Fire Detection Algorithm for Modis." *Remote Sensing of Environment* 87 2-3 (2003): 273-82
- Gimbert, L. J., and P. J. Worsfold. "Environmental Applications of Liquid-Waveguide-Capillary Cells Coupled with Spectroscopic Detection." *Trac-Trends in Analytical Chemistry* 26 9 (2007): 914-30
- Goetz, A., and R. Pueschel. "Basic Mechanisms of Photochemical Aerosol Formation." *Atmospheric Environment* 1 3 (1967): 287
- Gomez-Gonzalez, Y., et al. "Characterization of Organosulfates from the Photooxidation of Isoprene and Unsaturated Fatty Acids in Ambient Aerosol Using Liquid Chromatography/(-) Electrospray Ionization Mass Spectrometry." *Journal of Mass Spectrometry* 43 3 (2008): 371-82
- Graber, E. R., and Y. Rudich. "Atmospheric Hulis: How Humic-Like Are They? A Comprehensive and Critical Review." *Atmospheric Chemistry and Physics* 6 (2006): 729-53
- Graham, B., et al. "Water-Soluble Organic Compounds in Biomass Burning Aerosols over Amazonia - 1. Characterization by NMR and GC-MS." *Journal of Geophysical Research-Atmospheres* 107 D20 (2002)
- Grieshop, A. P., N. M. Donahue, and A. L. Robinson. "Laboratory Investigation of Photochemical Oxidation of Organic Aerosol from Wood Fires 2: Analysis of Aerosol Mass Spectrometer Data." *Atmospheric Chemistry and Physics* 9 6



(2009a): 2227-40

Grieshop, A. P., et al. "Laboratory Investigation of Photochemical Oxidation of Organic Aerosol from Wood Fires 1: Measurement and Simulation of Organic Aerosol Evolution." *Atmospheric Chemistry and Physics* 9 4 (2009b): 1263-77

Guinot, B., et al. "Beijing Aerosol: Atmospheric Interactions and New Trends." *Journal of Geophysical Research-Atmospheres* 112 D14 (2007)

Gunthe, S. S., et al. "Cloud Condensation Nuclei in Pristine Tropical Rainforest Air of Amazonia: Size-Resolved Measurements and Modeling of Atmospheric Aerosol Composition and Ccn Activity." *Atmospheric Chemistry and Physics* 9 19 (2009): 7551-75

Gustin, M. S., et al. "Atmospheric Mercury Concentrations Associated with Geologically Enriched Sites in Central Western Nevada." *Environmental Science and Technology* 30 (1996):2572-79

Guyon, P., et al. "Physical Properties and Concentration of Aerosol Particles over the Amazon Tropical Forest During Background and Biomass Burning Conditions." *Atmospheric Chemistry and Physics* 3 (2003): 951-67

Hallquist, M., et al. "The Formation, Properties and Impact of Secondary Organic Aerosol: Current and Emerging Issues." *Atmospheric Chemistry and Physics* 9 14 (2009): 5155-236

Hamilton, J. F., et al. "Reactive Oxidation Products Promote Secondary Organic Aerosol Formation from Green Leaf Volatiles." *Atmospheric Chemistry and Physics* 9 11 (2009): 3815-23

Hansen, A. D. A., and T. Novakov. "Real-Time Measurement of Aerosol Black Carbon During the Carbonaceous Species Methods Comparison Study." *Aerosol Science and Technology* 12 1 (1990): 194-99

Hansson, H. C., et al. "Experimental-Determination of the Hygroscopic Properties of Organically Coated Aerosol-Particles." *Journal of Aerosol Science* 21 (1990): S241-S44

Hansson, H. C., et al. "NaCl Aerosol Particle Hygroscopicity Dependence on Mixing with Organic Compounds." *Journal of Atmospheric Chemistry* 31 3 (1998): 321-346

Harrison, R. M., and J. X. Yin. "Particulate Matter in the Atmosphere: Which Particle Properties Are Important for Its Effects on Health?" *Science of the Total Environment* 249 1-3 (2000): 85-101

- Hastings, W. P., et al. "Secondary Organic Aerosol Formation by Glyoxal Hydration and Oligomer Formation: Humidity Effects and Equilibrium Shifts During Analysis." *Environmental Science & Technology* 39 22 (2005): 8728-35
- Havers, N., et al. "Characterization of Humic-Like Substances in Airborne Particulate Matter by Capillary Electrophoresis." *Chromatographia* 47 11-12 (1998): 619-24
- Haywood, J., and O. Boucher. "Estimates of the Direct and Indirect Radiative Forcing Due to Tropospheric Aerosols: A Review." *Reviews of Geophysics* 38 4 (2000): 513-43
- Haywood, J. M., et al. "The Mean Physical and Optical Properties of Regional Haze Dominated by Biomass Burning Aerosol Measured from the C-130 Aircraft During Safari 2000." *Journal of Geophysical Research-Atmospheres* 108 D13 (2003)
- Hearn, J. D., and G. D. Smith. "A Chemical Ionization Mass Spectrometry Method for the Online Analysis of Organic Aerosols." *Analytical Chemistry* 76 10 (2004a): 2820-26
- Hearn, J. D., and G. D. Smith. "Kinetics and Product Studies for Ozonolysis Reactions of Organic Particles Using Aerosol CIMS." *Journal of Physical Chemistry A* 108 45 (2004b): 10019-29
- Hearn, J. D., and G. D. Smith. "Reactions and Mass Spectra of Complex Particles Using Aerosol CIMS." *International Journal of Mass Spectrometry* 258 1-3 (2006): 95-103
- Helas, G., et al. "Airborne Measurements of Savanna Fire Emissions and the Regional Distribution of Pyrogenic Pollutants over Western Africa." *Journal of Atmospheric Chemistry* 22 1-2 (1995): 217-39
- Hennigan, C. J., et al. "Enhanced Secondary Organic Aerosol Formation Due to Water Uptake by Fine Particles." *Geophysical Research Letters* 35 18 (2008)
- Hennigan, C. J., et al. "Gas/Particle Partitioning of Water-Soluble Organic Aerosol in Atlanta." *Atmospheric Chemistry and Physics* 9 11 (2009): 3613-28
- Henze, D. K., and J. H. Seinfeld. "Global Secondary Organic Aerosol From Isoprene Oxidation." *Geophysical Research Letters* 33 9 (2006)
- Hildemann, L. M., et al. "Contribution of Primary Aerosol Emissions from Vegetation-Derived Sources to Fine Particle Concentrations in Los Angeles." *Journal of Geophysical Research-Atmospheres* 101 D14 (1996): 19541-49
- Hoffa, E. A., et al. "Seasonality of Carbon Emissions from Biomass Burning in a

- Zambian Savanna." *Journal of Geophysical Research-Atmospheres* 104 D11 (1999): 13841-53
- Hoffer, A., et al. "Optical Properties of Humic-Like Substances (Hulis) in Biomass-Burning Aerosols." *Atmospheric Chemistry and Physics* 6 (2006): 3563-70
- Hoffmann, T., and D. Klockow. "Chemistry of Atmospheric Biogenic Hydrocarbons." *Chemie in Unserer Zeit* 32 4 (1998): 182-91
- Honrath, R. E., et al. "Regional and Hemispheric Impacts of Anthropogenic and Biomass Burning Emissions on Summertime Co and O<sub>3</sub> in the North Atlantic Lower Free Troposphere." *Journal of Geophysical Research-Atmospheres* 109 D24 (2004)
- Horvath, H. "Atmospheric Light-Absorption - a Review." *Atmospheric Environment Part a-General Topics* 27 3 (1993a): 293-317
- Horvath, H. "Comparison of Measurements of Aerosol Optical-Absorption by Filter Collection and a Transmissometric Method." *Atmospheric Environment Part a-General Topics* 27 3 (1993b): 319-25
- Hoyle, C. R., et al. "Secondary Organic Aerosol in the Global Aerosol - Chemical Transport Model Oslo Ctm2." *Atmospheric Chemistry and Physics* 7 21 (2007): 5675-94
- Huey, L. G. "The Kinetics of the Reactions of Cl-, O-, and O-2(-) with Hno<sub>3</sub>: Implications for Measurement of Hno<sub>3</sub> in the Atmosphere." *International Journal of Mass Spectrometry and Ion Processes* 153 2-3 (1996): 145-50
- Huey, L. G., et al. "Reactions of Sf<sub>6</sub>- and I- with Atmospheric Trace Gases." *Journal of Physical Chemistry* 99 14 (1995): 5001-08
- Huey, L. G., et al. "Reactions of Cf<sub>3</sub>o- with Atmospheric Trace Gases." *Journal of Physical Chemistry* 100 1 (1996): 190-94
- Huey, L. G., et al. "CIMS Measurements of Hno<sub>3</sub> and So<sub>2</sub> at the South Pole During ISCAT 2000." *Atmospheric Environment* 38 32 (2004): 5411-21
- Huey, L. G. "Measurement of Trace Atmospheric Species by Chemical Ionization Mass Spectrometry: Speciation of Reactive Nitrogen and Future Directions. " *Mass Spectrometry Reviews* 26 2 (2007): 166-184
- Huey, L. G., et al. "Trends of SO<sub>2</sub> Concentrations Emitted from various Fires Measured during ARCTAS-2008." *In Preparation* (2010)
- Iinuma, Y., et al. "Source Characterization of Biomass Burning Particles: The Combustion of Selected European Conifers, African Hardwood, Savanna Grass, and German and Indonesian Peat." *Journal of Geophysical Research-Atmospheres*

112 D8 (2007)

- Jacob, D. J. "Heterogeneous Chemistry and Tropospheric Ozone." *Atmospheric Environment* 34 12-14 (2000): 2131-59
- Jacob, D. J., and S. C. Wofsy. "Photochemistry of Biogenic Emissions over the Amazon Forest." *Journal of Geophysical Research-Atmospheres* 93 D2 (1988): 1477-86
- Jacob, D.J. et al. "The ARCTAS Aircraft Mission: Design and Execution" Submitted to *Atmospheric Chemistry and Physics* (2010)
- Jaffrezo, J. L., et al. "Biomass Burning Signatures in the Atmosphere of Central Greenland." *Journal of Geophysical Research-Atmospheres* 103 D23 (1998): 31067-78
- Jang, M. S., et al. "Heterogeneous Atmospheric Aerosol Production by Acid-Catalyzed Particle-Phase Reactions." *Science* 298 5594 (2002): 814-17
- Jimenez, J. L., et al. "Evolution of Organic Aerosols in the Atmosphere." *Science* 326 5959 (2009): 1525-29
- Johnson, E. A., Kiyoko Miyonishi, and National Center for Ecological Analysis and Synthesis. *Forest Fires : Behavior and Ecological Effects*. San Diego, Calif.: Academic Press, 2001
- Justice, C. O., et al. "The Modis Fire Products." *Remote Sensing of Environment* 83 1-2 (2002): 244-62
- Kanakidou, M., et al. "Organic Aerosol and Global Climate Modelling: A Review." *Atmospheric Chemistry and Physics* 5 (2005): 1053-123
- Kang, C. M., et al. "Chemical Characteristics of Acidic Gas Pollutants and Pm2.5 Species During Hazy Episodes in Seoul, South Korea." *Atmospheric Environment* 38 28 (2004): 4749-60
- Kavouras, I. G., et al. "Measurement of Particulate Aliphatic and Polynuclear Aromatic Hydrocarbons in Santiago De Chile: Source Reconciliation and Evaluation of Sampling Artifacts." *Atmospheric Environment* 33 30 (1999): 4977-86
- Kawamura, K., L. L. Ng, and I. R. Kaplan. "Determination of Organic-Acids (C1-C10) in the Atmosphere, Motor Exhausts, and Engine Oils." *Environmental Science & Technology* 19 11 (1985): 1082-86
- Khwaja, H. A., S. Brudnoy, and L. Husain. "Chemical Characterization of 3 Summer Cloud Episodes at Whiteface Mountain." *Chemosphere* 31 5 (1995): 3357-81
- Kiehl, J. T. "Twentieth Century Climate Model Response and Climate Sensitivity."

*Geophysical Research Letters* 34 22 (2007)

- Kirchstetter, T. W., T. Novakov, and P. V. Hobbs. "Evidence That the Spectral Dependence of Light Absorption by Aerosols Is Affected by Organic Carbon." *Journal of Geophysical Research-Atmospheres* 109 D21 (2004)
- Kiss, G., et al. "Characterization of Polar Organic Compounds in Fog Water." *Atmospheric Environment* 35 12 (2001): 2193-200
- Kleindienst, T. E., et al. "Determination of Secondary Organic Aerosol Products from the Photooxidation of Toluene and Their Implications in Ambient PM<sub>2.5</sub>." *Journal of Atmospheric Chemistry* 47 1 (2004): 79-100
- Koppmann, R., et al. "Emissions of Organic trace Gases From Savanna Fires in Southern Africa During the 1992 Southern Africa Fire Atmosphere Research Initiative and Their Impact on the Formation of Tropospheric Ozone." *Journal of Geophysical Research-Atmospheres* 102 D15 (1997): 18879-88
- Krivacsy, Z., et al. "Study of Humic-Like Substances in Fog and Interstitial Aerosol by Size-Exclusion Chromatography and Capillary Electrophoresis." *Atmospheric Environment* 34 25 (2000): 4273-81
- Krivacsy, Z., et al. "Study on the Chemical Character of Water Soluble Organic Compounds in Fine Atmospheric Aerosol at the Jungfraujoeh." *Journal of Atmospheric Chemistry* 39 3 (2001): 235-59
- Krivacsy, Z., et al. "Study of Water-Soluble Atmospheric Humic Matter in Urban and Marine Environments." *Atmospheric Research* 87 1 (2008): 1-12
- Kroll, J. H., et al. "Secondary Organic Aerosol Formation from Isoprene Photooxidation under High-NO<sub>x</sub> Conditions." *Geophysical Research Letters* 32 18 (2005a)
- Kroll, J. H., et al. "Chamber Studies of Secondary Organic Aerosol Growth by Reactive Uptake of Simple Carbonyl Compounds." *Journal of Geophysical Research-Atmospheres* 110 D23 (2005b)
- Kroll, J. H., and J. H. Seinfeld. "Chemistry of Secondary Organic Aerosol: Formation and Evolution of Low-Volatility Organics in the Atmosphere." *Atmospheric Environment* 42 16 (2008): 3593-624
- Lacaux, J. P., et al. "Biomass Burning in the Tropical Savannas of Ivory-Coast - an Overview of the Field Experiment Fire of Savannas (Fos/Decafe-91)." *Journal of Atmospheric Chemistry* 22 1-2 (1995): 195-216
- Lawless, P. A., C. E. Rodes, and D. S. Ensor. "Multiwavelength Absorbance of Filter Deposits for Determination of Environmental Tobacco Smoke and Black

- Carbon." *Atmospheric Environment* 38 21 (2004): 3373-83
- LeCanut, P., et al. "Airborne Studies of Emissions from Savanna Fires in Southern Africa .1. Aerosol Emissions Measured with a Laser Optical Particle Counter." *Journal of Geophysical Research-Atmospheres* 101 D19 (1996): 23615-30
- Lee, S., et al. "Gaseous and Particulate Emissions from Prescribed Burning in Georgia." *Environmental Science & Technology* 39 23 (2005): 9049-56
- Lee, S., et al. "Diagnosis of Aged Prescribed Burning Plumes Impacting an Urban Area." *Environmental Science & Technology* 42 5 (2008): 1438-44
- Limbeck, A., M. Kulmala, and H. Puxbaum. "Secondary Organic Aerosol Formation in the Atmosphere Via Heterogeneous Reaction of Gaseous Isoprene on Acidic Particles." *Geophysical Research Letters* 30 19 (2003)
- Lindberg, J. D., R. E. Douglass, and D. M. Garvey. "Atmospheric Particulate Absorption and Black Carbon Measurement." *Applied Optics* 38 12 (1999): 2369-76
- Ludwig, J., et al. "Domestic Combustion of Biomass Fuels in Developing Countries: A Major Source of Atmospheric Pollutants." *Journal of Atmospheric Chemistry* 44 1 (2003): 23-37
- Lukacs, H., et al. "Seasonal Trends and Possible Sources of Brown Carbon Based on 2-Year Aerosol Measurements at Six Sites in Europe." *Journal of Geophysical Research-Atmospheres* 112 D23 (2007)
- Maleknia, S. D., T. L. Bell, and M. A. Adams. "Eucalypt Smoke and Wildfires: Temperature Dependent Emissions of Biogenic Volatile Organic Compounds." *International Journal of Mass Spectrometry* 279 2-3 (2009): 126-33
- Malm, W. C. "Atmospheric Haze - Its Sources and Effects on Visibility in Rural-Areas of the Continental United-States." *Environmental Monitoring and Assessment* 12 3 (1989): 203-25
- Malm, W. C., and P. K. Mueller. "Introduction to Special Section: Aerosol Atmospheric Optics." *Journal of Geophysical Research-Atmospheres* 101 D14 (1996): 19185-87
- Mang, S. A., et al. "Contribution of Carbonyl Photochemistry to Aging of Atmospheric Secondary Organic Aerosol." *Journal of Physical Chemistry A* 112 36 (2008): 8337-44
- Maria, S. F., et al. "Organic Aerosol Growth Mechanisms and Their Climate-Forcing Implications." *Science* 306 5703 (2004): 1921-24

- Marley, N. A., et al. "An Empirical Method for the Determination of the Complex Refractive Index of Size-Fractionated Atmospheric Aerosols for Radiative Transfer Calculations." *Aerosol Science and Technology* 34 6 (2001): 535-49
- Marley, N. A., et al. "Measurements of Aerosol Absorption and Scattering in the Mexico City Metropolitan Area During the MILAGRO Field Campaign: A Comparison of Results from the T0 and T1 Sites." *Atmospheric Chemistry and Physics* 9 1 (2009b): 189-206
- Martins, J. V., et al. "Spectral Absorption Properties of Aerosol Particles from 350-2500nm." *Geophysical Research Letters* 36 (2009)
- Mauzerall, D. L., et al. "Photochemistry in Biomass Burning Plumes and Implications for Tropospheric Ozone Over the tropical South Atlantic." *Journal of Geophysical Research-Atmospheres* 103 D15 (1998): 19281-82
- Mayol-Bracero, O. L., et al. "Water-Soluble Organic Compounds in Biomass Burning Aerosols over Amazonia - 2. Apportionment of the Chemical Composition and Importance of the Polyacidic Fraction." *Journal of Geophysical Research-Atmospheres* 107 D20 (2002)
- McKeen, S. A., et al. "Hydrocarbon Ratios During PEM-West A: A Model Perspective." *Journal of Geophysical Research-Atmospheres* 101 D1 (1996): 2087-109
- McNeill, V. F., G. M. Wolfe, and J. A. Thornton. "The Oxidation of Oleate in Submicron Aqueous Salt Aerosols: Evidence of a Surface Process." *Journal of Physical Chemistry A* 111 6 (2007): 1073-83
- Menon, S. "Current Uncertainties in Assessing Aerosol Effects on Climate." *Annual Review of Environment and Resources* 29 (2004): 1-30
- Mohler, O., and F. Arnold. "Flow Reactor and Triple Quadrupole Mass-Spectrometer Investigations of Negative-Ion Reactions Involving Nitric-Acid - Implications for Atmospheric HNO<sub>3</sub> Detection by Chemical Ionization Mass-Spectrometry." *Journal of Atmospheric Chemistry* 13 1 (1991): 33-61
- Mohler, O., T. Reiner, and F. Arnold. "A Novel Aircraft-Based Tandem Mass-Spectrometer for Atmospheric Ion and Trace Gas Measurements." *Review of Scientific Instruments* 64 5 (1993): 1199-207
- Moteki, N., and Y. Kondo "Effects of Mixing State on Black Carbon Measurements by Laser-Induced Incandescence." *Aerosol Science and Technology* 41 (2007): 398-417
- Moteki, N., and Y. Kondo "Method to Measure Time-Dependent Scattering Cross Sections of Particles Evaporating in a Laser Beam." *Journal of Aerosol Science*

39 (2008): 348-364

- Muhle, J., et al. "Trace gas and Particulate Emissions from the 2003 Southern California Wildfires." *Journal of Geophysical Research-Atmospheres* 112 D3 (2007)
- Mukai, H., and Y. Ambe. "Characterization of a Humic Acid-Like Brown Substance in Airborne Particulate Matter and Tentative Identification of Its Origin." *Atmospheric Environment* 20 5 (1986): 813-19
- Munoz, C., et al. "Analysis of Soil Humic Acids in Particle Size Fractions of an Alfisol from a Mediterranean-Type Climate." *Geoderma* 151 3-4 (2009): 199-203
- Myhre, C. E. L., and C. J. Nielsen. "Optical Properties in the Uv and Visible Spectral Region of Organic Acids Relevant to Tropospheric Aerosols." *Atmospheric Chemistry and Physics* 4 (2004): 1759-69
- Narukawa, M., et al. "Distribution of Dicarboxylic Acid and Carbon Isotopic Compositions in Aerosols From 1997 Indonesian Forest Fires." *Geophysical Research Letters* 26 20 (1999): 3101-04
- Noone, K. J., et al. "Ozone in the Marine Atmosphere Observed During the Atlantic Stratocumulus Transition Experiment Marine Aerosol and Gas Exchange." *Journal of Geophysical Research-Atmospheres* 101 D2 (1996): 4485-99
- Novakov, T., and C. E. Corrigan. "Cloud Condensation Nucleus Activity of the Organic Component of Biomass Smoke Particles." *Geophysical Research Letters* 23 16 (1996): 2141-44
- Novakov, T., D. A. Hegg, and P. V. Hobbs. "Airborne Measurements of Carbonaceous Aerosols on the East Coast of the United States." *Journal of Geophysical Research-Atmospheres* 102 D25 (1997): 30023-30
- Novakov, T., and J. E. Penner. "Large Contribution of Organic Aerosols to Cloud-Condensation-Nuclei Concentrations." *Nature* 365 6449 (1993): 823-26
- Nowak, J. B., et al. "A Chemical Ionization Mass Spectrometry Technique for Airborne Measurements of Ammonia." *Journal of Geophysical Research-Atmospheres* 112 D10 (2007)
- Nozriere, B., P. Dziejczic, and A. Cordova. "Products and Kinetics of the Liquid-Phase Reaction of Glyoxal Catalyzed by Ammonium Ions (Nh<sub>4</sub><sup>+</sup>)." *Journal of Physical Chemistry A* 113 1 (2009): 231-37
- Oliveira, J. L., et al. "Spectroscopic Investigation of Humic Substances in a Tropical Lake During a Complete Hydrological Cycle." *Acta Hydrochimica Et Hydrobiologica* 34 6 (2006): 608-17



- Orsini, D. A., et al. "Refinements to the Particle-into-Liquid Sampler (Pils) for Ground and Airborne Measurements of Water Soluble Aerosol Composition." *Atmospheric Environment* 37 9-10 (2003): 1243-59
- Pandis, S. N., et al. "Aerosol Formation in the Photooxidation of Isoprene and Beta-Pinene." *Atmospheric Environment Part a-General Topics* 25 5-6 (1991): 997-1008
- Pandis, S. N., et al. "Secondary Organic Aerosol Formation and Transport." *Atmospheric Environment Part a-General Topics* 26 13 (1992): 2269-82
- Paredes-Miranda, G., et al. "Primary and Secondary Contributions to Aerosol Light Scattering and Absorption in Mexico City During the Milagro 2006 Campaign." *Atmospheric Chemistry and Physics* 9 11 (2009): 3721-30
- Patashnick, H., et al. "Development of a Reference Standard for Particulate Matter Mass in Ambient Air." *Aerosol Science and Technology* 34 1 (2001): 42-45
- Peltier, R. E., et al. "Fine Aerosol Bulk Composition Measured on Wp-3d Research Aircraft in Vicinity of the Northeastern United States - Results from NEAQS." *Atmospheric Chemistry and Physics* 7 12 (2007a): 3231-47
- Peltier, R. E., R. J. Weber, and A. P. Sullivan. "Investigating a Liquid-Based Method for Online Organic Carbon Detection in Atmospheric Particles." *Aerosol Science and Technology* 41 12 (2007b): 1117-27
- Penner, J. E., et al. "Quantifying and Minimizing Uncertainty of Climate Forcing by Anthropogenic Aerosols." *Bulletin of the American Meteorological Society* 75 3 (1994): 375-400
- Penner, J. E., D. Hegg, and R. Leaitch. "Unraveling the Role of Aerosols in Climate Change." *Environmental Science & Technology* 35 15 (2001): 332A-40A
- Peuravuori, J., and Pihlaja K., "Molecular Size Distribution and Spectroscopic Properties of Aquatic Humic Substances." *Analytica Chemicia Acta* 337 2 (1997): 133-149
- Pope, C. A., et al. "Lung Cancer, Cardiopulmonary Mortality, and Long-Term Exposure to Fine Particulate Air Pollution." *Jama-Journal of the American Medical Association* 287 9 (2002): 1132-41
- Puxbaum, H., et al. "Levoglucosan Levels at Background Sites in Europe for assessing the Impact of biomass Combustion on the European Aerosol Background." *Journal of Geophysical research-Atmosphere* 112 D23 (2007)
- Ramanathan V., et al. "Atmosphere - Aerosols, Climate and the Hydrological Cycle."

- Science* 294 5549 (2001): 2119-2124
- Ravishankara, A. R., "Heterogeneous and Multiphase Chemistry in the Troposphere." *Science* 276 5315 (2007): 1058-65
- Reddy, M. S., and O. Boucher. "A Study of the Global Cycle of Carbonaceous Aerosols in the LMDZT General Circulation Model." *Journal of Geophysical Research-Atmospheres* 109 D14 (2004)
- Reid, J. S., et al. "Physical, Chemical, and Optical Properties of Regional Hazes Dominated by Smoke in Brazil." *Journal of Geophysical Research-Atmospheres* 103 D24 (1998): 32059-80
- Reid, J. S., et al. "A Review of Biomass Burning Emissions Part Iii: Intensive Optical Properties of Biomass Burning Particles." *Atmospheric Chemistry and Physics* 5 (2005): 827-49
- Rogge, W. F., et al. "Sources of Fine Organic Aerosol .1. Charbroilers and Meat Cooking Operations." *Environmental Science & Technology* 25 6 (1991): 1112-25
- Rogge, W. F., et al. "Sources of Fine Organic Aerosol .2. Noncatalyst and Catalyst-Equipped Automobiles and Heavy-Duty Diesel Trucks." *Environmental Science & Technology* 27 4 (1993a): 636-51
- Rogge, W. F., et al. "Sources of Fine Organic Aerosol .3. Road Dust, Tire Debris, and Organometallic Brake Lining Dust - Roads as Sources and Sinks." *Environmental Science & Technology* 27 9 (1993b): 1892-904
- Rogge, W. F., et al. "Sources of Fine Organic Aerosol .4. Particulate Abrasion Products from Leaf Surfaces of Urban Plants." *Environmental Science & Technology* 27 13 (1993c): 2700-11
- Rogge, W. F., et al. "Sources of Fine Organic Aerosol .5. Natural-Gas Home Appliances." *Environmental Science & Technology* 27 13 (1993d): 2736-44
- Rogge, W. F., et al. "Sources of Fine Organic Aerosol .9. Pine, Oak and Synthetic Log Combustion in Residential Fireplaces." *Environmental Science & Technology* 32 1 (1998): 13-22
- Rollins, A. W., et al. "Isoprene Oxidation by Nitrate Radical: Alkyl Nitrate and Secondary Aerosol Yields." *Atmospheric Chemistry and Physics* 9 (2009): 6685-6703
- Rosen, H., et al. "Soot in Urban Atmospheres - Determination by an Optical-Absorption Technique." *Science* 208 4445 (1980): 741-44

- Rubel, G. O., and J. W. Gentry. "Measurement of Water and Ammonia Accommodation Coefficients at Surfaces with Adsorbed Monolayers of Hexadecanol." *Journal of Aerosol Science* 16 6 (1985): 571-74
- Sachse, G. W., et al. "Fast-Response, High-Precision Carbon Monoxide Sensor Using a Tuneable Diode Laser Absorption Technique." *Journal of Geophysical Research* 92 (1987): 2071-81
- Salma, I., R. Ocskay, and G. G. Lang. "Properties of Atmospheric Humic-Like Substances - Water System." *Atmospheric Chemistry and Physics* 8 8 (2008): 2243-54
- Saxena, P., and L. M. Hildemann. "Water-Soluble Organics in Atmospheric Particles: A Critical Review of the Literature and Application of Thermodynamics to Identify Candidate Compounds." *Journal of Atmospheric Chemistry* 24 1 (1996): 57-109
- Saxena, P., et al. "Organics Alter Hygroscopic Behavior of Atmospheric Particles." *Journal of Geophysical Research-Atmospheres* 100 D9 (1995): 18755-70
- Schkolnik, G., and Y. Rudich "Detection and Quantification of Levoglucosan in Atmospheric Aerosols: A Review." *Analytical and Bioanalytical Chemistry* 385 1 (2006): 26-33
- Schmidl, C., et al. "Chemical Characterization of Particle Emissions from Burning Leaves." *Atmospheric Environment* 42 40 (2008): 9070-79
- Scholes, M., and M. O. Andreae. "Biogenic and Pyrogenic Emissions from Africa and Their Impact on the Global Atmosphere." *Ambio* 29 1 (2000): 23-29
- Seinfeld, J. H., et al. "Modeling the Formation of Secondary Organic Aerosol (SOA). 2. The Predicted Effects of Relative Humidity on Aerosol Formation in the Alpha-Pinene-, Beta-Pinene-, Sabinene-, Delta(3)-Carene-, and Cyclohexene-Ozone Systems." *Environmental Science & Technology* 35 9 (2001): 1806-17
- Seinfeld, J. H., and J. F. Pankow. "Organic Atmospheric Particulate Material." *Annual Review of Physical Chemistry* 54 (2003): 121-40
- Seinfeld, John H., and Spyros N. Pandis. *Atmospheric Chemistry and Physics : From Air Pollution to Climate Change*. New York: John Wiley, 1998
- Shapiro, E. L., et al. "Light-Absorbing Secondary Organic Material Formed by Glyoxal in Aqueous Aerosol Mimics." *Atmospheric Chemistry and Physics* 9 7 (2009): 2289-300
- Shinozuka, Y., et al. "Aerosol Optical Properties Relevant to Regional Remote Sensing of Ccn Activity and Links to Their Organic Mass Fraction: Airborne Observations

- over Central Mexico and the Us West Coast During MILAGRO/INTEX-B." *Atmospheric Chemistry and Physics* 9 18 (2009): 6727-42
- Sicre, M. A., et al. "Airborne and Vapor-Phase Hydrocarbons over the Mediterranean-Sea." *Geophysical Research Letters* 17 12 (1990): 2161-64
- Simoneit, B. R. T. "Organic-Matter in Eolian Dusts over Atlantic Ocean." *Marine Chemistry* 5 4-6 (1977): 443-64
- Simoneit, B. R. T. "Chemical Characterization of Sub-Micron Organic Aerosols in the Tropical Trade Winds of the Caribbean Using Gas Chromatography-Mass Spectrometry." *Atmospheric Environment* 36 33 (2002): 5259-63
- Skoog, D. A., et al. "Principles of Instrumental Analysis." *Thomspn Educational Publishing, Toronto ON, NY* 5 4-6 (1998)
- Slusher, D. L., et al. "A Chemical Ionization Technique for Measurement of Pernitric Acid in the Upper Troposphere and the Polar Boundary Layer." *Geophysical Research Letters* 28 20 (2001): 3875-78
- Slusher, D. L., et al. "A Thermal Dissociation-Chemical Ionization Mass Spectrometry (Td-CIMS) Technique for the Simultaneous Measurement of Peroxyacyl Nitrates and Dinitrogen Pentoxide." *Journal of Geophysical Research-Atmospheres* 109 D19 (2004)
- Spittler, M., et al. "Reactions of No<sub>3</sub> Radicals with Limonene and Alpha-Pinene: Product and SOA Formation." *Atmospheric Environment* 40 (2006): S116-S27
- Stankiewicz, B. A., et al. "Comparison of the Analytical Performance of Filament and Curie-Point Pyrolysis Devices." *Journal of Analytical and Applied Pyrolysis* 45 2 (1998): 133-51
- Stocks, B. J., et al. "Overview of the International Crown Fire Modelling Experiment (ICFME)." *Canadian Journal of Forest Research-Revue Canadienne De Recherche Forestiere* 34 8 (2004): 1543-47
- Stohl, A., et al. "Technical Note: The Lagrangian Particle Dispersion Model Flexpart Version 6.2." *Atmospheric Chemistry and Physics* 5 (2005): 2461-74
- Streets, D. G., et al. "An Inventory of Gaseous and Primary Aerosol Emissions in Asia in the Year 2000." *Journal of Geophysical Research-Atmospheres* 108 D21 (2003)
- Studnicka, M., et al. "Short-Term Effects of Acid Aerosols and Ozone on Lung-Function in Children." *American Review of Respiratory Disease* 147 4 (1993): A638-A638
- Subramanian, R., et al. "Positive and Negative Artifacts in Particulate Organic Carbon

- Measurements with Denuded and Undenuded Sampler Configurations." *Aerosol Science and Technology* 38 (2004): 27-48
- Sullivan, A. P., et al. "A Method for on-Line Measurement of Water-Soluble Organic Carbon in Ambient Aerosol Particles: Results from an Urban Site." *Geophysical Research Letters* 31 13 (2004)
- Sullivan, A. P., et al. "Airborne Measurements of Carbonaceous Aerosol Soluble in Water over Northeastern United States: Method Development and an Investigation into Water-Soluble Organic Carbon Sources." *Journal of Geophysical Research-Atmospheres* 111 D23 (2006). DOI: 10.1029/2006jd007072
- Talbot, M. M. B., and G. C. Bate. "The Relative Quantities of Live and Detrital Organic-Matter in a Beach Surf Ecosystem." *Journal of Experimental Marine Biology and Ecology* 121 3 (1988): 255-64
- Talbot, R. W., et al. "Aerosol Chemistry During the Wet Season in Central Amazonia - the Influence of Long-Range Transport." *Journal of Geophysical Research-Atmospheres* 95 D10 (1990): 16955-69
- Tanner, D. J., and F. L. Eisele. "Present Oh Measurement Limits and Associated Uncertainties." *Journal of Geophysical Research-Atmospheres* 100 D2 (1995): 2883-92
- Tanner, D. J., et al. "Selected Ion Chemical Ionization Mass Spectrometric Measurement of Oh." *Journal of Geophysical Research-Atmospheres* 102 D5 (1997): 6415-25
- Thompson, A., et al. "Reaction of Bromide Ions with Atmospheric Trace Gases and Aerosols." *PhD Thesis* Georgia Institute of Technology (2006)
- Trainer, M., et al. "Impact of Natural Hydrocarbons on Hydroxyl and Peroxy-Radicals at a Remote Site." *Journal of Geophysical Research-Atmospheres* 92 D10 (1987): 11879-94
- Trentmann, J., M. O. Andreae, and H. F. Graf. "Chemical Processes in a Young Biomass-Burning Plume." *Journal of Geophysical Research-Atmospheres* 108 D22 (2003)
- Tsigaridis, K., and M. Kanakidou. "Global Modelling of Secondary Organic Aerosol in the Troposphere: A Sensitivity Analysis." *Atmospheric Chemistry and Physics* 3 (2003): 1849-69
- Turpin, B. J., J. J. Huntzicker, and K. M. Adams. "Intercomparison of Photoacoustic and Thermal Optical Methods for the Measurement of Atmospheric Elemental Carbon." *Atmospheric Environment Part a-General Topics* 24 7 (1990): 1831-35

- van Donkelaar, A., et al. "Analysis of Aircraft and Satellite Measurements from the Intercontinental Chemical Transport Experiment (Intex-B) to Quantify Long-Range Transport of East Asian Sulfur to Canada." *Atmospheric Chemistry and Physics* 8 11 (2008): 2999-3014
- Varga, B., et al. "Isolation of Water-Soluble Organic Matter from Atmospheric Aerosol." *Talanta* 55 3 (2001): 561-72
- Vay, S. A., et al. "An Assessment of Aircraft-Generated Contamination on in Situ Trace Gas Measurements: Determinations from Empirical Data Acquired Aloft." *Journal of Atmospheric and Oceanic Technology* 20 11 (2003): 1478-87
- Viggiano, A. A., et al. "Stratospheric Negative-Ion Reaction-Rates with H<sub>2</sub>SO<sub>4</sub>." *Journal of Geophysical Research-Oceans and Atmospheres* 87 NC9 (1982): 7340-42
- Viggiano, A. A. "In-Situ Mass-Spectrometry and Ion Chemistry in the Stratosphere and Troposphere." *Mass Spectrometry Reviews* 12 2 (1993): 115-37
- Viskari, E., et al. "Ubiquity and Dominance of Oxygenated Species in Organic Aerosols in Anthropogenically-Influenced Northern Hemisphere Midlatitudes." *Geophysical Research Letters* 34 13 (2007)
- Volkamer, R., et al. "Seasonal and Diurnal Variation in Formaldehyde and Acetaldehyde Concentrations Along a highway in Eastern Finland." *Atmospheric Environment* 34 (2000):917-923
- Wang, H. B., K. Kawamura, and K. Yamazaki. "Water-Soluble Dicarboxylic Acids, Ketoacids and Dicarbonyls in the Atmospheric Aerosols over the Southern Ocean and Western Pacific Ocean." *Journal of Atmospheric Chemistry* 53 1 (2006): 43-61
- Warneke, C., et al. "Biomass Burning in Siberia and Kazakhstan as an Important Source for Haze over the Alaskan Arctic in April 2008 - Art. No. L02813." *Geophysical Research Letters* 36: : 2813-13 36
- Watson, J. G., et al. "Methods to Assess Carbonaceous Aerosol Sampling Artifacts for Improve and Other Long-Term Networks." *Journal of the Air & Waste Management Association* 59 8 (2009): 898-911
- Weber, R.J., et al. "A Particulate-into-liquid Collector for Rapid Measurement of Aerosol Bulk Chemical Composition. " *Aerosol Science and Technology*, 35 3 (2001): 718-727
- Weinheimer, A. J., et al. "Meridional Distributions of No(X), No(Y) and Other Species in the Lower Stratosphere and Upper Troposphere During Aase-II." *Geophysical Research Letters* 21 23 (1994): 2583-86

- Went, F. W. "On Nature of Aitken Condensation Nuclei." *Tellus* 18 2-3 (1966): 549
- Went, F. W. "Organic Matter in the Atmosphere, and Its Possible Relation to Petroleum Formation." *Proceedings of the National Academy of Sciences of the United States of America* 46 2 (1960): 212-21
- Wisthaler, A., et al. "Organic Trace Gas Measurements by PTR-MS During INDOEX 1999." *Journal of Geophysical Research-Atmospheres* 107 D19 (2002)
- Yamasoe, M. A., et al. "Chemical Composition of Aerosol Particles from Direct Emissions of Vegetation Fires in the Amazon Basin: Water-Soluble Species and Trace Elements." *Atmospheric Environment* 34 10 (2000): 1641-53
- Yang, M., et al. "Attribution of Aerosol Light Absorption to Black Carbon, Brown Carbon, and Dust in China - Interpretations of Atmospheric Measurements During East-AIRE." *Atmospheric Chemistry and Physics* 9 6 (2009): 2035-50
- Yokelson, R. J., et al. "The Tropical Forest and Fire Emissions Experiment: Laboratory Fire Measurements and Synthesis of Campaign Data." *Atmospheric Chemistry and Physics* 8 13 (2008): 3509-27
- Yokelson, R. J., et al. "Emissions from Biomass Burning in the Yucatan." *Atmospheric Chemistry and Physics* 9 15 (2009): 5785-812
- Yu, J. Z., et al. "Gas-Phase Ozone Oxidation of Monoterpenes: Gaseous and Particulate Products." *Journal of Atmospheric Chemistry* 34 2 (1999a): 207-58
- Yu, J. Z., et al. "Observation of Gaseous and Particulate Products of Monoterpene Oxidation in Forest Atmospheres." *Geophysical Research Letters* 26 8 (1999b): 1145-48
- Zappoli, S., et al. "Inorganic, Organic and Macromolecular Components of Fine Aerosol in Different Areas of Europe in Relation to Their Water Solubility." *Atmospheric Environment* 33 17 (1999): 2733-43
- Zhang, J., et al. "Characteristics of Aldehydes: Concentrations, Sources, and Exposures for Indoor and Outdoor Residential Microenvironments." *Environmental Science and Technology* 28 (1994):146-52
- Zhang, Q., et al. "Hydrocarbon-Like and Oxygenated Organic Aerosols in Pittsburgh: Insights into Sources and Processes of Organic Aerosols." *Atmospheric Chemistry and Physics* 5 (2005): 3289-311
- Zhang, Q., et al. "Ubiquity and Dominance of Oxygenated Species in Organic Aerosols in Anthropogenically-Influenced Northern Hemisphere Midlatitudes."

*Geophysical Research Letters* 34 13 (2007)

Zhang, X., et al. "On the Spatial Variability of Fine Particle Water-Soluble Organic Carbon in the Southeastern United States" *Atmospheric Chemistry and Physics Discussions* (2010b): *In Preparation*

Zhang, X., et al. "Biomass Burning Impact on PM<sub>2.5</sub> Over the Southeastern U.S.: Integrating Chemically Speciated FRM Filter Measurements, MODIS Fire Counts and PMF analysis" *Atmospheric Chemistry and Physics Discussions* 10 (2010b): 7037-77